The Southern Termination of the East Madagascar Current

Adrian Myles Webb

Department of Oceanography, University of Cape Town,
Rondebosch, South Africa.

Submitted in fulfilment of the requirements of the M.Sc degree at the
University of Cape Town, 2007

Abstract

The Agulhas Current system is a vital part of the global thermohaline circulation. This global thermohaline overturning of the oceans has in turn an inextricable link to world climate. Although this current is so important, relatively little is known on its sources. One of these proposed sources of the Agulhas Current is the southern limb of the East Madagascar Current (EMC). Previously the EMC was primarily studied through the use of drifters, remote sensing and ships' drift methods. In an attempt to increase the understanding of this possible source region a first dedicated cruise was organised for the southern termination of the EMC. The cruise took place in March 2001. The hydrographic and other data from the cruise have the potential to describe the EMC termination in a seminal way.

The EMC is shown to consist of Tropical Surface Water, Subtropical Surface Water and South Indian Central Water. In the region of the EMC Antarctic Intermediate Water, North Indian Deep Water and North Atlantic Deep Water/Circumpolar Deep Water were found. There is clear evidence of the presence of Red Sea Intermediate Water with salinities greater than 34.5 psu at temperatures between 4 and 6.5°C from 800–1250 m, inshore of the EMC. The width of the current during the cruise period was 100 km, the maximum speed of the current was 1.1 m/s and the depth of the current was 1000 m. The maximum transport of the EMC was calculated to be 39.3 Sv. An EMC undercurrent was found with a depth range of 1000–2000 m. The maximum speed of the undercurrent was seen to be 0.3 m/s and the transport of the undercurrent was 0.8 Sv.

No retroflection of the EMC emerges from this data set. Satellite geostrophics over a period of 13 years give evidence of eastward flow being associated with eddies in the region of the EMC termination. References have suggested that such eddies may give the appearance of a retroflection.

From the observations there was ample evidence for the presence of a relatively weak upwelling cell inshore of the EMC. The temperature at the surface of the upwelling cell was 26°C (2 degrees less than the surrounding water) and the chlorophyll concentration was 0.63 mg Chl-a/m^3. Nitrate concentration was 6.4 µmol/kg at 100 m, phosphate 0.53 µmol/kg, silicate 5.69 µmol/kg and oxygen was 107.5 µmol/kg. At 45 km from the coast there was an average movement of water offshore down to a depth of 40 m. The maximum speed of the offshore flow was 0.5 m/s.

Declaration

This study is my own unaided work, except for the normal assistance received from my supervisor and the teaching staff at the University of Cape Town.

Work in this study has in part been published in a paper of which I was not the first author but contributed substantially to the results and analysis:
Machu, E., Lutjeharms, J.R.E., Webb, A.M. and van Aken, H.M. (2002). First hydrographic evidence of the southeast Madagascar upwelling cell. Geophysical Research Letters 29, 10.1029/2002GL015381.

Other publications to which I contributed, but which did not form part of this study are:
Froneman, P.W., Ansorge, I.J., Vumazonke, L., Gulekana, A., Bernard, K.S., Webb, A.M., Leukes, W., Risien, C.M., Thomalla, S., Hermes, J., Knott, M., Anderson, D., Hargey, N., Jennings, M.E., Veitch, J., Lutjeharms, J.R.E., McQuaid, C.D. (2002). Physical and biological variability in the Antarctic Polar Frontal Zone : report on research cruise 103 of the MV SA Agulhas. South African Journal of Science 98, 534-536.

Walter, S., Peeken, I., Lochte, K., Webb, A. and Bange, H.W. (2005). Nitrous oxide measurements during EIFEX, the European Iron Fertilzation Experiment in the subpolar South Atlantic Ocean. Geophysical Research Letters 32, 10.1029/2005GL024619.

Acknowledgements

Firstly I would like to thank my supervisor Prof. Johann Lutjeharms for his excellent guidance, assistance and facilitation even during his extended illness.

I am thankful to the Netherlands Sea Research institute (NIOZ) for letting me use the ACSEX data to do this study, and for funding my trip to the European Geophysical Union meeting in Vienna.

Many thanks to my office mate Dr Juliet Hermes for her great friendship and unfailing willingness to help me.

I am also very grateful to Mr Emlyn Balarin and Dr Isabelle Ansorge for their encouragement and assistance in many diverse matters.

A final expression of gratitude to my parents for their support and patience.

Contents

List of figures

List of tables

1. Introduction

In the Indian Ocean the South Equatorial Current (SEC) flows from east to west in a band from 6° to 25°S (Swallow et al., 1988), and by other reports between 8° to 22°S (Woodberry et al., 1989; Hastenrath and Greishar, 1991). On encountering the coast of Madagascar, the fourth largest island in the world (Ho et al., 2004), the SEC splits into a northern and southern branch of the East Madagascar Current (EMC). The southern EMC flows southward from 18°S following the eastern coastline of Madagascar. The EMC transports waters of relatively high temperature, high salinity and low nutrients (Ho et al., 2004). The current flows to the southern end of the continent at 27°S (Hastenrath and Greishar, 1991; Sætre, 1985). There is uncertainty about the further course of the current from this southern position. Figure 1.1. shows the main features of the greater Agulhas Current system including the EMC.

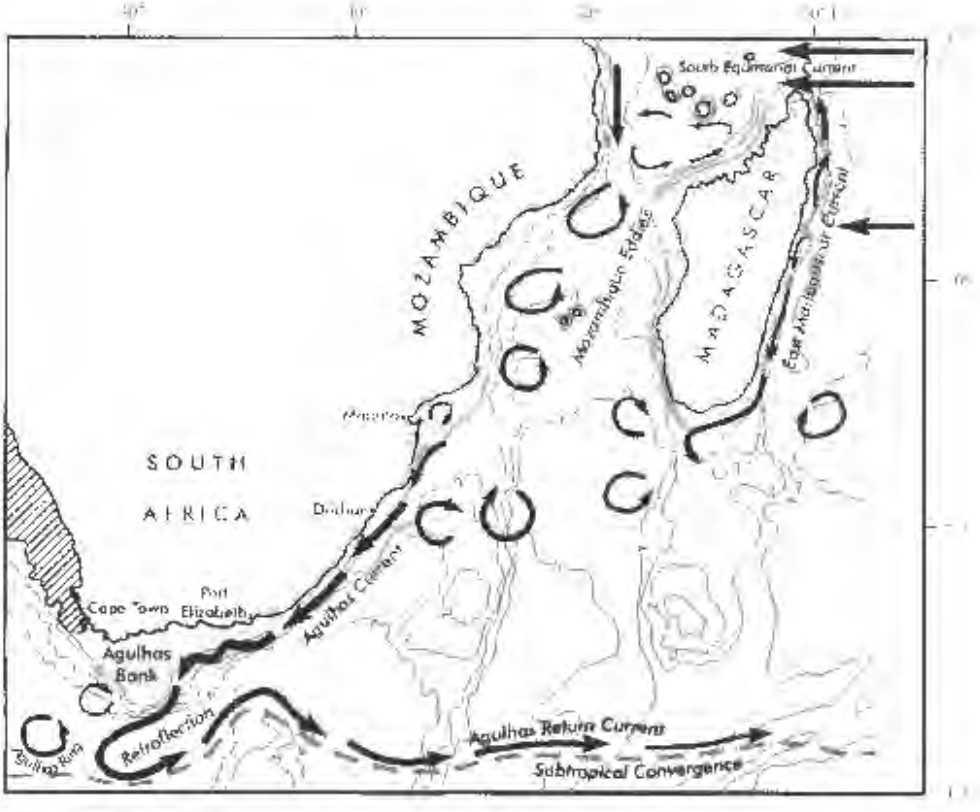

Figure 1.1. Agulhas Current and associated features (from Lutjeharms 2006). Shelf regions shallower than 1000 m are shaded and hatching indicates upwelling.

Early portrayals of the flow in this southern region show the EMC continuing to the west to join up with the Agulhas Current at about 25°S making it an important source of the Agulhas Current (Figure 1.2). On further investigation, Lutjeharms found that there was only a westward component of flow at deeper levels (greater than 200 m), while the surface flow was to the east (Lutjeharms, 1976). Satellite investigation of this topic led to the concept of an East Madagascar Current retroflection (Lutjeharms, 1988b). However the true nature of the flow can only be determined with *in situ* hydrographic data. Unfortunately there have been relatively few hydrographic studies performed in this region to clarify the situation.

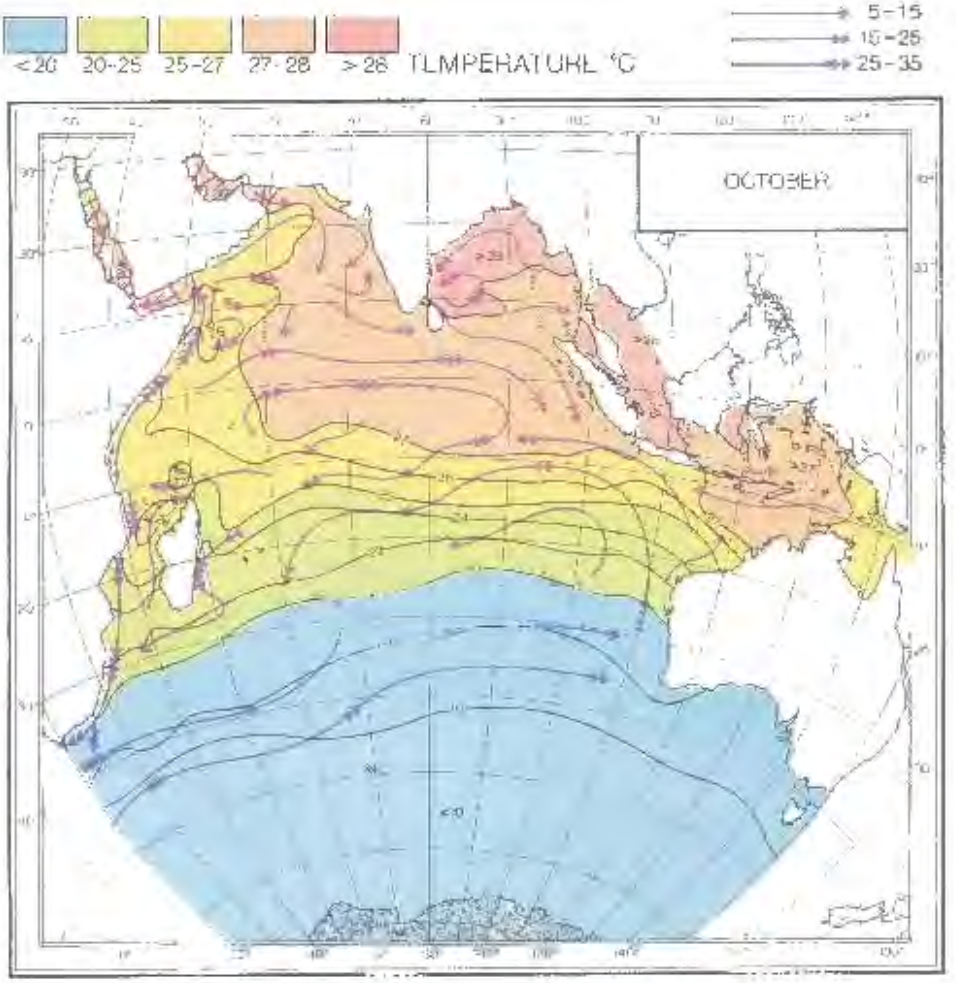

Figure 1.2. *Currents derived from ships' drift (from Krey and Babenerd 1976). Streamlines indicate direction and velocity of currents in nautical miles per day. (5-15 nm/day=0.11-0.33 m/s, 25-35 nm/day=0.54-0.75 m/s).*

The other supposed important sources of the Agulhas Current are its own recirculation cell and the flow through the Mozambique Channel (Figure 1.2). The Mozambique Current was portrayed as flowing down the western side of the Mozambique Channel and then joining the northern Agulhas Current. As with the EMC there have been relatively few appropriate hydrographic stations to investigate the flow in this channel. Most knowledge of the current initially came from the analysis of ships' drift data (Sætre, 1985). This method is not sufficient in resolving the current, as it is only an indication of the surface flow. Recent studies have questioned this portrayal of a continuous flow and demonstrated that the flow in the channel consist of a train of eddies (de Ruijter et al., 2002, Biastoch and Krauß, 1999).

The EMC might have an indirect effect on the northern European climate. This possible link between the EMC and the northern European climate (and in fact the global climate) is made through the Agulhas Current. As a source of the Agulhas Current the EMC could have a controlling influence on this current. The Agulhas Current in turn is a very important link in the global thermohaline circulation (Lutjeharms, 1996). This global circulation is responsible for moving salt and heat around the oceans and between the oceans (Figure 1.3). The Agulhas Current moves the water through a flow peculiarity that exists at the southern tip of Africa.

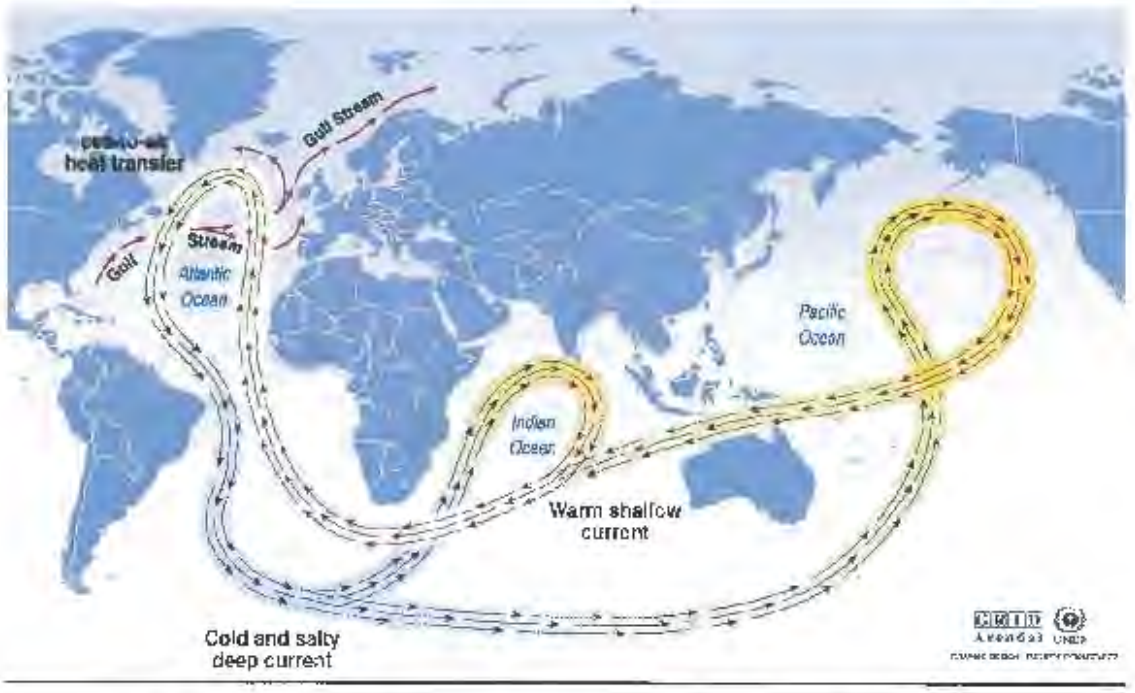

Figure 1.3 Global ocean thermohaline circulation. (from Broecker 1991. cited http://www. grida.no/climate/vital/32.htm). The Agulhas Current plays a vital role in the link between the warm Indian Ocean and the Atlantic Ocean.

The Agulhas Current flows in a western direction down the eastern side of South Africa (Figure 1.1). The current then turns to head east at the southern tip of Africa and heads back into the Indian Ocean as an eastward return current, this is called a retroflection. At the retroflection the south-westward flowing limb and the eastward limb regularly "short-circuit" and this forms large anti cyclonic eddies called Agulhas rings. These rings, which contain Indian Ocean water, then move northwest into the Atlantic Ocean (Byrne et al., 1995). This movement of Indian Ocean water adds salt and heat to the southern Atlantic Ocean. In the Atlantic Ocean the surface component of the global thermohaline circulation then moves this water to the north. Once in the North Atlantic the heat is lost to the atmosphere and North Atlantic Deep Water is formed (Figure 1.3). The atmosphere, which is warmed by the ocean, maintains the relatively warm climate of North Western Europe. Hence the Agulhas Current has an important role to play in the global thermohaline circulation.

The best understood and documented trigger mechanism for the Agulhas rings, which are shed about 6 to 9 times a year (Feron et al., 1992), is believed to be perturbations in the flow of the Agulhas Current (van Leeuwen et al., 2000). These perturbations can take the form of single meanders in the course of the Agulhas Current and are called Natal Pulses (Lutjeharms and Roberts, 1988). The generation of the Natal Pulses has been observed to be related to the shedding of Agulhas rings about six months later. These meanders, in the usually very stable flow of the Agulhas Current, form close to Durban. The eastern coastline of South Africa is noted as having a relatively narrow continental shelf and steep continental slope. The Agulhas Current follows the shelf break quite persistently. An exception to this narrow shelf is in a region upstream of Durban where the shelf slope is relatively weak; this region is called the Natal Bight. The current in this region is in a stable state, but it is close to being unstable. It is believed that anti-cyclonic eddies move to just east of the Natal Bight and from this position they enhance and perturb the current (Schouten et al., 2002). These perturbations can then grow into Natal Pulses. The Natal Pulse then moves down the coast at a rate of about 10-20 km per day (Lutjeharms and Roberts, 1988). When a pulse gets close to the Agulhas retroflection the southward extension of the current can result in the closing of the retroflection loop and the pinching off of an Agulhas ring.

The anti-cyclonic eddies which are involved in the formation of the Natal Pulse have been shown to arrive from the Mozambique Channel (Schouten et al., 2002). Schouten et al. (2002) have also shown a synchronisation between anomalies arriving at the region of the Natal Pulse from the EMC and from the Mozambique Channel (Figure 9 in Schouten et al., 2002). Eddy dipoles, which head towards the Natal Pulse region, have been seen to come from the EMC region and are possibly related to the EMC (de Ruijter et al., 2004). With a better understanding of the southern termination of the EMC we would be able to determine if these eddies are linked to the proposed retroflection of the EMC. These eddies might also originate further to the east in the Indian Ocean, and move through the EMC region. So, through a chain of events the EMC might be linked to the maintenance of the climate in Europe.

The EMC has another interesting, but poorly understood element. This is the question of upwelling inshore of the current southeast of Madagascar. The shelf configuration in this area is similar to that found in two other places along the Agulhas Current, Port Alfred and the Natal Bight (Figure 1.5). At these regions along the Agulhas Current intense and persistent upwelling cells have been found. Off Port Alfred the upwelling cell has been shown to have a surface expression for about 45% of the time that was analysed (Lutjeharms et al., 2000c). At the Natal Bight, distinct upwelling has been seen in 56% of the satellite pictures analysed by Lutjeharms et al. (1989) (if all uncertain cases are included then this number rises to 90%). At all these sites the shelf width increases along the course of the current (Figure1.5). This upwelling is a result of the flow past this particular shelf configuration and is not wind induced (Gill and Schumann, 1979). Using satellite measured ocean colour and temperature (Figure 1.4) it has been shown that there is a very strong possibility that a similar upwelling cell is present off the coast of southeast Madagascar (Lutjeharms and Machu, 2000). In order to verify this upwelling cell *in situ* measurement need to be made.

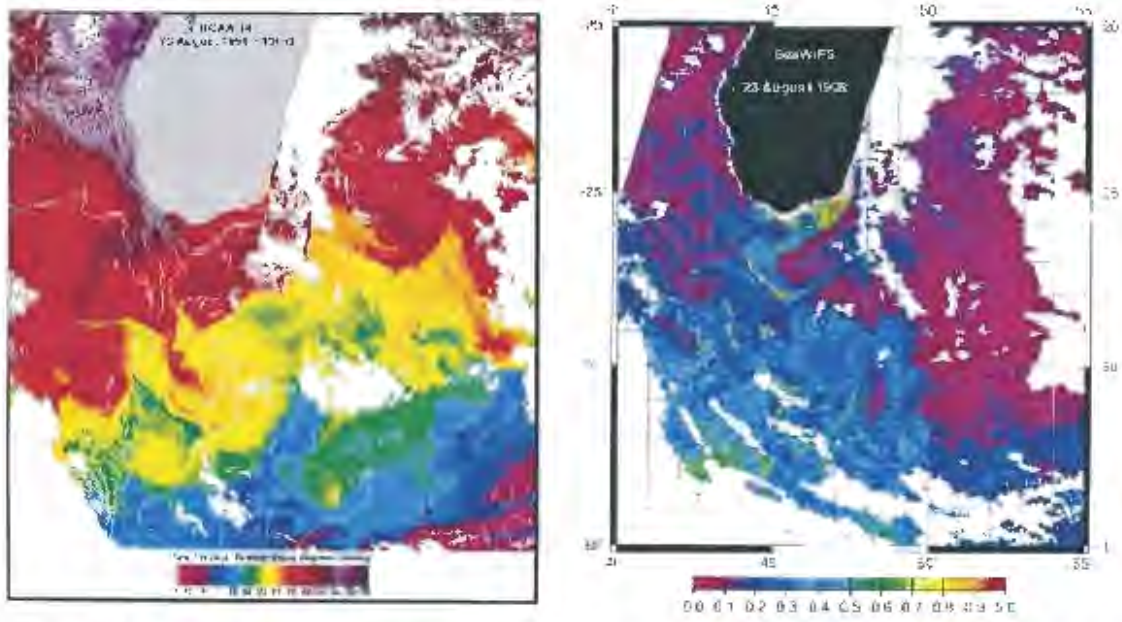

Figure 1.4. *Upwelling inshore of the East Madagascar Current. Left hand side panel shows the composite of sea surface temperature. The right hand side panel shows chlorophyll-a concentration. (from Lutjeharms and Machu, 2000).*

To summarise, the EMC may possibly have a controlling effect on the Agulhas Current and the behaviour of that current's retroflection. The Agulhas Current is known to be a notable component of the global thermohaline circulation, therefore the area of the southern termination of the EMC may possibly have a link to world climate. It has also been concluded that there is an upwelling cell inshore of the southern limb of the EMC that might well be driven by the passing current. In order to establish what research needs to be done in this important ocean region, it is crucial to determine precisely what already is known.

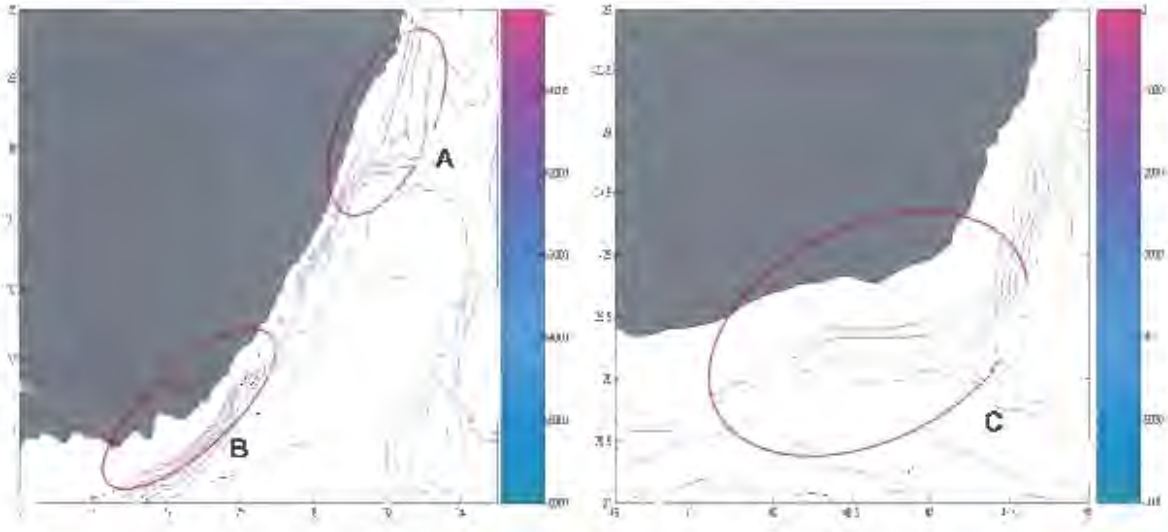

Figure 1.5. *Widening shelf configurations. (A) The Natal Bight (B) Port Alfred and (C) the south-eastern tip of Madagascar.*

2. What is known about the East Madagascar Current?

In the literature a few different methods have been employed to study the region of the EMC. As commercial ships pass the southern tip of Madagascar on their way between South Africa and Asia, the Far East and Middle East they can be used to gather data. The drift of ships off their course as they pass through the waters south of Madagascar is possibly the simplest way to garner information about the current. However, a much better method for the description of a current is to use data from deep hydrographic stations, but there is a shortage of hydrographic data for the EMC. Nevertheless there are other modern sophisticated methods that have been used. An example of these modern methods is remote sensing satellite information, which can give an insight into the water movement through sea level, sea temperature and sea colour. Drifting buoys released in the current can be tracked by satellite, and so the movement of the water into which the drifter was entrained can be established. A method that can give a long term view of the current is the deployment of moored current meters in the current over long periods. This can give information on the intensity and seasonality of the flow. All of this knowledge can also be assimilated in computer models, which should be able to give an impression of the larger picture, and also make it possible to predict flow patterns.

2.1 Ships' Drift

From the analysis of ships' drift in the early part of the previous century it was thought that the EMC continued west past the southern tip of Madagascar and was a permanent and direct source for the Agulhas Current (Michaelis, 1923; Paech, 1926). Ships' drift has limited use in the description of a current because it only gives an idea of the water movement of the surface water, but cannot give an indication of deep water movement. The use of ships' drift for the determination of surface movement cannot be done with any great accuracy either, because strong wind force acting on the ship's superstructure can change the resultant drift of the ship. As wind force acting on ships varies because of different ship profiles this factor cannot be accurately removed.

The large data set of ships drift has, however, been considered satisfactory in resolving seasonal current patterns (Sætre, 1985). Analysis of ships drift in the region by Sætre (1985) showed the EMC to be directionally stable. He found that part of the water from the current was deflected to the east at about 22° to 27°S, although the main part of the current rounded the southern tip of Madagascar and fed the Agulhas Current.

Figures from a climatic atlas of the Indian Ocean (Hastenrath and Greischar, 1989) show the EMC rounding the southern tip of Madagascar in January and April. Figures from the US Navy atlas (Anonymous, 1970) also show a similar situation (Figure 2.1). Lutjeharms et al. (2000b) have recently performed a reanalysis of the ships' drift data. They found that the EMC lies between 18°S and 26°S, which is a similar range to that found in previous analyses (Hastenrath and Greishar, 1991; Sætre, 1985). Lutjeharms et al. (2000b) found the current to have a maximum width of 2 degrees of latitude (about 220 km). This is similar to the previous findings of about 200 km (Lutjeharms et al., 1981) based on hydrographic observations across the current.

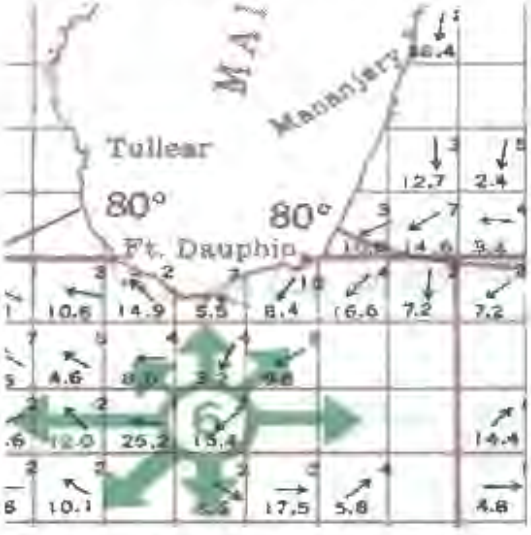

Figure 2.1. Surface currents south of Madagascar in January (from Anonymous 1970). Black arrows show the average direction of the current in each 1-degree quadrangle. The number in the upper right hand corner of the quadrangle represents the total number of current observations used in the calculation. The number in the bottom left corner of the quadrangle represents the drift in miles per day. The green rose represents the prevailing currents in the general area.

The maximum observed surface speed for the EMC as reported by Hastenrath and Greishar (1991) was about 25 cm/s. Sætre (1985) found higher values, which ranged between 50 and 74 cm/s. These higher values agree with Lutjeharms et al.'s (2000b) more recent analysis where the average current speeds were calculated as exceeding 50 cm/s. Individual speeds as high as 150 cm/s have been reported (Duncan and Schladow, 1981). Lutjeharms et al. (2000b) have found high values of eddy kinetic energy seaward of the EMC from 21°S to 25°S (Figure 2.2). High kinetic energy suggests current instability in this region, which could be caused by the formation of eddies or meanders in the current (Lutjeharms et al., 2000b).

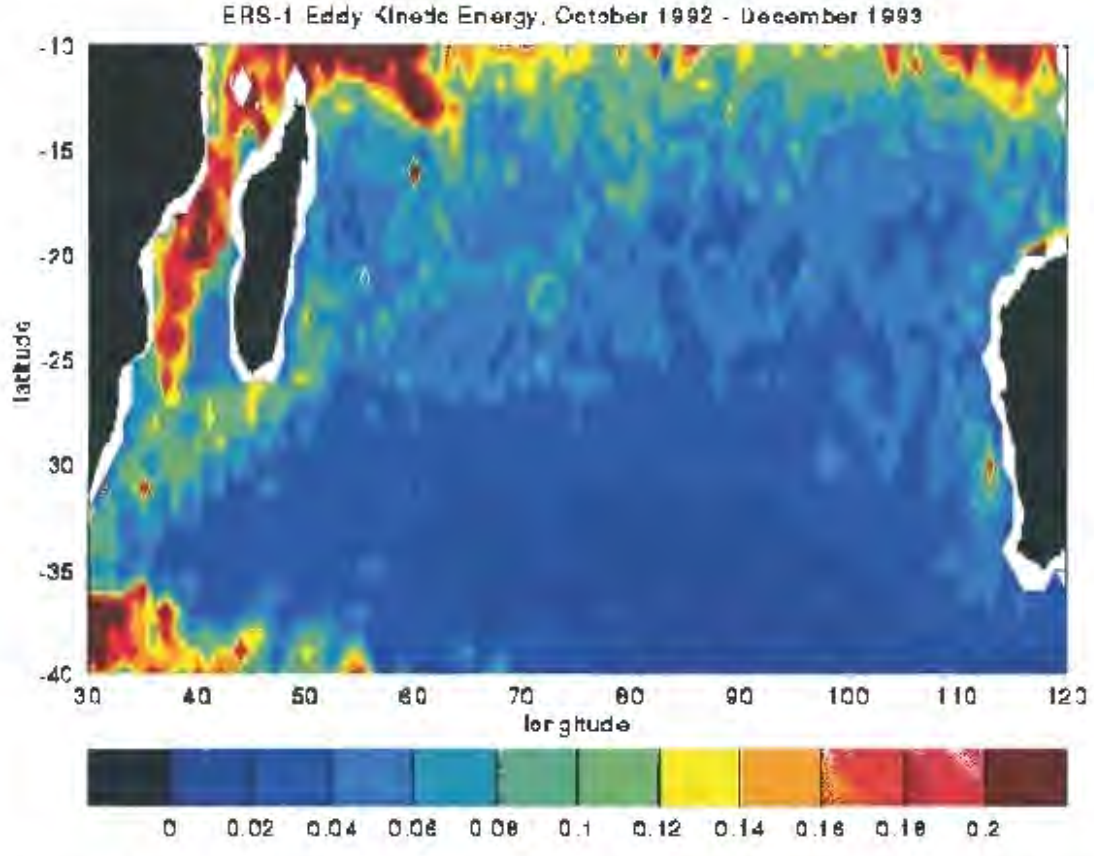

Figure 2.2. Mean eddy kinetic energy ($m^2 s^{-2}$), October 1992 - December 1993, from ERS-1 altimeter (from Heywood and Somayajulu 1997). The figure shows the relatively high eddy kinetic energy east and south of southern Madagascar.

Another region of high eddy kinetic energy is south of Madagascar. This region is the proposed site of retroflection of the current (Lutjeharms et al., 1981). However the existence of the high kinetic energy alone does not verify a retroflection. This geographical area of high eddy kinetic values south of Madagascar, which have been calculated from the ships' drift data, show a good correlation with the area suggested by remotely sensed altimetry data (Lutjeharms 2000b; Heywood and Somayajulu, 1997; Quartly et al., 2006). The region of high variability south of Madagascar extends westward along the path taken by eddies that have been observed in the South West Indian Ocean (Gründlingh et al., 1991). However, in an analysis of sea surface temperature data, Quartly and Srokosz (2002b) found that the path taken by warm features shed from the EMC was in a south and then southwest direction. They suggest that the features going west might not be detected because they do not have a big enough anomaly to the background.

Although ship's drift was considered satisfactory in resolving seasonal current patters, both the Hastenrath and Greishar (1991) and Sætre (1985) studies of the ships' drift data did not show any seasonality. This could be due to the fact that they averaged the results over large areas. However Lutjeharms et al. (2000b) in their refined analysis found that there is a suggested seasonal signal in the EMC. The winter and spring seasons were found to have the highest speeds, while summer and autumn had lower speeds. The difference between October and February was more than 30 cm/s. However, Lutjeharms et al. (2000b) caution that the standard deviation of these results is large. The seasonality in the EMC may be related to the seasonality of the South Equatorial Current, which Hastenrath and Greishar (1991) have demonstrated to have the highest speeds in winter. The seasonality of the current may also be related to the local winds and their seasonal intensification and direction change (Lutjeharms et al., 2000b).

With the large ships' drift data set it has been possible to calculate a few characteristics of the surface of the EMC. Some of the characteristics are; speed, size, seasonality and stability of the EMC. Unfortunately, due to the inherent limitations of ships drift, it is not possible to clearly and decisively

show the path of the EMC and possible retroflection. Satellite remote sensing could in principle help in solving this conundrum.

2.2 Remote Sensing

As mentioned previously, satellite data can be used to calculate the movement of the current trajectory. Altimeter data from TOPEX/Poseidon between 1992 and 1998 show there is a region of high variability south of Madagascar at the southern termination of the EMC (Lutjeharms et al., 2000a). Heywood and Somayajulu (1997) have also found this region to exhibit high eddy kinetic energy when they analysed ERS-1 altimetry data from October 1992 to December 1993. They found that this region extended from the EMC towards the Agulhas Current. Quartly et al. (2006) have recently looked at the combined altimetry data of TOPEX/Poseidon and ERS-2 from April 1995 to August 2001. After applying EOF analysis and removing large scale signals they found a band of significantly high variability south and southwest of Madagascar. They suggest that this variability is caused by eddies which arrived from the east along a band at 25°S. Quartly et al. (2006) have also found signals of eddies along the EMC which had joined the current between 22°S to 24°S after arriving from the east. These smaller features in the EMC were seen at times to merge with the larger features that had arrived along 25°S. They have compared their altimetry findings with previously published studies of ocean colour and temperature images which displayed signs of retroflection. These studies show that the signs of retroflection in ocean colour were caused when chlorophyll rich upwelled water was wrapped around the circulation of an anti-cyclonic eddy. These eddies were located east of the current termination, causing an arc of cold chlorophyll rich water which headed towards the east (Quartly et al., 2006; cf Figure 1.4 right hand side panel). The EMC is in fact low in nutrient concentration and therefore was not well resolved in ocean colour. Sea surface temperature is perhaps better suited to delineating the current.

Unfortunately, persistent cloud cover restricts the infrared and visible wavelengths in the region of the EMC for a large proportion of the time, and furthermore, the sea surface temperature ranges in the region are small, and

features often loose their sea surface signal quickly (Quartly et al., 2006) making it difficult to identify the current and its features. Notwithstanding this, Lutjeharms (1988b) has highlighted the circulation pattern of the sea south of Madagascar using infrared images from the satellite NOAA 7. From the images he estimated the width of the surface expression of the EMC to be about 60 km. For the Agulhas Current (which bears many similarities to the EMC) it has been demonstrated that the surface temperature on occasion is a good indicator of the position of the general flow (Lutjeharms, 1988b). A loop of about 200 km diameter, which first turned west, was seen south of the southern most tip of Madagascar by Lutjeharms (1988b). The water then seemed to flow back east into the central Indian Ocean, against the background flow in this region. A similar situation can be seen in Figure 2.3. Harris et al. (1978) have performed a cursory investigation of the EMC using infrared images for the whole Agulhas Current system. They found that the termination first headed poleward past the southern tip of Madagascar and then turned northwest and then finally it headed southwest.

Quartly and Srokosz (2004) have analysed SeaWiFS (Sea-viewing Wide Field-of-view Sensor) data and noted eddies southwest of Madagascar. These cyclonic eddies are formed elsewhere in the Mozambique Channel and then move towards southwest Madagascar. Quartly and Srokosz (2004) have suggested that it is likely that a drifter caught in one of these eddies would give the impression of the EMC rounding the southern tip of Madagascar and heading northwest into the Mozambique Channel. In the same SeaWiFS study they found chlorophyll patterns that represented a retroflection of the EMC. They have also found a number of instances where the SeaWiFS data showed chlorophyll rich water, entrained in the EMC, heading past the southern tip of Madagascar in a west-southwest direction.

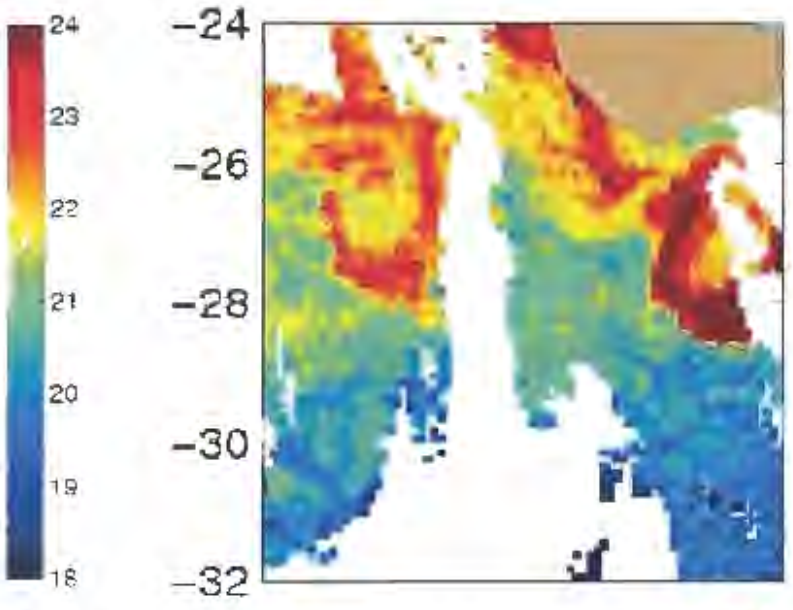

Figure 2.3. Sea surface temperature at the southern tip of Madagascar (from Quartly and Srokosz, 2001). The figure shows a composite, for 25-27 July 1994. A retroflection of the EMC is seen at 28°S. Relatively cooler water can be seen at the south-eastern end of Madagascar.

Quartly and Srokosz (2003) have studied a series of Along Track Scanning Radiometer (ATSR) infrared emissions of the EMC region. They have observed the anti-cyclonic flow along the EMC retroflection loop gradually progressing westwards. A warm ring was visible to the west of the retroflection, and they surmised that it could have been shed from the EMC. They also looked at a series of chlorophyll concentration images from ocean colour sensors for the same region but for a different date. Ocean colour sensors are able to record information from within the upper few metres of the water column rather than just the surface (Ho et al., 2004). These SeaWiFS images show the edge of the current delineated by high chlorophyll concentration and an eddy that had originated from the EMC moving south-westwards.

SeaWiFS images have also shown that the EMC has in general a lower chlorophyll concentration than the surrounding water masses (Quartly and Srokosz, 2002a). This is due to the EMC's origin in the low nutrient waters of the tropical Indian Ocean (Ho et al., 2004). Using this contrast Quartly and Srokosz (2002a) have been able to show that at the south-eastern tip of

Madagascar, the position of the front on the western side of the current is most variable during summer. They have also shown that the core of the current lies closest to the coast in winter (150 km south of the southern tip of Madagascar), but moves further away in summer (as far as 300 km from the coast at the southern tip of Madagascar).

These satellite data give us a strong indication as to what the current may be doing, but in general it is only a reflection of the surface properties. A very informative method of investigating a current is to undertake a research cruise to the region and perform hydrographic measurements.

2.3 Hydrographic Observations

Some of the few hydrographic measurements in the core of the EMC were undertaken as part of a mooring project. From the mooring data Swallow et al. (1988) found that the EMC had no seasonal signal below 150 m. Unfortunately all the moorings were deeper than 150 m so there is no data for the surface waters. The hydrographic sections that were carried out to complement the moorings were also too few and variable to determine a signal in the upper layer.

Geostrophic currents were calculated from the hydrographic profiles that complemented the mooring project in the EMC (Swallow et al., 1988). It was found that there was a weak counter current at 110 to 167 km from the coast at 23°S (Swallow et al., 1988). The maximum surface speed of the EMC was 67 cm/s and this was found at about 40 km from the coast (Figure 7 in Swallow et al., 1988). The total volume flux calculated from the geostrophic currents was 20.6 Sv. The total flow calculated for the moorings was 20.3 Sv (Schott et al., 1988). In a study of a line of stations occupied in 1995 as part of WOCE, Donohue and Toole (2003) have calculated the transport of the EMC to be 21.6 Sv. They found the EMC to be flowing at 80 cm/s close to the sea surface at 25°S. The maximum velocity at the surface of the EMC was calculated to be up to 100 cm/s through a section along 23°S (Lutjeharms et al., 1981). They also calculated the volume transport through this section to be 41 Sv.

Water masses:

Swallow et al. (1988) have found four distinct water masses in the core of the EMC at 23°S. At the surface (approximately 0-100 m with a geostrophic transport of 4.0 Sv) they found a low salinity surface layer. This Tropical Surface Water (TSW) is the result of an excess of precipitation over evaporation (Read and Pollard, 1993) and to the influence of low salinity Indian through flow waters carried westward in the South Equatorial Current (Donahue and Toole, 2003). Beneath the TSW there was a high salinity core of Subtropical Surface Water (STSW), which had an oxygen minimum (approximately 100-400 m with a geostrophic transport of 8.5 Sv). This STSW layer, which was seen to have its core at 150 m in the WOCE line analysis (Donohue and Toole, 2003), was also noted as having high nutrient concentrations. These high nutrient tracers of the STSW are believed to be due to *in situ* bacterial breakdown of organic matter (Donohue and Toole, 2003). In the southwest Indian Ocean STSW is defined as having a salinity greater than 35.5 psu (Gründlingh et al., 1991).

In the deep thermocline (approximately 400-800 m with a geostrophic volume transport of 6.7 Sv) there was South Indian Central Water (SICW) with an oxygen maximum. In this region SICW is recognised by its relatively linear Θ/S relationship between approximately 9°C and 14°C (Gründlingh et al., 1991).

In the deep layer at 23°S (approximately 800-1200 m with a geostrophic volume transport of 2,0 Sv) Swallow et al.(1988) found Antarctic Intermediate Water (AAIW) with a salinity minimum at around 1050 m. In the southwest Indian Ocean AAIW is defined as having a salinity less than 34.6 psu and a temperature range of roughly 4-6°C (Gründlingh et al., 1991). Off Cape Amber, at 12°S, Swallow et al. (1988) found that the minimum salinity Antarctic Intermediate Water had experienced some mixing with Red Sea Intermediate Water (RSIW) of high salinity. There was however no sign of deep mixing with RSIW at 23°S (Swallow et al., 1988). At its origin RSIW has a salinity of about 38 psu, but as it progresses south the core salinity is

reduced due to interaction with other water masses. In the region between 10°S and 30°S in the Western Indian Ocean, AAIW and RSIW experience intermingling and mixing. By the time the RSIW has reached the Mozambique Channel the salinity is roughly 34.7 psu (Gründlingh, 1985). At greater depths Donahue and Toole (2003) found Circumpolar Deep Water (CDW) hugging the coast of Madagascar at 25°S. Further offshore they found NIDW, indicated by its silicate maximum, centred at a density of 28.1 $kg.m^{-3}$

The portrayal of the EMC rounding the southern tip of Madagascar was questioned by Lutjeharms (1976). He found that the flow in this region was to the east near the surface, while the flow at deeper levels was to the west. The data used for his analysis came from selected hydrographic stations occupied during the Northeast Monsoon season. The analysis was restricted to data from the Northeast Monsoon season because it was decided that during this period the currents might be most strongly developed (Lutjeharms, 1976).

Directly south of Madagascar, the water movement at the surface as determined by an XBT line, was found to be to the east (Lutjeharms et al., 1981). Since there was no evidence of the EMC rounding the southern tip of Madagascar and continuing westward this finding supports the concept of a sharp retroflection of the current when it overshoots the southern end of Madagascar (Lutjeharms et al., 2000b). It would therefore seem that the EMC is not a direct or permanent source of the Agulhas Current.

The question of whether the EMC is a source of the Agulhas Current was also investigated using chemical tracers. It has been shown that the waters of the Agulhas Current consist of two distinct portions near Durban (Harris, 1972; Gordon, 1986). On the coastal side of the current Gordon (1986) has found a salinity profile that was almost identical to that found in the Mozambique Channel, while further offshore in the current the profile matched that of the EMC. Harris (1972) has found low oxygen water close to the coast. This water is derived from the Mozambique Channel and not from the Indian Ocean east of Madagascar. The outer portion had water with high oxygen concentrations,

which could have been supplied by two sources, via the EMC and through recirculation of the Agulhas Return Current (Harris, 1972).

DiMarco et al. (2002), in a study of WOCE hydrographic data, have found high oxygen concentrations along a zonal line (WHP line I4) from the southern tip of Madagascar to the east coast of Africa. They stated that this high oxygen water was possibly due to contributions from water transported in the EMC, which then rounded the southern tip of Madagascar. However, Lutjeharms (1976) has shown that during the months November to April both sides of the Mozambique Channel above 120 m had water which clearly came from north and not from east of Madagascar.

On the eastern side of the southern tip of Madagascar, Donohue and Toole (2003) have found strong flow offshore heading to the northeast. This flow at 49°E, which was seen in WOCE Hydrographic data, was not believed to be a retroflection but rather a cyclonic eddy (Donohue and Toole, 2003). The support for this flow not being a retroflection of the EMC was that the low oxygen core in the STSW that was seen in the EMC was not seen in this offshore northward flow. High salinity levels, which were found in the EMC, were also missing from the northeast flow. Lowered Acoustic Current Profiler Data also showed that the EMC extended to about 1000 m, while the northward flow was only about 800 m deep (figure 10 in Donohue and Toole, 2003). They believed that the northward flow was caused by a cyclonic eddy to the east of the EMC, which was evident in sea level anomaly data.

Unfortunately, a full suite of hydrographic measurements at appropriately placed stations needed to answer the retroflection question have not been performed yet. Apart from the retroflection conundrum suffering from a lack of hydrographic data, there are other interesting phenomena that are still not completely understood and quantified. Such a phenomenon is the proposed upwelling, which has been seen at the southeast of Madagascar.

Upwelling

Upwelling inshore of the EMC at the southeastern tip of Madagascar was first observed using satellite remote sensing (Lutjeharms and Machu, 2000; DiMarco et al., 2000). The signs of the upwelling were seen in ocean colour data (Figure 2.4) and sea surface temperature data. However, due to high atmosphere to ocean heat fluxes, SST differences between cold upwelled water and ambient water are not always large enough in this region to be sensed by infra-red sensors (Ho et al., 2004). The upwelling was most prominent at about 26°S. At this point the shelf widens abruptly along the course of the EMC and the continental slope becomes less steep (Lutjeharms and Machu, 2000). It is believed that this change in the shelf configuration along the course of the EMC induces upwelling (Lutjeharms and Machu, 2000). The upwelling cell had an area of about 2° longitude by 1° latitude and its surface water was about 3-5°C colder than the surrounding water during February and March 2000 (DiMarco et al., 2000). Another possible cause for the cell is upwelling favourable winds (DiMarco et al., 2000).

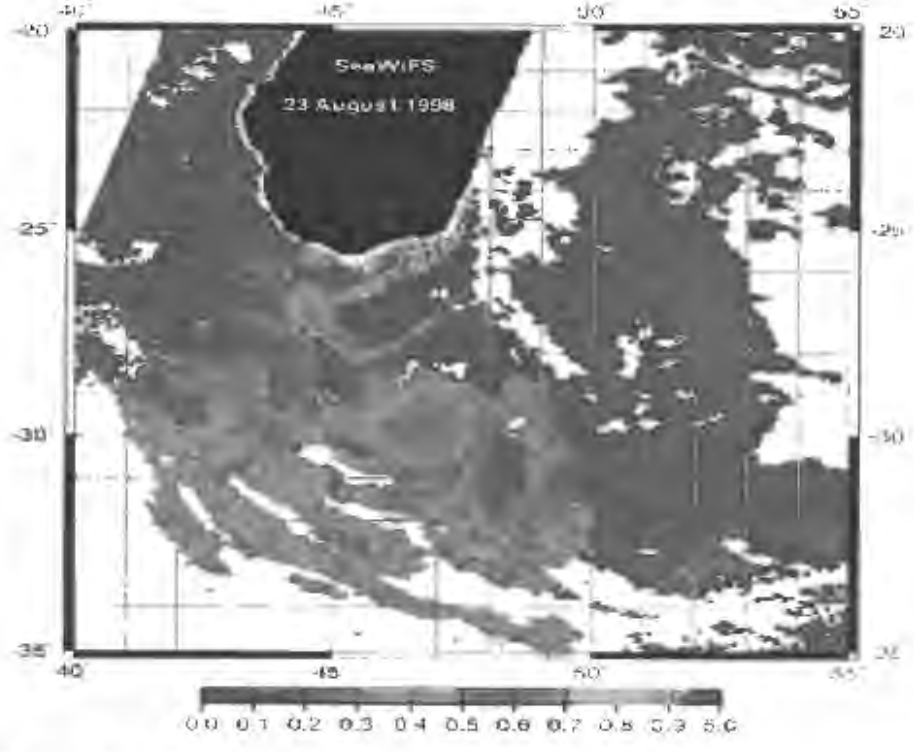

Figure 2.4. *Chlorophyll-a distribution at the southern tip of Madagascar (from Lutjeharms and Machu, 2000). The figure shows the situation on 23 August 1998. Upwelling of nutrient rich waters southeast of Madagascar would have caused the increased concentration of chlorophyll-a seen here.*

In a review of the use of various satellite products Quartly and Srokosz (2001) also noted the upwelling. They have found that ATSR (Along Track Scanning Radiometer) data from the ERS satellites showed surface waters in the upwelling cell to be about 21°C in July with the ambient water being about 2°C warmer. They also found the region to have heightened chlorophyll content in their analysis of SeaWiFS data. Lutjeharms and Machu (2000) have looked at all cloud free SeaWiFS ocean colour images of the upwelling region for 1998. Of the 42% of the days of the year that had useful images, 94% showed clear signs of upwelling (Lutjeharms and Machu, 2000). Ho et al. (2004) have studied the SeaWiFS data from September 1997 to November 2001. They found that there is a peak in the upwelling signal in winter of each year except for 1999 and in summer of each year except 2001.

There is a need for *in situ* observations of this upwelling cell to validate the existence, and quantify the upwelling cell. A hydrographic cruise to the region would definitely be a step in the right direction. Unfortunately a single cruise cannot tell us about the seasonality of the current, or if the situation that was measured was a true reflection of the current. If a current has various flow paths it will be necessary to return to measure all of these. This would be a very costly and difficult exercise. A relatively cheap method of getting *in situ* flow data is to use drifting buoys. These can be released into the current by volunteer observation ships so there is no need for a dedicated cruise to the region.

2.4 Drifters

Since the 1970's a number of satellite tracked drifting buoys have passed through the EMC and the surrounding region. Lutjeharms, Bang and Duncan were the first to carry out an analysis of a collection of drifter data in a paper in 1981. Three of the buoys in this study moved to the eastern coast of Madagascar. Here at the coast they headed south following the continental shelf break. The temperature reported from the buoys with working sensors remained relatively constant for this leg of their tracks (Lutjeharms et al., 1981). This movement down the coast suggests that they were being

entrained by the EMC. At the southern tip of Madagascar, where one of the buoys drifted off the continental shelf, the reported water temperature dropped by 3°C. The drift speeds of the buoy also decreased at this point as it was probably out of the current. When another of the buoys left the continental shelf break the temperature also dropped, and as this buoy passed the southern tip of Madagascar the speed first picked up and then dropped off again. A buoy that approached the southern tip of Madagascar from the southeast also showed temperature and velocity change once it reached the southern tip of Madagascar. All the drifters moved in cyclonic and anti-cyclonic motions south of Madagascar, this behaviour suggests that the buoys were not in the EMC at this point, and that the circulation is highly variable in this region. Lutjeharms (1988a) has suggested that the eddy-scale motions and general wandering of the drifters at the southern tip of Madagascar indicates that the drifters were imbedded in eddies or filament offshoots of the EMC.

Tomczak and Godfrey (2003) have reviewed a number of satellite-tracked buoys in their description of the East Madagascar Current extension. They found that the current has three flow patterns (Figure 2.5). They described a flow past the southern tip of Madagascar and then north into the Mozambique basin. This flow then moves west to the coast of Africa before joining up with the Agulhas Current. The next flow they described was directly west from the southern tip of Madagascar to the coast of Africa to join the Agulhas Current. The last flow pattern they described was a retroflection directly south of Madagascar. Tomczak and Godfrey (2003) have noted that drifting buoys rarely followed the retroflection, but it was occasionally seen in satellite images. Looking at a set of 15 drifters that passed into the EMC, Quartly et al. (2006) have observed only two drifters loop back to head in a north-easterly direction. Three drifters left the region of the EMC to the east at 25°S and another three left the region to the southeast.

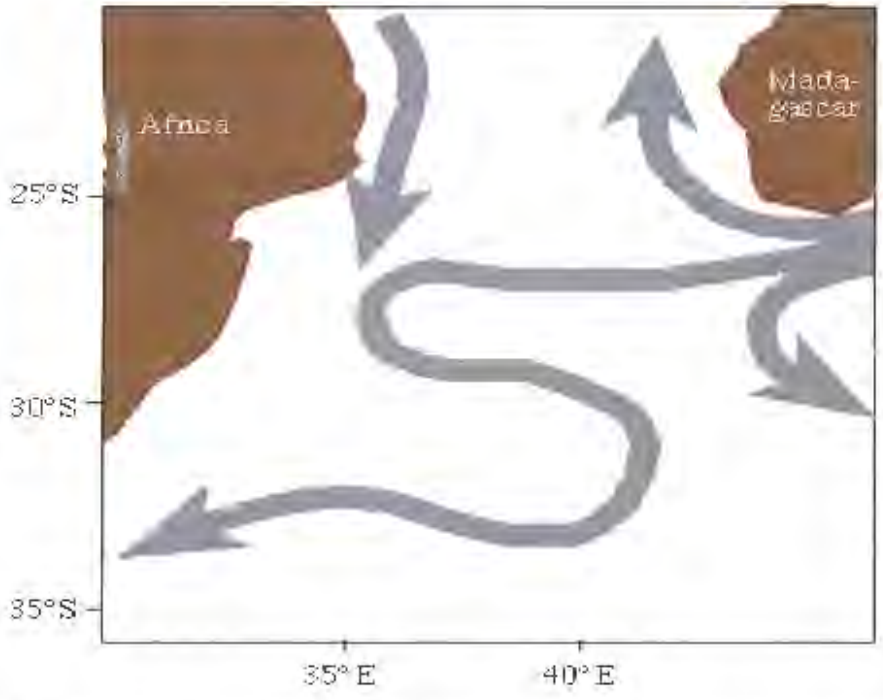

Figure 2.5. *Three main flow patterns of drifter buoys past the southern tip of Madagascar (from Tomczak and Godfrey, 2003).*

Chapman et al. (2003) have reported on profiling floats around Madagascar. Their data show that a float did follow a path that retroflected south of Madagascar. Other interesting findings to come out of the profiling float data is the first evidence of bifurcation of the South Equatorial Current on reaching the coast of Madagascar at intermediate depths. They also noted that there was no evidence for Red Sea Intermediate Water to the east of Madagascar from their data (Chapman et al., 2003).

Quartly et al. (2006) do not believe that the EMC flows persistently north into the Mozambique Channel, as has been suggested by Tomczak and Godfrey (2003). Quartly et al. (2006) have shown that the drifters arriving in the Mozambique Channel from the EMC did not stay close to the coast, but moved in paths consistent with them being caught in cyclonic eddies which are found here. Quartly et al. (2006) have also questioned the concept of the EMC heading due west from the south of Madagascar to join the Agulhas Current as there is an abundance of eddies in this area and there is a lack of a steady current.

Drifting buoys are very helpful in giving us *in situ* measurements of the current, but they are not the final word on current flow. Drifters can often be ejected from a current especially if a current branches or has rings that are pinched off. Another informative method of looking at a current that does not require a research cruise is to use computer models.

2.5 Models

Numerical computer models can give us information about the flow and water properties at various depths, depending on how sophisticated the model is. In an analysis of a simple reduced gravity model Schott et al. (1988) have found that there was a transport of 16.5 Sv at 23°S with a seasonal variation of 1.5 Sv. This was regarded to be in fairly good agreement with their mooring data. The mooring data had returned a transport of 20.3 Sv ± 6.6 Sv with no obvious seasonal variation (Schott et al., 1988). The authors have mentioned however that the model might have been in good agreement with the *in situ* data for the wrong reasons. The model did not include barotropic Rossby waves, which might have had an effect on the annual changes.

Matano et al. (2002) have used a more sophisticated model to analyse the flow in the Indian Ocean. The model showed that the EMC south of Madagascar had a mean flow of 30 Sv ± 5 Sv heading west. This was regarded as close to the flow calculated from *in situ* measurements. They noted that there was a small seasonal signal with a maximum flow in March and April. The minimum in the flow was during December and January (Matano et al., 2002). This seasonal signal was compared with the seasonality north of Madagascar, in the Mozambique Channel and in the Agulhas Current. It was found that the EMC's seasonal signal was significantly smaller and out of phase with the other three (Matano et al., 2002).

The EMC was found to feed into the Agulhas Current at 27°S, mostly by anti-cyclonic eddies. This was shown in an eddy-permitting model used by Biastoch and Krauß (1999). These eddy features were also seen when looking at the mean eddy kinetic energy calculated from the model. There was

a maximum along the southeast coast of Madagascar where the eddies were seen to form. The model also showed that a mean of 20 Sv flows past 23°S in the EMC. The model was also used to calculate the sea surface height. This result showed that there was a definite increase in height along the southeast coast. However this was not seen in the surface height as detected by satellite (Biastoch and Krauß, 1999). It would seem that the model produces eddies which do not appear in the real world.

Through the combination of hydographic sections in an inverse box model Sloyan and Rintoul (2001) were able to compute the circulation of the waters in the Southern Ocean. Their model showed 28.1 Sv moving south in the EMC at 18°S.

Quartly et al. (2006) have released virtual drifters into the EMC using a model called OCCAM. They have found that a few drifters were advected to the northeast out of the EMC. This model does not have a retroflection at the EMC, only anti-cyclonic eddies heading south along the course of the EMC. Quartly et al. (2006) have explained the signs of a retroflection in remotely sensed chlorophyll and SST to this eddy-eddy interaction.

2.6 Summary

From previous research we have gained valuable insight on the EMC. Ships' drift data has shown the current to be directionally stable. The use of ships' drift data has also shown us that the current is about 200 km wide. Unfortunately the various studies of the ships' drift data set have given highly variable speed results, with calculations ranging from 25 to 150 m/s.

Possible upwelling inshore of the EMC was first identified by satellite remote sensing. The factors forcing this upwelling remain unclear. A hydrographic survey of the proposed upwelling site may verify the existence of this cell.

An area of high SSH variability at the termination of the EMC has been made apparent through the use of remote sensing. This area of high variability is probably caused by eddies which have arrived there from the east. The width

of the surface expression of the EMC was calculated from satellite SST to be 60 km. Remotely sensed SST and chlorophyll data also give possible evidence of a retroflection of the EMC. Satellite data have furthermore shown that eddies originating from the current move in a SW direction. Satellite data have made evident lower chlorophyll concentration of the current compared to the surrounding waters.

Hydrographic observations were the first to highlight the possibility of a retroflection of the EMC south of Madagascar. The hydrographic studies have shown that there is no seasonal signal in the EMC. The maximum speed of the current was found to be between 67 cm/s and 100 cm/s. The total flow has been calculated to range between 21 Sv to 41 Sv. The current was found to have TSW, STSW, SICW and AAIW but no Red Sea Intermediate Water.

Drifters have shown that there are three possible flow paths south of Madagascar: the rarely followed path of retroflection; a path past the south of Madagascar and then north into the Mozambique channel, and a path west to join the Agulhas Current. However, drifters that have followed erratic paths through the region south of Madagascar have called these set pathways into question.

Models have been shown to be very useful as they are unconstrained by ship logistics and give relatively inexpensive results, but these results can not always be verified. The models have given conflicting results for transport and seasonality and these need to be verified. None of the models have shown a retroflection, but rather eddies at the termination.

As can be seen, there are questions that have not been answered or not conclusively answered. The most topical question is probably the fate of the EMC termination and the possible existence of a retroflection of the EMC at the southern tip of Madagascar. Linked to this question is the contribution of the EMC to the Agulhas Current. The upwelling that was seen in satellite data also needs to be explored further. These questions will be expanded on in the next section.

3. What is unknown about the East Madagascar Current termination?

From the literature review it is clear that there are substantial gaps in our knowledge of the southern termination of the East Madagascar Current (EMC). These gaps are centred on the fact that no dedicated cruises have been undertaken to study this region. The three main questions that have arisen from the literature study and will be addressed here are: What are the main water masses at the southern termination of the EMC; what is the probable trajectory of the EMC termination; and does upwelling exist inshore of the southern termination of the EMC? These main questions will be discussed in this chapter.

3.1 What are the main water masses at the southern termination of the EMC?

Although there have been cruises in the broader region of the EMC, they have been inappropriate to properly describe the hydrology of the southern termination of the EMC or the water masses involved.

The research cruises on the research vessel Marion Dufresne in 1984, 1985 and 1986 were possibly the best attempts at improving the knowledge of the hydrography of the southern termination of the EMC. The hydrographic measurements were made using eXpandable Bathy Thermograph (XBT's) and Conductivity Temperature Depth (CTD) systems. A second aspect of the cruise was the mooring of current meters. The hydrographic stations were limited to an area around the current meter moorings at 23°S.

Based on these cruises Swallow et al. (1988) have found four water masses: 0-100 m contained low salinity surface water, 100-400 m had high salinity, low oxygen Subtropical Surface Water. Between 400-800 m South Indian Central Water was found with an oxygen maximum. Between 800-1200 m was Antarctic Intermediate Water. In a hydrographic section at 12°S the Antarctic Intermediate Water was seen to have experienced some mixing with Red Sea Intermediate Water. This deep mixing was not detected in the section at 23°S, and this could be because the water column was not measured deeper than

1500 m. North Indian Deep Water, North Atlantic Deep Water and Circumpolar Deep Water have also been found in deeper waters adjacent to the EMC (Donohue and Toole, 2003). Profiling floats, which have passed the region, have also offered the opportunity to investigate the water masses. Chapman et al. (2003) have reported on profiling float data. In these data they also did not find any evidence of Red Sea Intermediate Water to the east of Madagascar.

These profiling floats were unfortunately parked at a depth of 900 m so they are limited in what they can establish. If the measurements could go down to the bottom this would highlight features that were previously unknown. The understanding of the hydrography of the southern termination of the EMC would benefit from a group of stations that are not limited in their distribution by any other scientific research.

3.2 What is the probable trajectory of the termination of EMC?

The exact details of the EMC vary for the different reports on the current. One of the main variations is in the description of the fate of the EMC. What happens to the current once it passes the southern tip of Madagascar may influence the Agulhas Current.

The first attempts at determining if the EMC flows towards the Agulhas Current were made using the ships' drift data set (Michaelis, 1923; Paech, 1926). From these early studies it was deduced that the EMC flowed directly towards the Agulhas Current and was a permanent source of the Agulhas Current. Ships' drift is not a very accurate means of determining a current flow. Ships' drift can only give an indication of the surface layer, and even this surface layer portrayal is not very accurate.

Lutjeharms (1976) has investigated the data from a limited set of *in situ* stations in the region. He found that the surface waters were retroflecting and flowing to the east while the deeper waters flowed west. In 1981 Lutjeharms et al. reported on an XBT line that headed southwest past the southern tip of Madagascar. Here they found that the surface movement was to the east,

while there was a deeper component to the west. They proposed that the current termination had an obvious retroflection that cast off eddies that moved west towards the Agulhas Current. In the same paper the XBT findings were corroborated by drifter data. Further evidence for the retroflection of the current has come from satellite data. Lutjeharms (1988b) showed a satellite picture of sea surface temperature in which the current was visible. In this picture the current was seen to have a marked eastward retroflection when it passed south of Madagascar. Gründlingh et al. (1989) have also shown a similar representation of a retroflection of the current from a satellite picture. However not all research on the subject agrees.

Research by Harris et al. (1978) on the satellite sea surface temperature images of the region showed a slightly different picture. The water from the EMC was seen to approach the Agulhas Current in a complicated path. First the current was seen to round the southern tip of Madagascar then turn to head south for a while then head northwest into the Mozambique basin before turning towards the Agulhas Current. DiMarco et al (2000) have supported a similar concept with the current flowing past the southern tip of Madagascar into the Mozambique Channel and then onto the Agulhas Current. Their conclusion comes form the fact that they found high concentrations of oxygen in the water on the south-western side of Madagascar, and they believe that this water was possibly from the EMC.

Calculations of the current's path by different researchers using ships' drift data also vary. An atlas by Hastenrath and Greischar (1989) clearly shows the EMC rounding the southern tip of Madagascar for a few months of the year. This agrees with the early results of Michaelis (1923) and Paech (1926). In slight contrast the results from Sætre (1985) show that the ships' drift data set displays a small component of the current heading east. However the greater part of the current was seen to round the southern tip of Madagascar. A reanalysis of the ships' drift data (Lutjeharms et al., 2000b) has shown that there is a high degree of eddy kinetic energy at the termination of the current. The existence and positioning of the eddy kinetic energy is in agreement with

the idea of a retroflection here. Other methods such as drifter tracking have also been used to look at the path of the current.

Drifter data have not given a conclusive depiction of the termination of the EMC. It is clear though from the tracked drifters that the region south of Madagascar is highly variable (Lutjeharms et al., 1981, Quartly et al., 2006). Tomczak and Godfrey (2003) who have analysed drifter data, found three paths for the EMC. They found a direct flow towards the Agulhas Current, a flow past the southern tip of Madagascar then into the Mozambique Channel, and a rare retroflection path. The profiling float report by Chapman et al. (2003) shows a float that did retroflect south of Madagascar.

Quartly et al. (2006) question these three paths. They have analysed the movements of 15 floats in the region and suggest that there is no direct path to the Agulhas Current as this pathway is littered with eddies. They imply that the signs of a retroflection are due to drifters being caught in eddies to the east of the EMC. Furthermore they believe that the signs of a path into the Mozambique Channel are due to drifters getting caught in cyclonic eddies.

Looking at model data we see that the Madagascar Current feeds into the Agulhas Current through anticyclonic eddies which travel along a path at 27°S (Biastoch and Krauß, 1999). The OCCAM model also does not show a retroflection at the EMC termination; only anticyclonic eddies travelling down the current (Quartly et al., 2006).

There is obviously no certainty in the description of the path of the termination of the EMC. Even when the same ships' drift data set is used a different representation of the current can emerge depending on the analysis method employed. Drifter data is not conclusive either so there is a need to clarify this picture.

3.3 Does upwelling exist inshore of the EMC termination?

An indication of the presence of an upwelling cell was first identified in 2000 by Lutjeharms and Machu (2000). By studying remotely sensed sea surface temperature in the region they described a patch of water at 25°S that was relatively cold. They also noted that in the remotely sensed chlorophyll data there were high concentrations of chlorophyll at this proposed upwelling site. These findings of lower temperature were independently supported in a paper by DiMarco et al. (2000), who used sea surface temperature remotely sensed by satellite from different dates and saw indications of the same upwelling cell. Lutjeharms and Machu's findings of the high chlorophyll concentrations were subsequently confirmed by Quartly and Srokosz (2001). Although numerous researchers have identified the upwelling cell by using remotely sensed data, there has to date been no *in situ* verification of this phenomenon.

The causes of the upwelling cell have also been difficult to detect. Lutjeharms and Machu (2000) have suggested that the forcing is probably due to current and bathymetric controls, similar to the upwelling cells seen inshore of the Agulhas Current. DiMarco et al. (2000) have surmised that it was most probably due to a combination of wind forcing and interaction between the EMC and the continental shelf slope. However, Lutjeharms and Machu (2000) have claimed that it was not necessarily linked to the wind. The forcing mechanism for the proposed upwelling cell south of Madagascar therefore needs to be clarified.

The only way to possibly get any closer to understanding this remotely sensed upwelling cell is to go to the site and perform *in situ* measurements.

These questions on the termination of the EMC as it passes the southern tip of Madagascar are to be addressed. For this the appropriate data and methods are required.

4. Data and methods

In order to address the lack of clarity surrounding the sources of the Agulhas Current a project called the Agulhas Current Sources Experiment (ACSEX) was initiated. ACSEX I & III were cruises to assess the nature of the Mozambique Current (Lutjeharms et al., 2000a; de Ruijter et al., 2006). The ACSEX I cruise has given a dramatically different picture of the situation by showing a train of eddies moving through the Channel instead of a continuous current (de Ruijter et al., 2002).

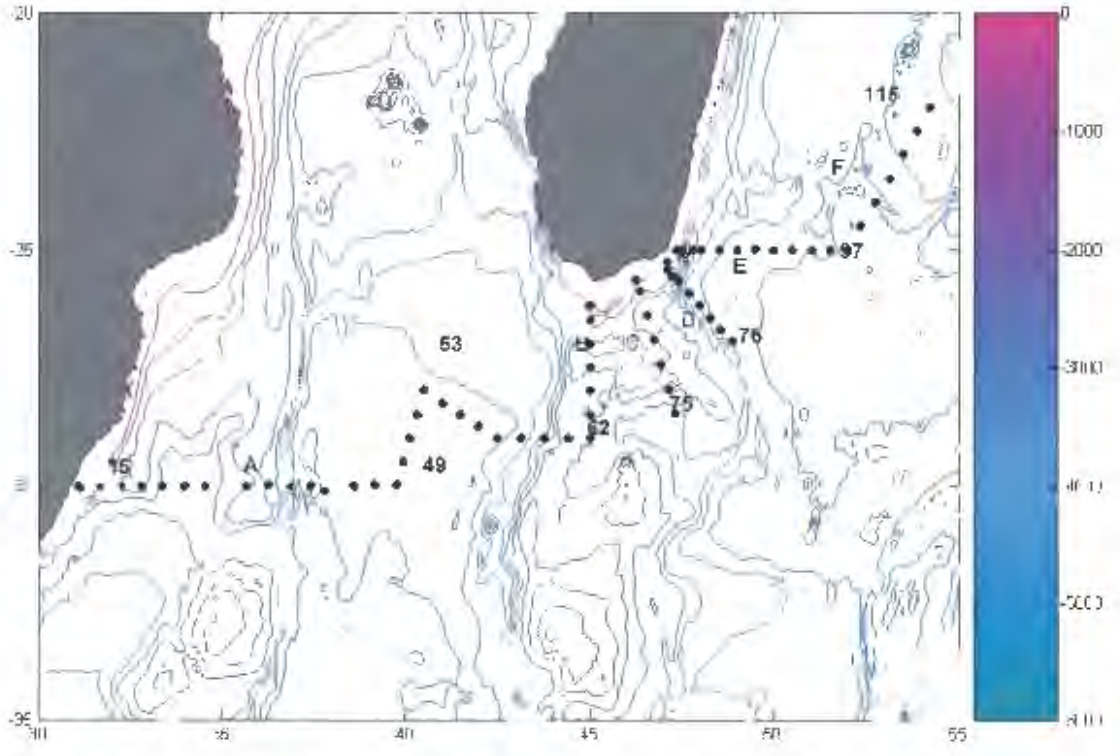

Figure 4.1. Distribution of CTD stations during ACSEX II. Contours show bathymetry in meters as per the colour bar.

ACSEX II in March 2001 was the first cruise devoted to addressing the lack of hydrographic data for the termination of the EMC (Figure 4.1). The cruise sections radiated from the south-eastern tip of Madagascar in such a way that they might intersect aspects of the EMC termination. The west-east section (E) was positioned furthest north in order to intersect the EMC before it

entered the termination region. The sections C and D were positioned to intersect a retroflection if one was present, and section B was placed to measure what was leaving the retroflection region. This research was undertaken by the Netherlands Institute of Sea Research (NIOZ), IMAU of Utrecht University, the Royal Dutch Meteorological Institute (KNMI), as well as the Department of Oceanography at the University of Cape Town.

4.1 Hydrographic data

During the ACSEX II cruise on the RV Pelagia, hydrographic data were collected using the rosette sampler/CTD array. The rosette sampler was made up of a sturdy stainless steel frame on which 24 NOEX bottles were mounted. Set in the middle of the frame was a Seabird Conductivity Temperature Depth system (CTD), which measures conductivity in the water in order to calculate the salinity. The CTD also houses a temperature sensor, and a pressure sensor in order to calculate depth. The readings from the CTD were relayed back to the deck unit; and commands sent to the sampler through a coaxial cable. The measurements were relayed and recorded at a frequency of 24 data cycles per second (van Aken, 2001). Ideally the temperature sensor has an accuracy of 0,001°C, the conductivity sensor an accuracy of 0.003 practical salinity units (psu), and the pressure sensor is accurate to 0.015% of the pressure (http://www.seabird.com). A continual real time graphical display of the measurements from the CTD was given on a PC, which was connected to the deck unit. The PC connected to the deck unit was also used to give commands such as bottle closure.

In order to check and calibrate the pressure sensor three electronic reversing pressure sensors were fitted to the rosette sampler. These were made by Sensoren Instrumente Systeme GmbH in Germany and give a digital display of the mean value of a burst of 16 individual readings that are taken at the time of triggering. A standard deviation for the readings is also displayed (http://www.sis-germany.com). The three electronic pressure sensors were calibrated using the national Dutch pressure standard (van Aken, 2001).

A high precision thermometer (Seabird SBE 35) was mounted on the frame. This laboratory standards thermometer records the temperature at the time of bottle closure. These temperature readings were then used as the reference temperatures to calibrate the CTD's temperature sensor.

The rosette sampler had a Chelsea Technologies fluorometer mounted to it. The fluorometer measures chlorophyll and particle concentration through optical backscatter. On the side of the rosette sampler was a Lowered Acoustic Doppler Current Profiler (LADCP). The two synchronised RD Instruments LADCP's were used to measure current direction and velocity. One of the instruments pointed upward, the other down. The data from the memory of the instruments were downloaded onto a PC at the end of every cast. The raw data were then processed using a MATLAB script developed at NIOZ (van Aken, 2001).

Technicap made the 10 l NOEX bottles on the rosette sampler in co-operation with NIOZ. These bottles had a polypropylene and polyethylene terephthalate polyester body, with Teflon taps, making them trace metal free. The entire closing mechanism for the NOEX bottles on the rosette sampler was developed and built at NIOZ. The lids of the bottles were closed using *in situ* water pressure. The valves, which distributed the water pressure to the required bottle, were controlled by a stepping motor, which in turn was triggered as required using the deck unit. (http://www.nioz.nl/en/facilities/-dmg/niop/themes/theme-d/thmdspre.htm).

The CTD-rosette frame was weighted in order to keep the frame stable in the water while it was lowered at a speed of between 1 and 1.5 m/s. Measurements during the down-cast went down to within 4 m of the bottom, until the bottom switch indicated the proximity of the bottom. During the up-cast water samples where taken at prescribed depths. The CTD winch was stopped while bottles were being closed. After each cast the CTD/rosette frame was placed on deck. Subsequently water samples were drawn and the readings of the electronic reversing pressure sensors were recorded.

Water from the NOEX bottles was first subsampled for oxygen analysis in 100-130 ml glass bottles. A piece of Tygon tube was attached to the outlet tap of the NOEX bottle to allow the water to enter the sample bottle with minimum air contact and turbidity. The sample was allowed to overflow to 3 times its volume in order to flush the sample bottle. Care was taken not to introduce air into the sample. Once the samples were collected the oxygen in the samples was chemically fixed and the bottles capped. The basic Winkler (Grasshoff et al., 1983) method was used to fix the dissolved oxygen and liberate it as iodine. The NIOZ method however differs from the standard method in that the concentration of the iodine is measured using a spectrophotometer and not through titration. At the time of the cruise an automated system was being developed for the measurement of dissolved oxygen.

Polyethylene bottles of about 100 ml each were used to collect subsamples for the nutrient analysis. The bottles were rinsed 3 times and care was taken not to contaminate the samples. The samples were analysed for the concentration of the following nutrients: silicate, phosphate, nitrate and nitrite (van Aken, 2001). A Technicon TRAACS autoanalyser was used to colourmetricly measure the nutrients using standard chemistries (Grassoff et al., 1983).

Subsamples for the analysis of salinity were taken from water collected below 2000 m. The samples were drawn into 250 ml glass bottles that were rinsed out 3 times. The bottles were tightly closed with a plastic stopper as well as a screw lid. The salinity of the samples was determined using a Guildline Autosal 8400b salinometer (van Aken, 2001). The results from this analysis were used to calibrate the CTD.

The graphical representations of the temperature/salinity, nutrient/salinity and oxygen/salinity plots in this study were produced using Ocean Data View. This computer program for the graphical display of oceanographic data has been developed by Reiner Schlitzer (Schlitzer, 2006). The remainder of the plots in this study were produced using Matlab.

The large calculations in the study such as geostrophic currents were computed with the aid of Matlab. The deepest value was used as the reference level for calculating the geostrophic flow. A Matlab script developed by Phil Morgan (http://www.marine.csiro.au/~morgan/seawater) was used for the geostrophic calculations.

Four Argos surface drifters were deployed close to Madagascar during the cruise (Figure 4.2). These drifters are designed to measure the lagrangian current. The drifters, which can be deployed while the ship is steaming, consist of a buoy with a reinforced tether to a holey sock drogue. The holey sock, which is a cylinder of 1 meter by 7 meters, hangs in the water column at about 15 m. The buoy houses a satellite reporting aerial, controlling and recording device and enough battery power to run the system for over a year. There is a thermometer with a 0.1°C accuracy, attached to the lower part of the buoy. The temperature data gets reported to satellites in orbit around the earth. The satellites then transmit the data to the satellite control centre where the position of the drifter is triangulated and the data are made available through the Argos service (http://www.argosinc.com).

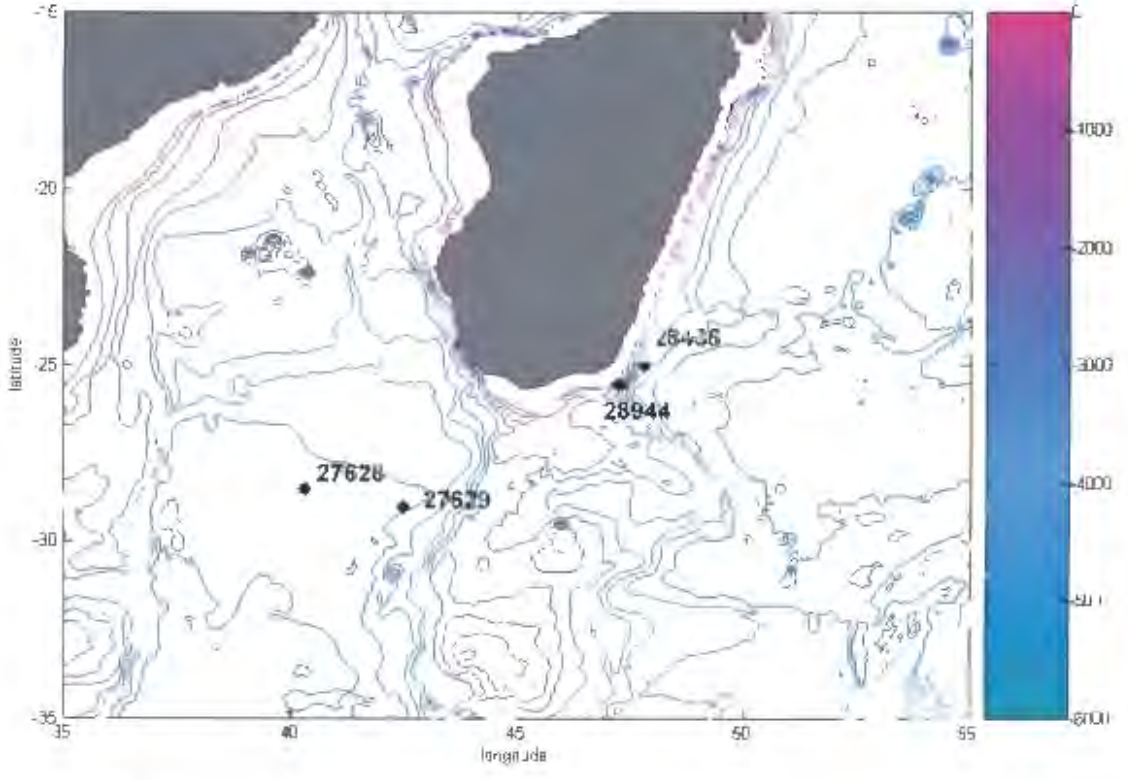

Figure 4.2. Deployment sites of Argos surface drifters during ACSEX II.

All of these hydrographic methods are very useful and relatively accurate. However, exclusively using these methods to understand the current only gives a snapshot view. To aid in an understanding of where the snapshot fits into the longer time scale we can use remote sensing.

4.2 Remotely sensed measurements

Sea Level Anomaly (SLA) satellite data are useful in remotely determining changes in the height of the sea surface from the mean. These changes in the surface are caused by phenomena such as waves, tides, currents and eddies. The data are retrieved from satellites that have radar altimeters on board. The radar altimeter works by transmitting an electromagnetic signal to the sea surface and then timing how long it takes for the echo to return. This measurement is performed many times a second and then averaged per second. These data are then downloaded from the satellite for processing.

Processing involves correcting the time taken for the electromagnetic signal to pass through the atmosphere. Water vapour and the ionosphere slow the signal down, so the known state of the atmosphere through which the signal travelled is used to correct the travel time (CLS, 2006). The signal travel times also have to be corrected for any changes in the height of the satellite. The ocean tides then have to be removed from the sea surface height measurements, and waves can also be removed (http://www-7320.nrlssc.navy.mil/altimetry/proc.html). The mean sea surface height for a particular point is then subtracted from the altimeter measurement for that point in order to get the SLA. The mean sea surface height for the TOPEX/Poseidon altimeter has been calculated from January 1993 to December 1995 (CLS, 2006). For the ERS-2 altimeter the mean is calculated from ERS-1 for a 3 year mean compatible with TOPEX/Poseidon (Aviso, 1998). The altimeter products were produced by SSALTO/DUACS (Data Unification and Altimeter Combination System) and distributed by AVISO with support from CNES. The data are merged TOPEX/Poseidon and ERS-1/2 satellite data. The resolution of the data is 1/3°.

Remotely sensed sea surface temperature (SST) is useful in detecting surface water that has a contrasting temperature signature to that of its surroundings. This means that cold upwelled water can be identified, or the course of a warm current or eddies as they move through a colder ocean region. Two different SST products have been used in this study. The highest resolution data was obtained from the Advanced Very High Resolution Radiometer (AVHRR). This sensor carried on the NOAA-15 polar-orbiting satellite records electromagnetic radiation from the sea surface in the 11.5-12.5 μm (mid-infrared range) (http://noaasis.noaa.gov/NOAASIS/-ml/avhrr.html). The raw data are downloaded from the satellite and post processing is applied. The processed data are distributed by the Jet Propulsion Laboratory through the PO.DAAC Ocean ESIP Tool (http://poet.jpl.nasa.gov). The data has a resolution of about 9 km. Unfortunately cloud cover attenuates the transmission of this frequency range. As the region of the EMC is often covered with cloud there are considerable data blanks (addendum Figure A1).

The third product used was from the Tropical Rainfall Measuring Mission (TRMM) which is able to overcome the cloud cover problem. The TRMM Microwave Imager (TMI) measures at a frequency of 10.7 GHz (wavelength of approximately 3 cm). However, the microwave radiometer only has a resolution of 25 km. Close to the land there is interference due to hot thermal emission and side-lobe contamination, therefore data less than 100 km from the coast are excluded. Direct comparison with ocean buoys has shown a root mean square difference of 0.6°C between the buoys and the satellite data (Wentz et al., 2000). Areas of missing data can be caused by rainfall and sunlight reflecting off the sea surface (Ricciardulli and Wentz, 2004). The TMI data are produced by Remote Sensing Systems and sponsored by the NASA Earth Science REASoN DISCOVER Project. Data are available at http://www.remss.com.

Remotely sensed ocean colour can give a representation of the chlorophyll-a in the surface layer of the ocean. The Sea-viewing Wide Field-of-view Sensor (SeaWiFS) project has a satellite-mounted sensor that is able to view the ocean in the visible and near infrared wavelength (412-865 nm)

(http://www.sat.dundee.ac.uk/seawifs.html). Persistent cloud cover in the region of the EMC causes many data blanks. On views with minimal cloud cover the chlorophyll-a data are able to show probable upwelling sites due to increased phytoplankton in the nutrient rich waters. The course of the current can also be identified if phytoplankton rich water is entrained.

Wind data in this study have been obtained from NASAS's Quick Scatteromerter (QuikSCAT) (http://poet.jpl.nasa.gov). This satellite radiometer transmits high frequency microwave radiation towards the ocean surface. The backscatter is then measured by the satellite. The roughness of the sea surface due to wind results in a varying strength of backscatter. The radiometer is able to measure wind speed between 3 and 20 m/s with an accuracy of 2 m/s and at a direction accuracy of 20 degrees. The resolution of the calculated wind vectors is 25 km (http://winds.jpl.nasa.gov/-missions/quikscat/index.cfm).

The methods described are all useful in giving an understanding of the EMC. They will be used in combination to answer the proposed key questions of: what are the main water masses at the southern termination of the EMC; what is the probable trajectory of the termination of the EMC; and does upwelling exist inshore of the EMC termination? The next chapter will present all the results and findings of the investigations using the methods described in this chapter.

5. Water masses of the East Madagascar Current termination

An anticipated application of the ACSEX II data was to clarify the water mass distribution in the area. Evidence has previously been provided that the EMC and adjacent waters consist of Tropical Surface Water (TSW) between 0 and 100 m depth; Subtropical Surface Water (STSW) between 100 and 400 m depth; South Indian Central Water (SICW) between approximately 400 and 800 m and Antarctic Intermediate Water (AAIW) between 800 and 1200 m (Swallow et al., 1988). It was suggested in this study that the AAIW associated with the northern EMC had experienced some mixing with Red Sea Intermediate Water (RSIW) off Cape Amber, at 12°S, but no mixing had taken place at 23°S. In the deep layers adjacent to the EMC, North Indian Deep Water (NIDW), North Atlantic Deep Water (NADW) and Circumpolar Deep Water (CDW) have also been found (Donohue and Toole, 2003).

The ACSEX II cruise surveyed further south than the Swallow et al. (1988) study. The ACSEX II stations also covered a larger geographical portion of the termination of the EMC than the Swallow et al. (1998) and Donahue and Toole (2003) studies. The ACSEX II cruise occupied four CTD station lines which radiated out from the south-eastern tip of Madagascar (Figure 5.1). The most northern section adjacent to Madagascar was zonally along 25°S, and the most westerly section was meridionaly along 45°E. The larger area of coverage in the ACSEX II cruise and the repeated crossing of the EMC were undertaken in order to resolve the characteristics of the southern EMC more thoroughly than had previous been possible (Donohue and Toole, 2003; Swallow et al., 1988). Although there were problems with the CTD cable on the ACSEX II cruise limiting the maximum cast depth to 2500 m these were deeper than the deep CTD casts of the Swallow et al. (1988) study, which were deployed down to a maximum depth of only 1500 m. The Donohue and Toole (2003) study had CTD casts which were not limited in depth so were deployed down to 10 m from the bottom.

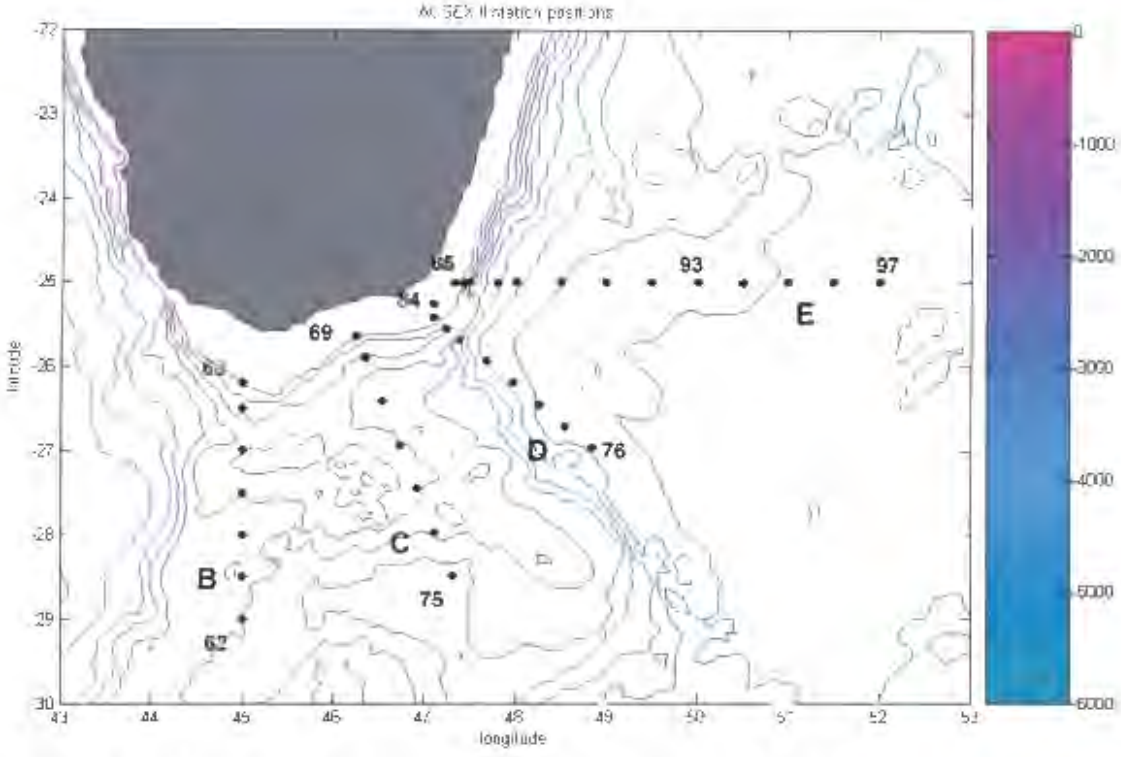

Figure 5.1. ACSEX II station positions southeast of Madagascar. The bathymetry is contoured in 500 m intervals.

To establish the existence of the aforementioned water masses and to determine the occurrence of any other water masses during the ACSEX II cruise, the θ/S relationships (Potential temperature/Salinity) for the cruise lines B, C, D and E have been plotted. Looking at the Θ/S relationships for these sections (Figure 5.2) it is evident that the surface layer consisted of TSW and associated with the TSW there was STSW with a depth down to 350 m during the cruise. The central water was SICW with a depth range of 350 m to 800 m and there was AAIW from about 800 m to 1500 m. The rectangles and ellipses in the figure have been positioned in order to highlight the water masses more clearly. The observations from this largely confirm the results of Swallow et al. (1988). However, in contrast to the previous work there were certainly signs of RSIW south of 23°S during the ACSEX II cruise, as is highlighted in Figure 5.2. This RSIW had a depth range of approximately 800 to 1200 m. As the CTD casts of the ACSEX II cruise went as deep as 2500 m, NIDW was also detected in the lower depths from 1500 m to 2500 m, which confirms the findings of Donohue and Toole (2003).

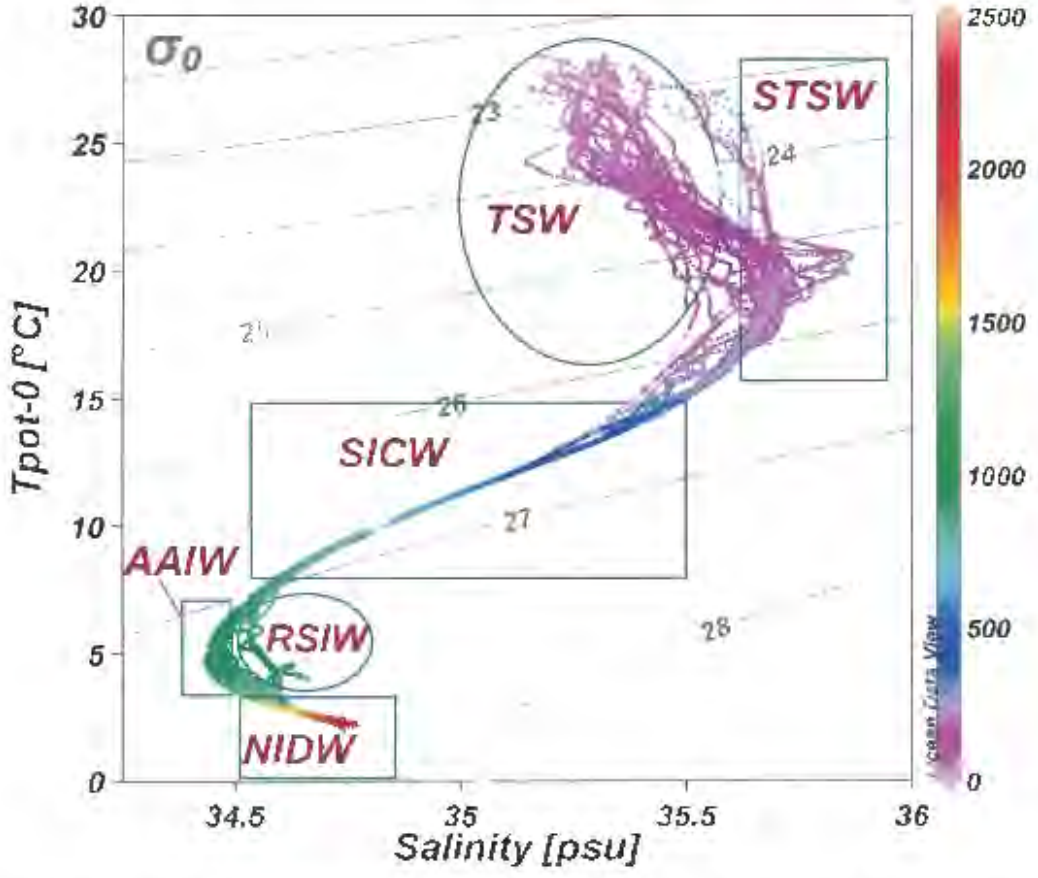

Figure 5.2. Potential temperature/Salinity plot for all ACSEX II stations under investigation (Figure 5.1). Labels show main water masses identified. Colours indicate depths according to the right hand scale.

Looking more closely at the respective water masses we see that the surface water masses during the ACSEX II cruise (Figure 5.3) had a potential temperature range of 25.5-15.75°C. The salinity range was 35.075-35.868 psu and the density range as per σ_t was 22.38-26.23 kg.m^{-3}. Fresher surface waters closer to the Madagascar coastline were observed (highlighted in Figure 5.3). These fresher waters existed to a depth of about 200 m. The more saline waters at 200 m depth that were described by Nauw et al. 2006 as an intra-thermocline eddy are also seen at the salinity range of 35.7-35.868 psu. The World Ocean Circulation Experiment (WOCE) is a source of additional high quality data in the region, although the coverage is very sparse. A section of the WOCE data were used as part of the Donohue and Toole (2003) study.

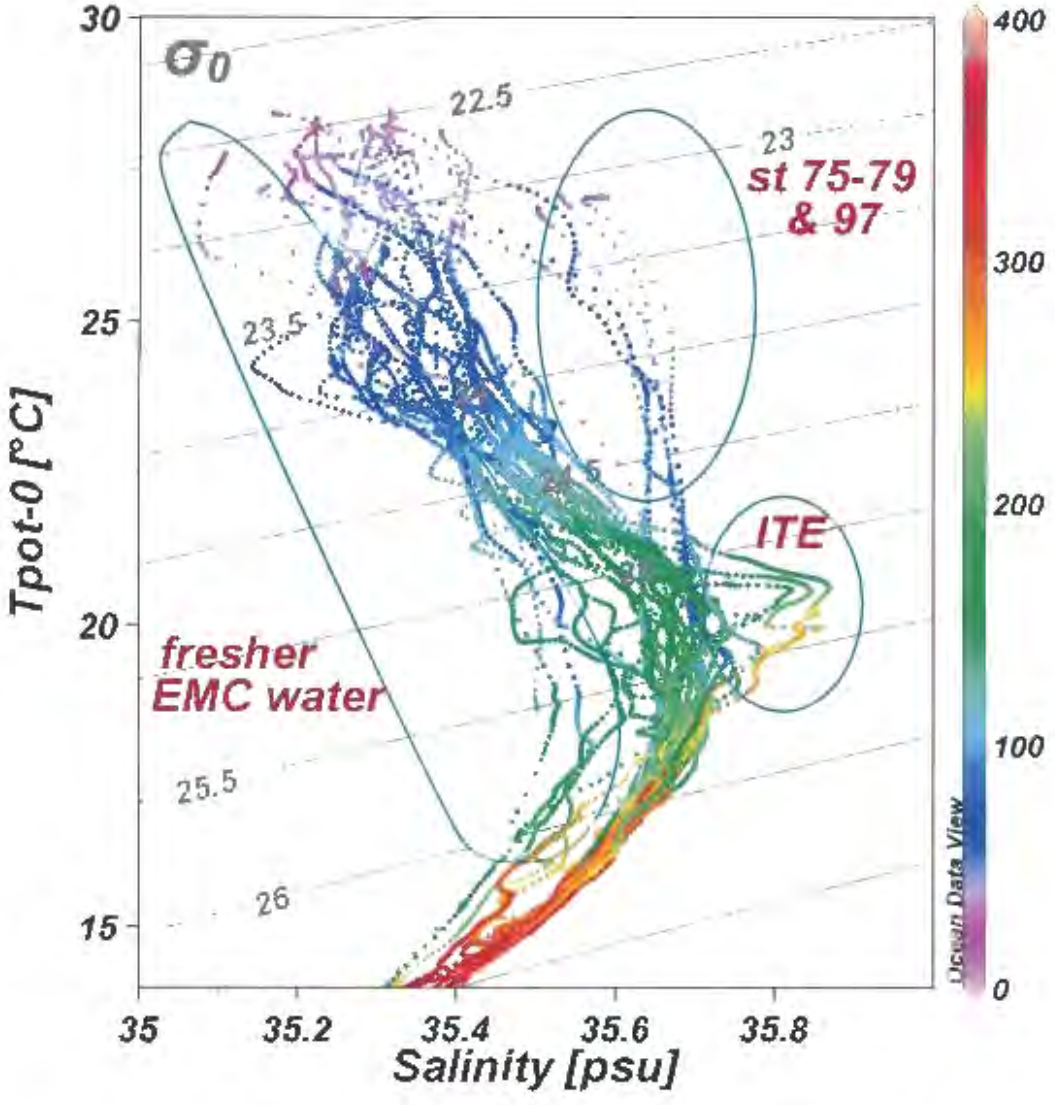

Figure 5.3. Surface water Potential temperature/Salinity plot for all ACSEX II stations under investigation (Figure 5.1). The water associated with the intra-thermocline eddy (ITE) is labelled, as well as the fresher coastal water of the EMC and the more saline eastern water. Colours indicate depths according to the right hand scale.

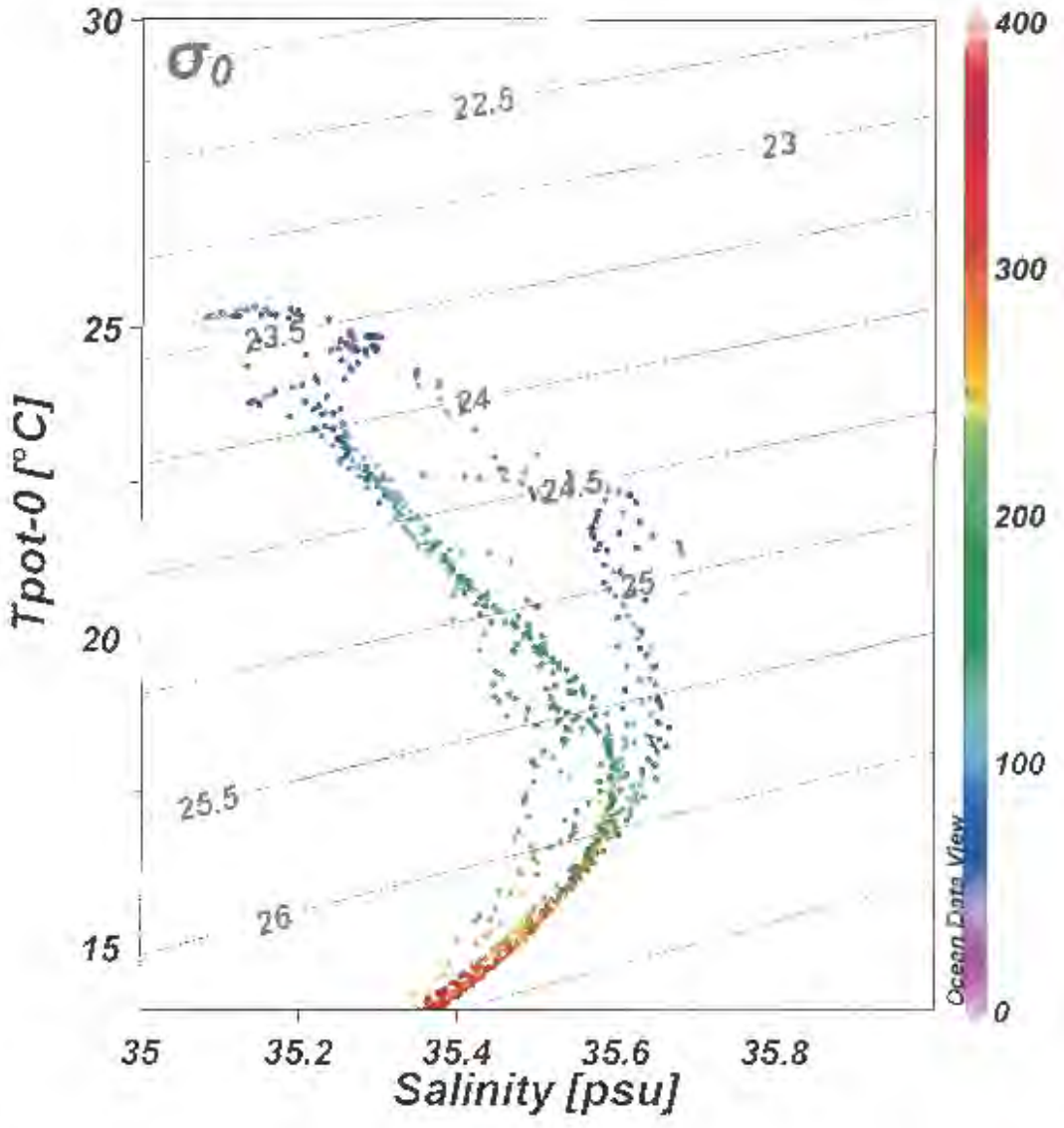

Figure 5.4. Surface water Potential temperature/Salinity plot for all WOCE stations under investigation (Figure 5.5). Colours indicate depths according to the right hand scale.

Only 14 appropriate WOCE stations were studied from the region southeast of Madagascar in this study. The WOCE surface water Θ/S plot (Figure 5.4) showed a very similar distribution of characteristics to that of the ACSEX II data although the surface waters in the WOCE data were generally fresher and cooler. A similar batch of less saline waters as were apparent in the ACSEX II data was also evident in the WOCE plot. These fresher Θ/S relationships for both the WOCE and ACSEX II data correspond to the stations in the EMC proper as seen in the LADCP (Figure 6.1) and

geostrophic data (as discussed in the chapter 6 'Flow dynamics of the EMC'). This characteristic demonstrates the fresher tropical origins of this current.

Of interest in the ACSEX II Θ/S profile were stations 75-79 and 97, which were all located on the eastern side of the survey region (Figure 5.1). These stations displayed high surface salinities of between 35.502 and 35.58 psu from the surface down to a depth of 60 m. This 0.2 psu increase in salinity could be explained by the eastern waters having had less diluted STSW while the stations close to the EMC displayed water that had experienced slight mixing with the fresher TSW of the EMC. However the saltier water could also have been associated with the anti-cyclonic features in the area (Figure 6.11). Does this explanation of an anti-cyclonic feature bringing saline water to the region apply when looking at previous data?

In the WOCE Θ/S plot (Figure 5.4) a grouping of stations in a density range between 23.8 and 26 $kg.m^{-3}$ which were about 0.2 psu more saline than the core of the surface waters were apparent. These more saline water masses in the WOCE data were also located on the eastern side of the region under investigation. However, the SLA data contemporaneous with the WOCE stations of 1995 (Figure 5.5) shows no anti-cyclonic feature close to the stations. So it would appear that the elevated surface salinities to the east of Madagascar were less diluted STSW and are a permanent feature and not brought on by transient anticyclones.

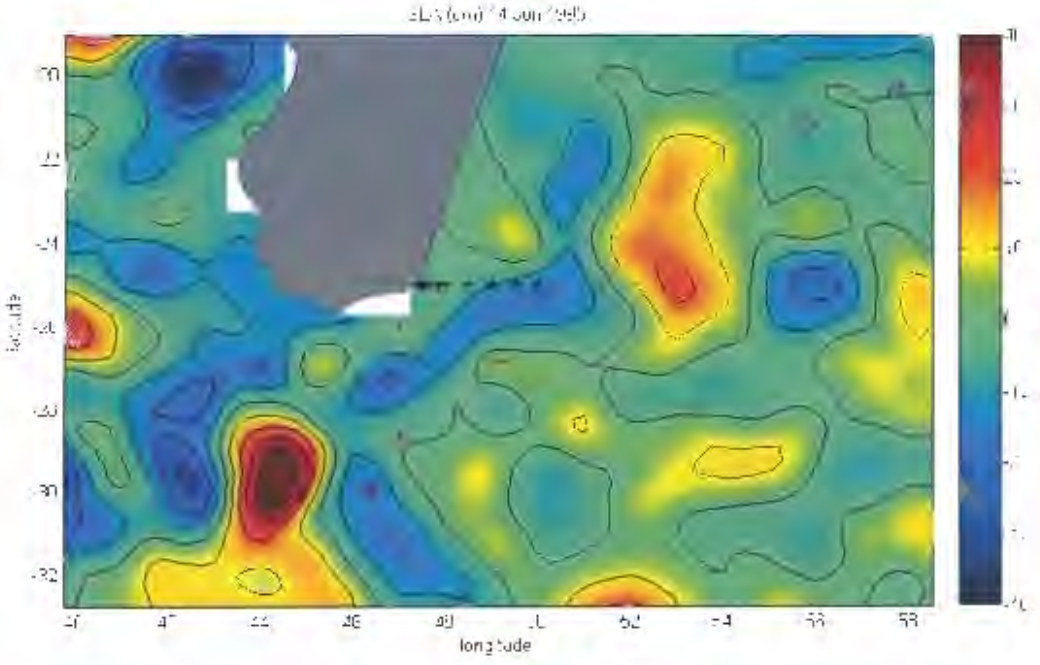

Figure 5.5. *Sea Level Anomaly (SLA) for the waters around southern Madagascar. SLA data are for 14 June 1995. Black symbols indicate the position of the WOCE stations that are concurrent with the date of the SLA map. Red symbols indicate the remaining WOCE stations under investigation, but which are not concurrent with the SLA map.*

Of further interest in the surface waters are stations 90-92, which showed extensive subsurface interleaving between depths 140-268 m (plot of station 92 can be seen in Figure 6.6). In this region maximum subsurface salinities of 35.821-35.868 psu were observed between 25-25.5 $kg.m^{-3}$. LADCP data at these stations showed an opposing flow indicative of an eddy (bottom right panel of Figure 6.1). This feature has been explained by Nauw et al. (2005) as an intra-thermocline eddy (ITE). These ITE's have a salinity maximum and a potential temperature range of between 18 and 22°C. These features are most likely formed in the subtropical South Indian Ocean east of 90°E and south of 25°S (Nauw et al., 2005). The core of the more saline ITE has been highlighted in Figure 5.3.

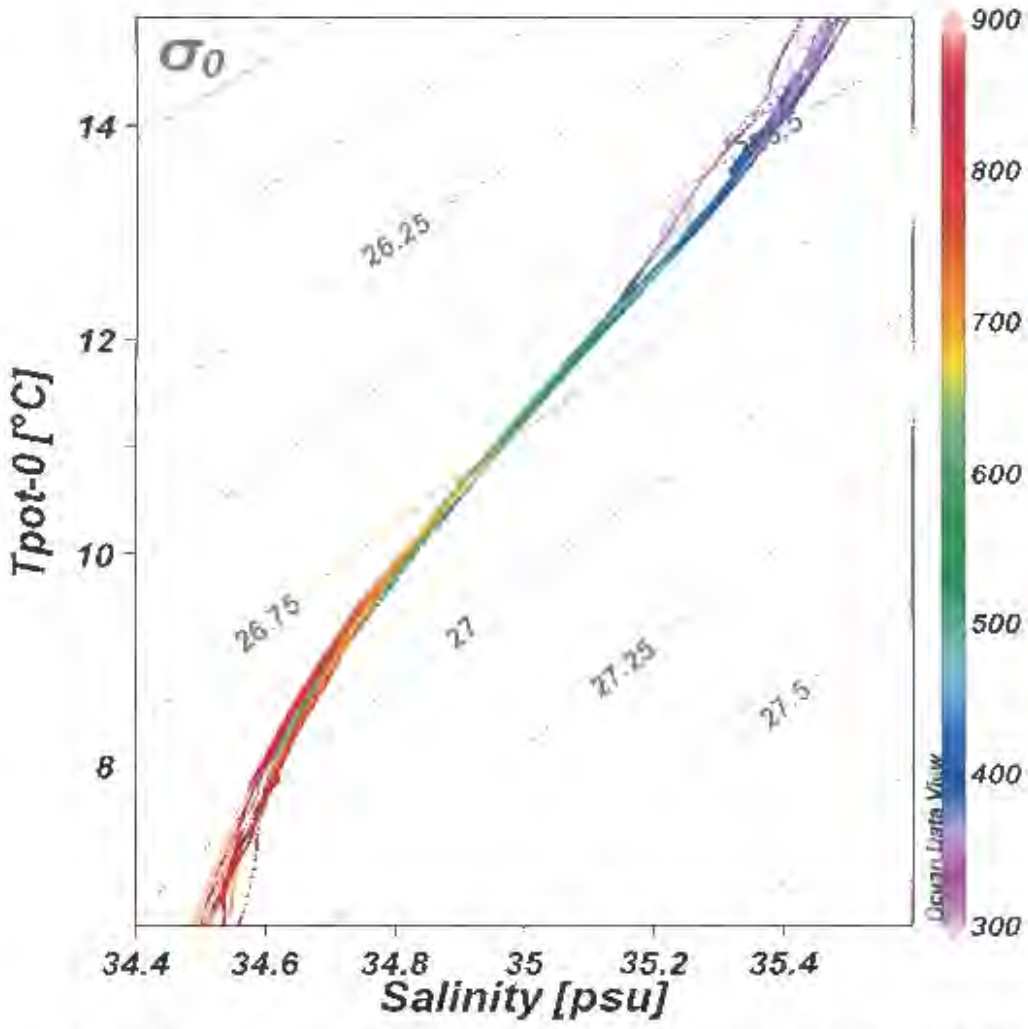

Figure 5.6. Central water Potential temperature/Salinity plot for all ACSEX II stations under investigation (Figure 5.1). Colours indicate depths according to the right hand scale.

The Θ/S profile for the central water masses is shown in Figure 5.6. The salinity range of this SICW was 35.413-34.566 psu, and the temperature range was 7.40-14.80°C which gives a density range of 26-27 $kg.m^{-3}$. The WOCE data for the central water in this area display a plot (addendum Figure A3) almost identical to the ACSEX II data. These ranges are also comparable to other results in the area (Gründlingh et al., 1991). The very linear profile of the SICW mass as observed in Figure 5.6 highlights the nature of the thermocline in this region.

Between the depths of 800-1500 m (Figure 5.7) the AAIW mass was found with a temperature range of 2.85-8°C, and the salinity range was 34.432-

34.650 psu. The density range of the AAIW was 27.6-26.96 kg.m^{-3}. The Swallow et al. (1988) study of the EMC reported that there was no RSIW mixed with AAIW associated with the southern EMC. The initial impression of the ACSEX II data certainly alluded to the existence of an intermediate water mass with a more saline signature than the AAIW. This water mass was up to 0.1 psu more saline then the AAIW. The WOCE data of June 1995 (Figure 5.8) also showed the existence of this saltier water mass at this depth. Whether this was in fact RSIW can be determined with the use of oxygen as a tracer.

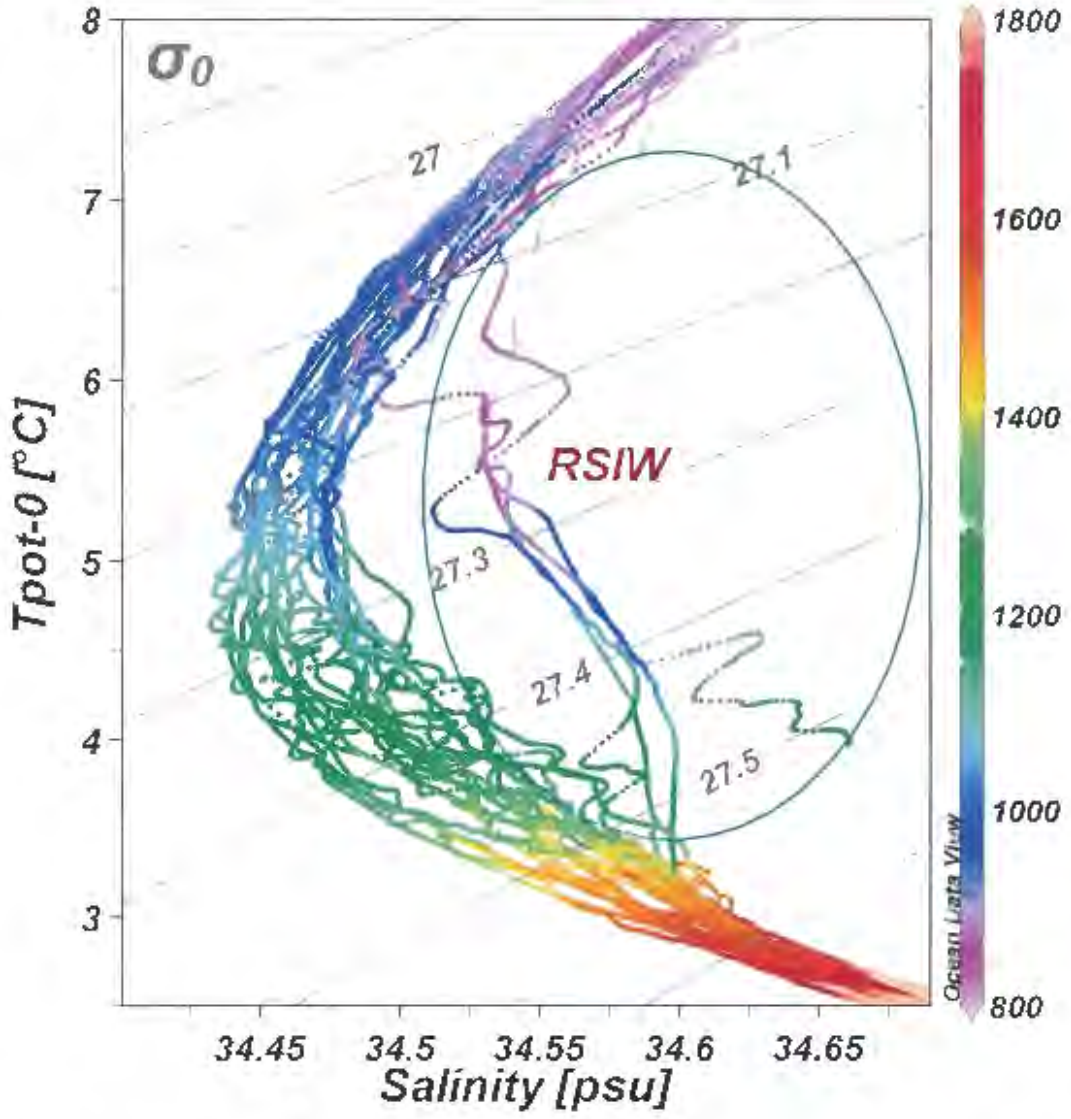

Figure 5.7. Intermediate water Potential temperature/Salinity plot for all ACSEX II stations under investigation (Figure 5.1). The proposed RSIW has been circled. Colours indicate depths according to the right hand scale.

As the Red Sea has a relatively high surface temperature and salinity the dissolved oxygen concentrations of this water mass are relatively low (Green and Carrit, 1967). Plotting oxygen against salinity for all the stations of sections B, C, D and E (Figure 5.9) it was found that the lowest oxygen concentrations of between 140 and 150 $\mu mol.kg^{-1}$ correspond to a salinity range of 34.55-34.66. The depth of this low oxygen concentration water was 800-1250 m. Furthermore the stations in which the low oxygen concentrations were found correspond to the stations which display the more saline intermediate waters. This confirms that the salty intermediate waters certainly do have a Red Sea Water influence with its characteristic low dissolved oxygen concentration. The definition for this RSIW was chosen as having a temperature range of 3.5-7°C and a salinity range of 34.51-34.66 psu. The RSIW lay within the density range of 27.05-27.51 $kg.m^{-3}$. The interesting flow pattern of this RSIW will be discussed further in chapter 6 'Flow dynamics of the EMC'.

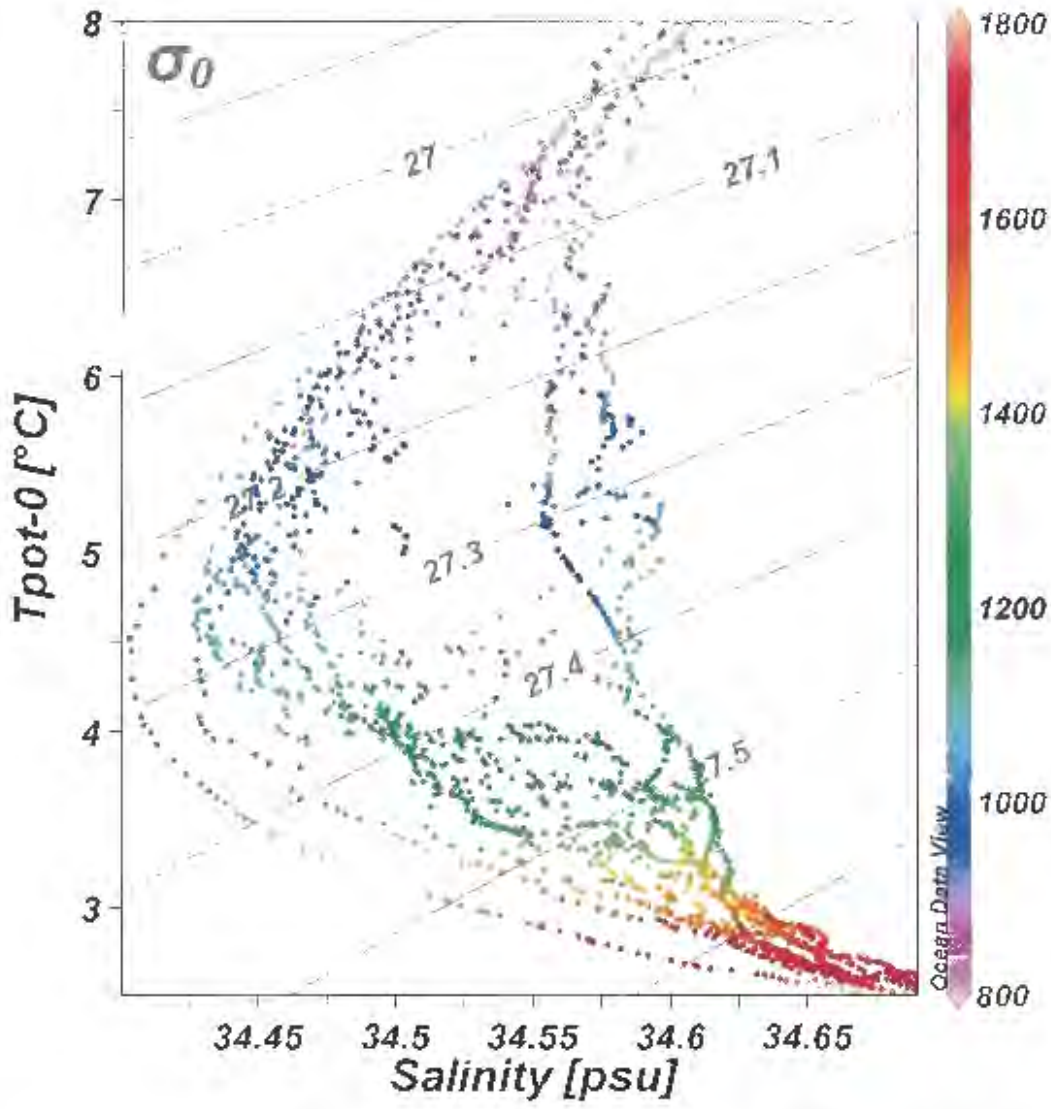

Figure 5.8. Intermediate water Potential temperature/Salinity plot for all WOCE stations under investigation (Figure 5.5). Colours indicate depths according to the right hand scale.

Due to cable problems which limited the maximum depth of the CTD casts, only the upper layer of the deep water masses was observed (Figure 5.10). The core of deep water was identified with a temperature range of 2.0-2.7°C, a salinity range of 34.630-34.742 psu and density of 27.630-27.765 kg.m^{-3}. Separate from this core were a number of outliers which had an increase in salinity of up to 0.03 psu. These outlying values correspond to stations on the distal end of sections B and C (Figure 5.1). The WOCE data for the deep waters in the region under investigation also displayed this dichotomy (Figure 5.11). Donohue and Toole (2003) mention that in the deep waters of the

Southwest Indian Ocean, NIDW, NADW and CDW are found. NADW and CDW have higher oxygen and lower nutrient concentrations compared to NIDW. The silicate/Salinity plot for all the ACSEX II stations (Figure 5.12) shows a bifurcation in the 1800-2000 m range. There was a grouping of silicates at about 76 $\mu mol.kg^{-1}$ and 34.75 psu while there was a second group that extended from 80-110 $\mu mol.kg^{-1}$ at 34.71 psu. The grouping of lower silicate concentration samples corresponded to an oxygen concentration range of 178-199 $\mu mol.kg^{-1}$ (Figure 5.13). The higher silicate concentration grouping corresponded to a lower oxygen concentration range of between 160 and 181 $\mu mol.kg^{-1}$ (Figure 5.13). The higher silicate/lower oxygen concentration grouping corresponded to the less saline core of the deep waters as seen in the Θ/S plot (Figure 5.10). This implies that the core of fresher water was representative of NIDW. The more saline low silicate/high oxygen water could have been either NADW or CDW. The ACSEX II stations on the northern most line only went down to 800 m after station 93 (50°E) therefore it was not possible to determine the existence of the NADW - CDW in the Mascarene basin. The WOCE data did however go to full depth, and was able to show that this NADW - CDW water was also found in the stations in the Mascarene basin.

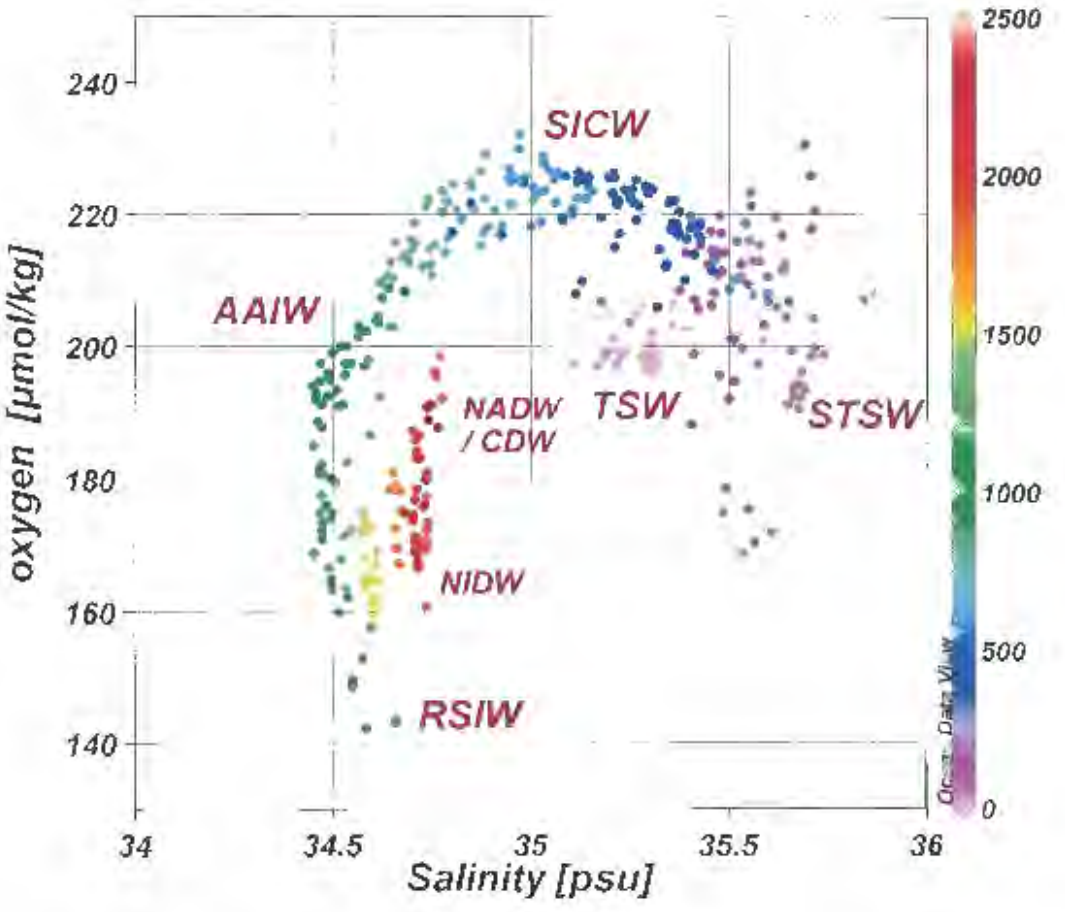

Figure 5.9. Oxygen/Salinity plot for all ACSEX II stations under investigation (Figure 5.1). The labels show the major water masses identified. Colours indicate depths according to the right hand scale.

The various water masses of the southern termination of the EMC have now been examined. The region was shown to have the previously recognised TSW, STSW, SICW and AAIW. At greater depths NIDW and NADW - CDW were also confirmed. A new conclusive discovery was that of RSIW adjacent to the EMC. However the pathways taken by these water masses are unclear. Through the use of geostrophics, LADCP, drifter and SLA data an attempt to highlight some of these flow dynamics will be made in the next chapter.

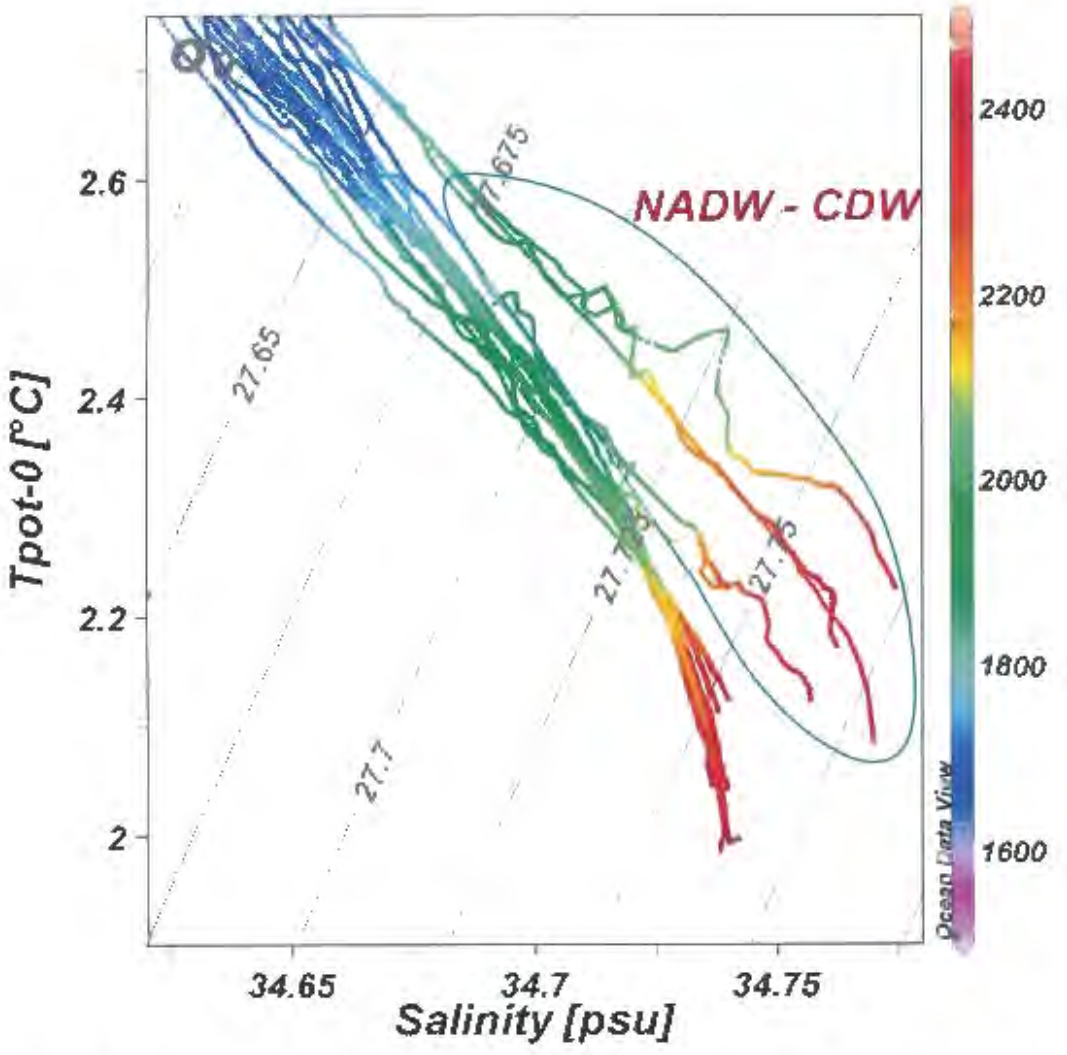

Figure 5.10. Deep water Potential temperature/Salinity plot for all ACSEX II stations under investigation (Figure 5.1). The Saline NADW - CDW has been labelled. Colours indicate depths according to the right hand scale.

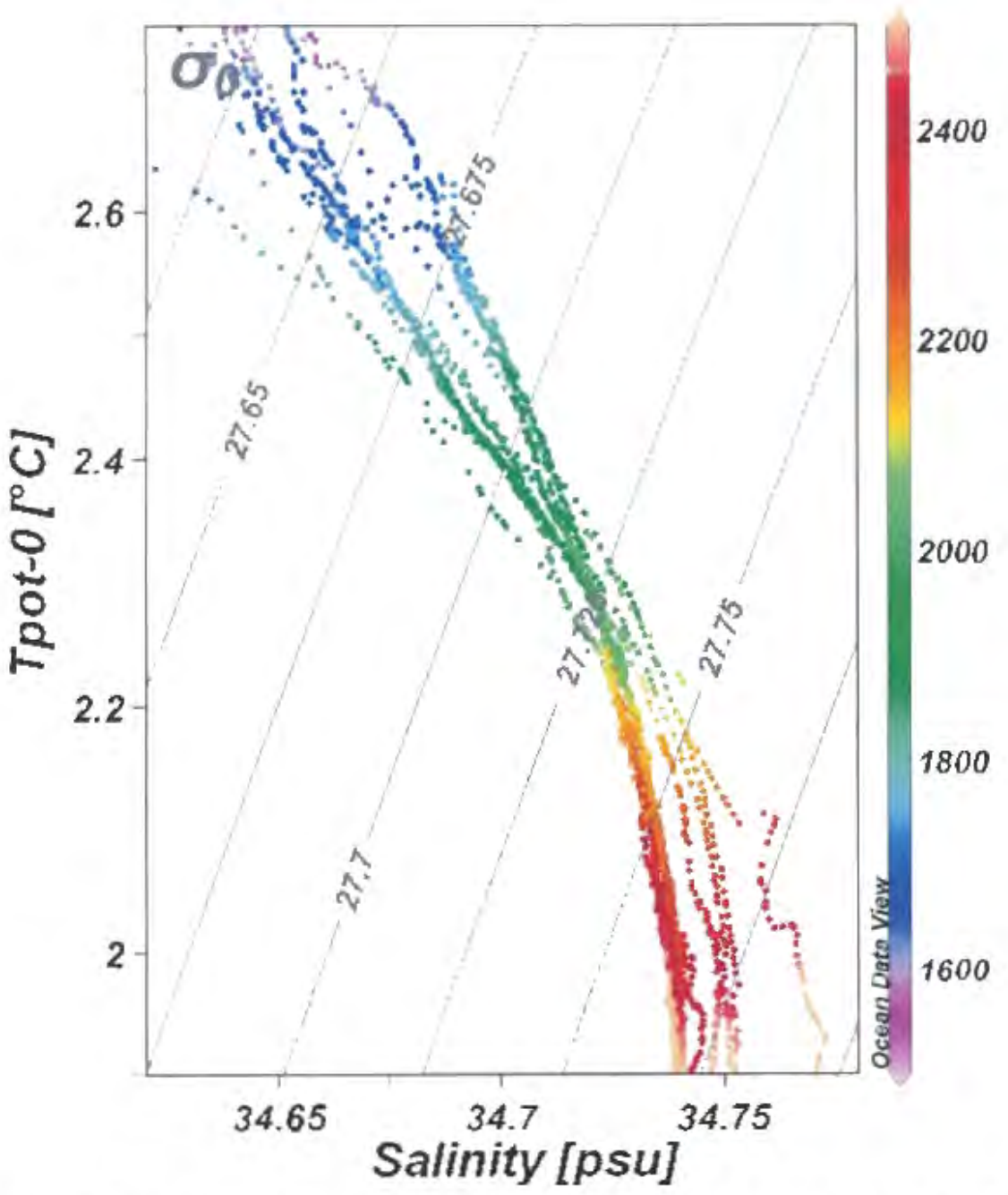

Figure 5.11. Deep water Potential temperature/Salinity plot for all WOCE stations under investigation (Figure 5.5). Colours indicate depths according to the right hand scale.

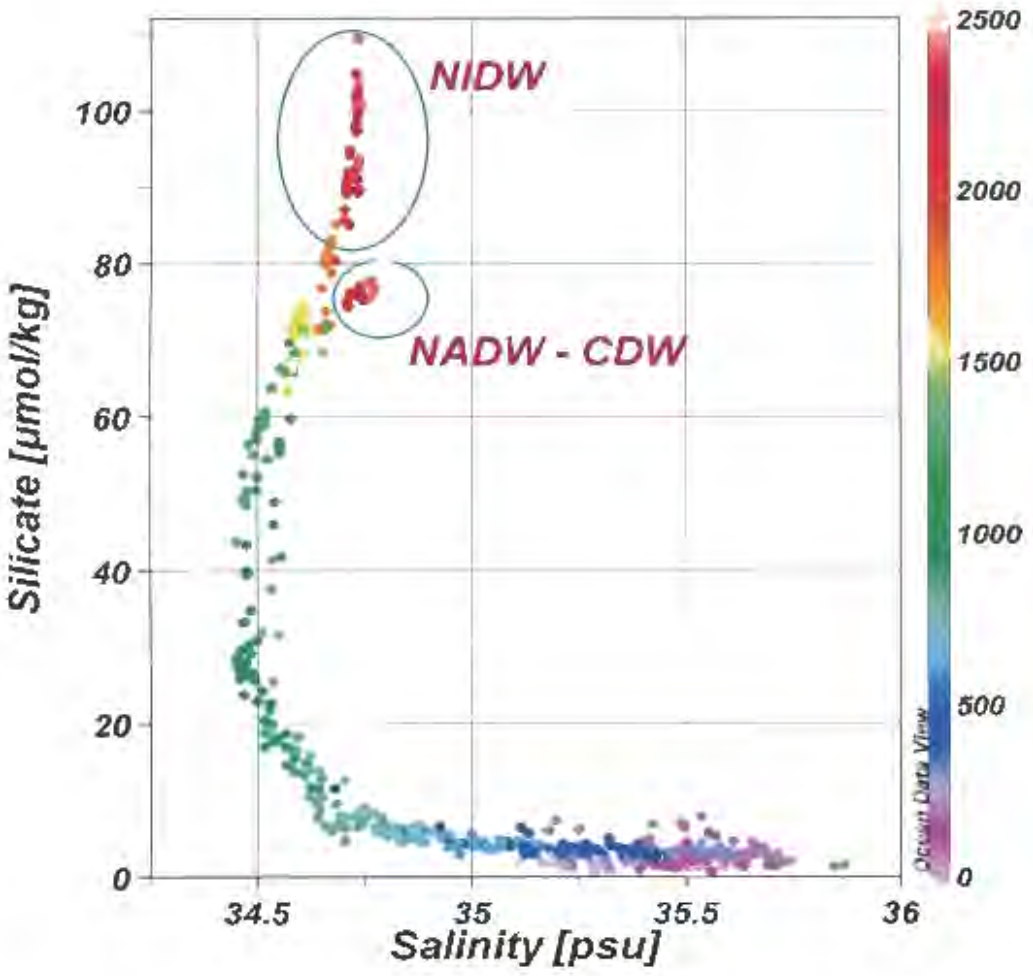

Figure 5.12. Silicate/Salinity plot for all ACSEX II stations under investigation (Figure 5.1). The low silicate concentration NADW - CDW has been labelled, as well as the high silicate concentration NIDW. Colours indicate depths according to the right hand scale.

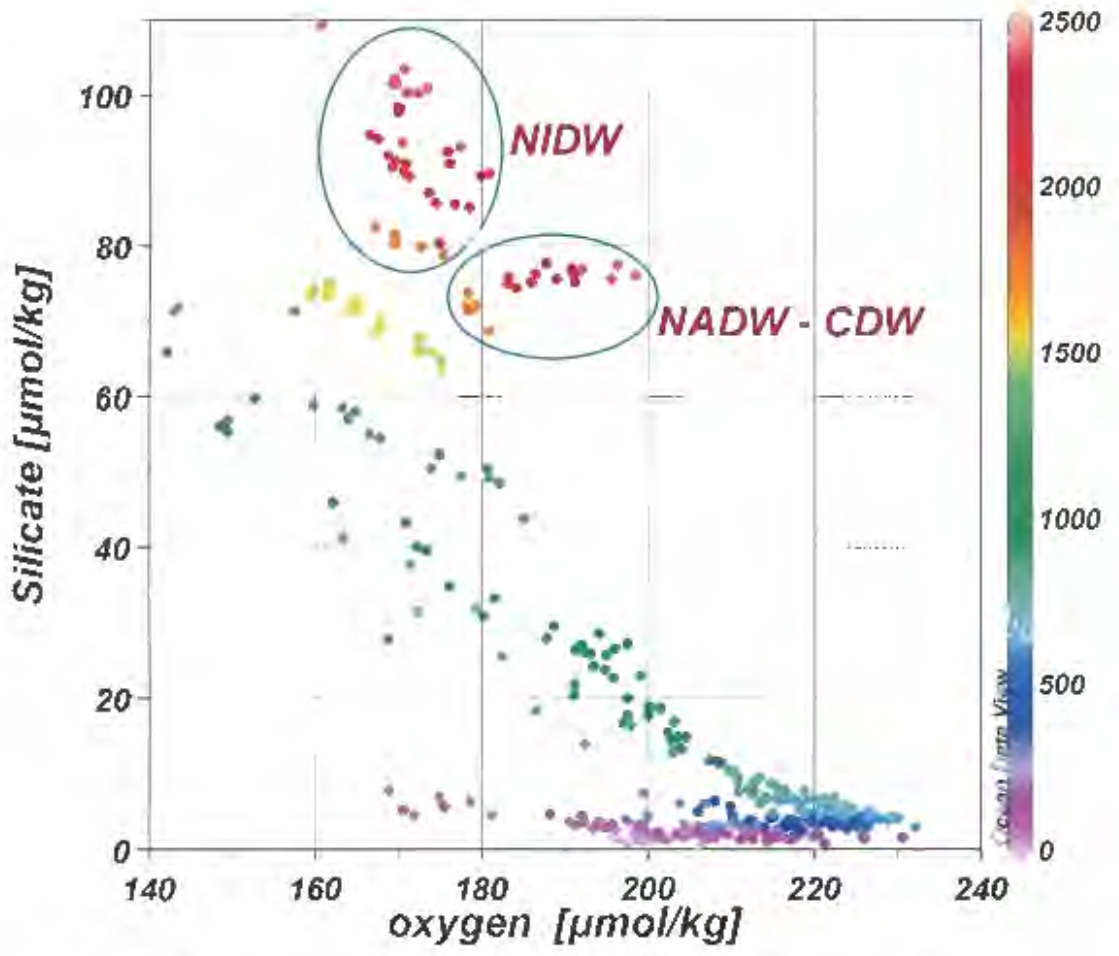

Figure 5.13. Silicate/Oxygen plot for all ACSEX II stations under investigation. The low oxygen high silicate concentration NIDW is circled as well as the high oxygen low silicate concentration NADW - CDW. Colours indicate depths according to the right hand scale.

6. Observed flow dynamics of the termination of the EMC

Uncertainty around the course of the EMC at its termination has prevailed for many years. With the ACSEX II cruise being the first cruise focused on this region there are some fundamental questions that can now be addressed. As the ACSEX II cruise was a dedicated hydrographic cruise the stations were chosen to highlight the main features. Four sections (B, C, D and E) of the cruise were orientated to intersect the EMC at its termination. The sections radiated out from the south-eastern corner of Madagascar. The length of the sections ranged from 141-294 km and the distance between stations was from about 8-30 km on the shelf and 40-60 km further offshore (Figure 5.1).

Lowered Acoustic Doppler Current profiler analysis:

The LADCP velocity profiles for the stations occupied on the four sections B, C, D and E are shown in Figure 6.1. The blue colour (negative values) represents flow in a southerly (westerly) direction and the red (positive values) flow in a northerly (easterly) direction. The contour lines are drawn every 0.1 m/s. In all of these sections there was visible a core of water flowing in a southerly to westerly direction close to the coast (represented by blue colours). The maximum velocity of this core perpendicular to section B (to the west) was 1.1 m/s; section C was 0.47 m/s; section D was 0.90 m/s and section E (to the south) was 0.94 m/s. The position of this relatively fast flowing core between 20 and 80 km from the coast leads to the conclusion that this was the EMC (Lutjeharms et al., 1981; Swallow et al., 1988). In the ACSEX II sections the current displayed a maximum depth of about 1000 m and a maximum width of about 100 km if 0.1 m/s was chosen as the boarder of the current. The volume transported by the EMC through section B was calculated to be 36.0 Sv. The transport through section C was calculated as 17.3 Sv, through section D it was calculated to be 11.4 Sv and through section E it was 14.6 Sv. The maps showing these values can be found in the addendum (Figure A10 and A11). Previous analysis of the EMC has recorded the current as flowing at 0.80 m/s at 25°S (the same position as ACSEX II section E) (Donohue and Toole, 2003); 1.00 m/s at 23°S (Lutjeharms et al.,

1981) and 0.67 m/s at 23°S (Swallow et al., 1988). The volume transport of the current has previously been calculated as ranging between 20.3 Sv (Schott et al., 1988) and 41 Sv (Lutjeharms et al., 1981).

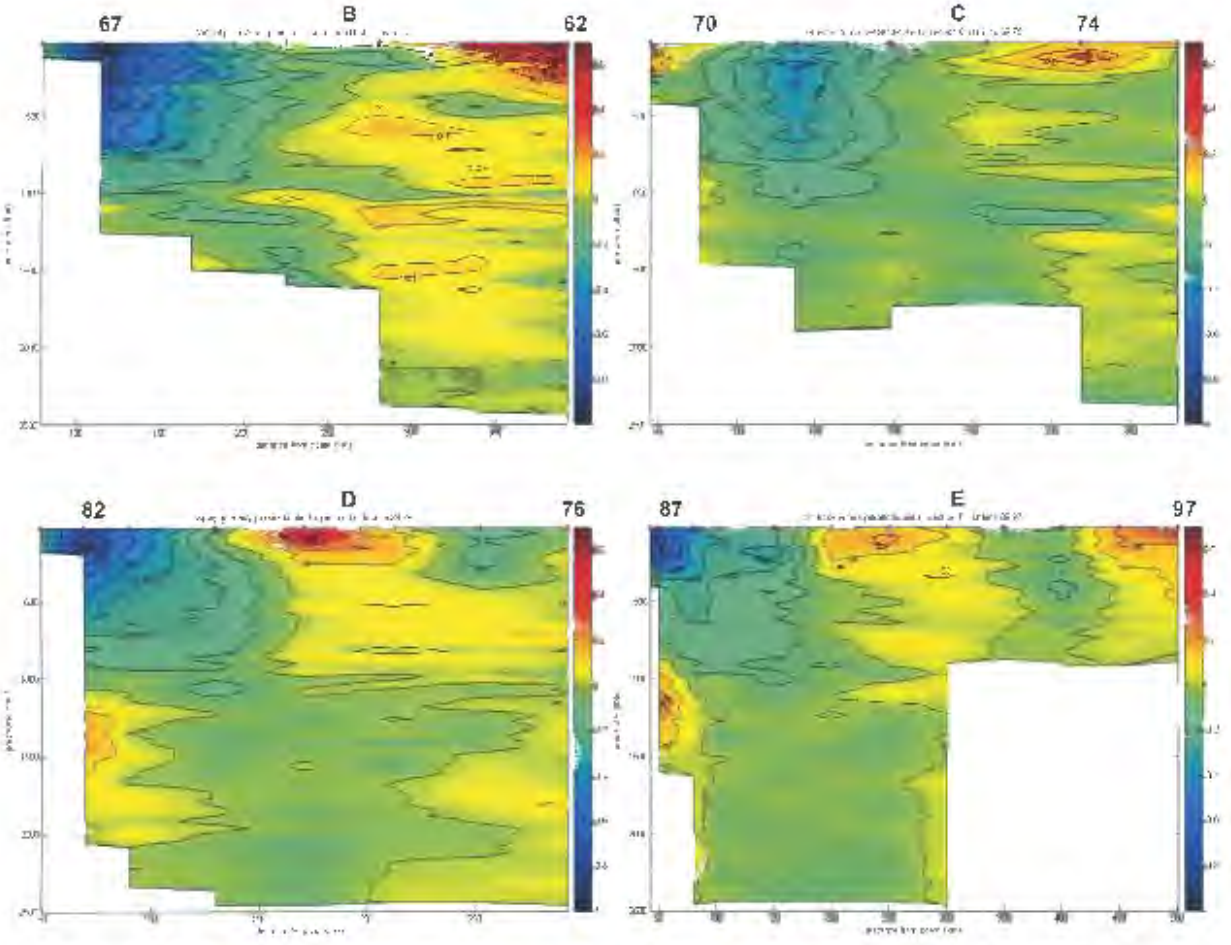

Figure 6.1. Water velocity through ACSEX II sections B, C, D and E. Measurements taken by Lowered Acoustic Doppler Current Profiler (LADCP). The East Madagascar Current (EMC) is seen close to the coast (blue colour). The EMC Undercurrent is seen against the shelf between 1000 and 2000 m depth in section D and E (orange colour). Counter current flow is seen at the surface between 80 km from the coast (section D) and 300 km from the coast (section B).

The calculated geostrophic flows for section B, D and E are shown in the addendum (Figure A9). From these figures it can be seen that in general there was good agreement on the position and strength of the EMC between the LADCP results and velocities obtained using geostrophic calculations referenced to the bottom. The maximum geostrophic speed of the EMC for all

the sections was 1 m/s. The depth of the current was down to 1200 m and the width was about 50 km. In most sections the geostrophic results tended to slightly underestimate the EMC compared to the directly measured LADCP data. However in section C the LADCP results (Figure 6.1) showed a weaker EMC flow of 0.4 m/s compared to the geostrophically calculated flow of 1 m/s (Figure 6.2). The depth of the current in the LADCP data for section C was about 1000 m while the depth of the current from the geostrophic data for this section was about 1200 m. This weaker representation of the current in the LADCP results for section C could have been due to the station spacing. Insufficient and inappropriately placed stations could have resulted in stations straddling the current and not sampling the current core properly with the LADCP. As the geostrophically calculated flow shows a possibly better representation of the current in section C this was used to calculate the volume transport and gives a flow of 39.3 Sv.

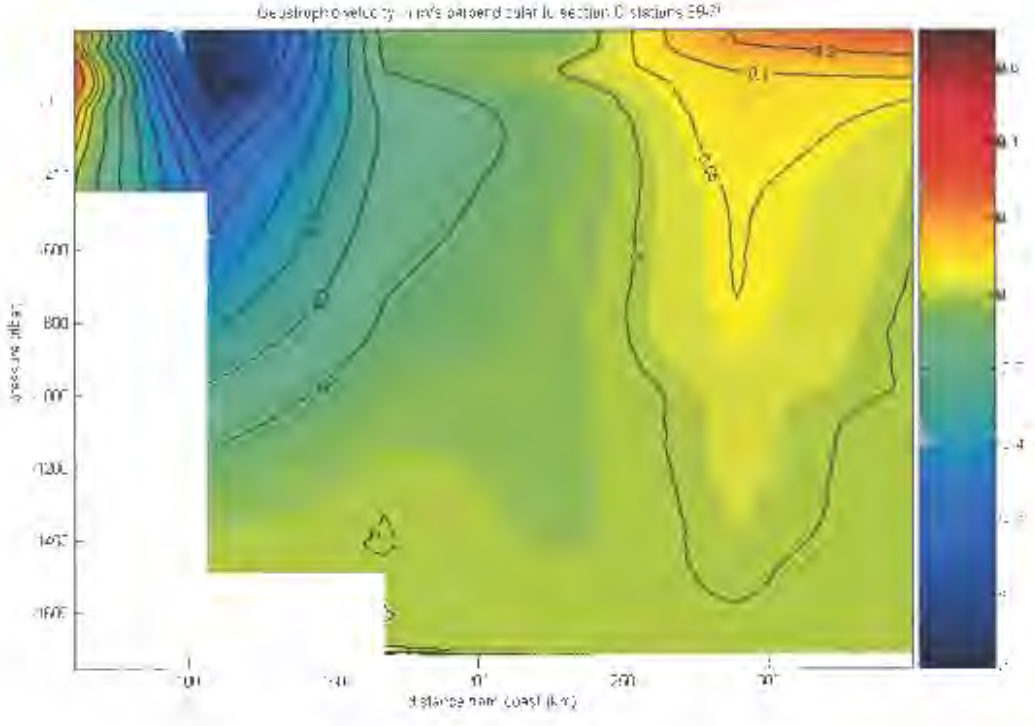

Figure 6.2. *Geostrophic flow through section C. This representation of the flow through section C seems more accurate than the LADCP data for this section.*

The LADCP and geostrophic data of the four sections of the ACSEX II cruise perpendicular to the coast of Madagascar all confirmed that the EMC closely follows the continental slope. Furthermore the LADCP section plots (Figure 6.1) showed a weak current below the EMC flowing in a north-easterly direction. This EMC undercurrent was found to be most prominent in sections D and E with a core velocity of up to 0.3 m/s. The undercurrent flowed very weakly in section C at only 0.05 m/s and in section B it was almost nonexistent. The undercurrent in sections D and E had a depth range of 1000 to 2000 m with a core at about 1400 m and a width of about 30 km. The volume transported by the undercurrent through sections D and E was calculated from the LADCP data to be about 0.8 Sv. Figure 6.3 shows the averaged direction and speed between 1000 and 2000 m, which was the depth range of the undercurrent at stations 70, 82 and 87. These arrows have been plotted with their origin at each station position. In this figure the undercurrent was seen to be heading in an easterly to north-easterly direction. An EMC undercurrent has never been reported before, but other undercurrents in the South Indian Ocean have been studied.

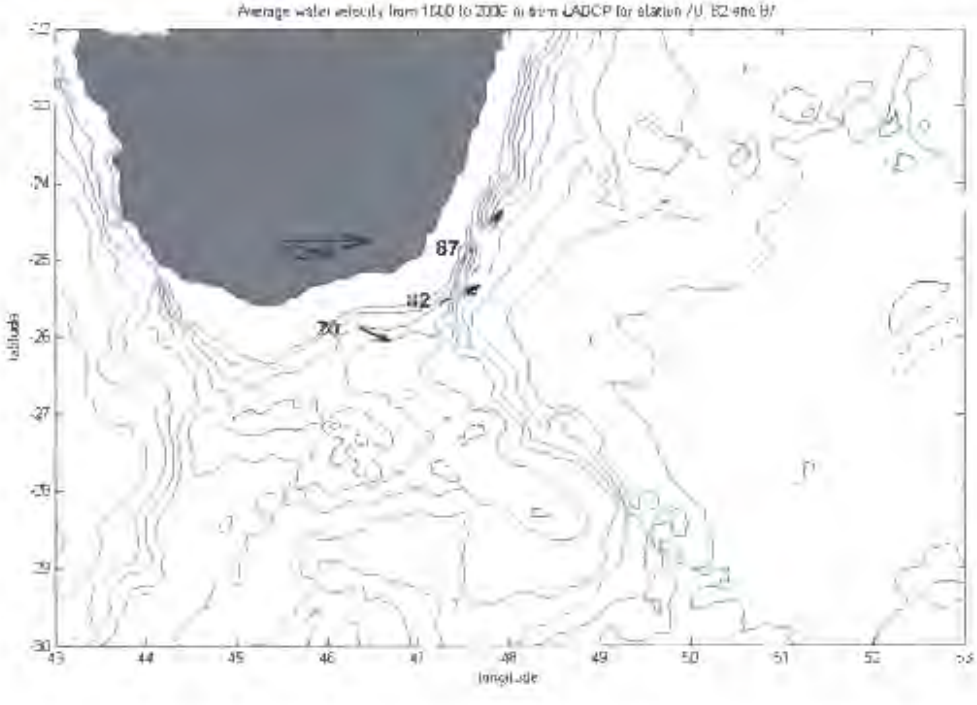

Figure 6.3. Average speed and direction of water between 1000 and 2000 m. Arrows depict flow for stations 70, 82 and 87. This is the average flow of the EMC undercurrent.

Water mass analysis:

Beal and Bryden (1999) have shown the existence of an Agulhas Undercurrent which consisted predominantly of North Atlantic Deep Water and Antarctic Intermediate Water. It was calculated that this northerly flowing Agulhas Undercurrent was a persistent feature. It was found to have a core at around 1200 m depth and was positioned next to the continental slope and below the Agulhas Current. As such, the Agulhas Undercurrent bears similarities in relative position to the coast and the overlying current to the current found flowing under the EMC during the ACSEX II cruise. The maximum velocity of the Agulhas Undercurrent was observed to be 0.3 m/s and its volume transport northeast was calculated to be about 6 Sv. A deep northward flowing current was also found in the Mozambique Channel (De Ruijter et al., 2002). The Mozambique Undercurrent displayed a maximum speed of 0.39 m/s north and an average of 0.077 m/s. It has been suggested that this large variability in speed was due to eddies that had been observed in the channel. The northward transport in the channel was estimated to be 2 Sv (van Aken et al., 2004). Ridderinkhof and de Ruijter (2003) have suggested that the Mozambique Undercurrent is a continuation of the Agulhas Undercurrent. Beal and Bryden (1999) have in turn suggested that the Agulhas Undercurrent might be considered as part of a localised deep recirculation cell.

Interestingly Beal and Bryden (1999) have found that there was a flow of RSIW being carried north towards its source by the Agulhas Undercurrent. However they calculated that the majority of the Red Sea Intermediate Water (RSIW) seen in their section at 32°S was being carried south. The depth range of the RSIW seen previously in chapter 5 'Water masses of the East Madagascar Current termination' was about 800 m to 1250 m (Figure 5.8). With the EMC Undercurrent displaying an overlapping depth range of 1000 to 2000 m it is expected to have had a RSIW component. Figure 6.4 shows the Potential temperature/Salinity (Θ/S) plot of intermediate water in the EMC region. The colours represent current velocity, with red representing flow to the north (east) and blue flow to the south (west). From this figure it is

apparent that as with the RSIW in the Beal and Bryden (1999) section most of the RSIW seems to have been moving south, away from its source. The LADCP data from the ACSEX II cruise and the geostrophic current flow has certainly verified the presence of the fast flowing western boundary EMC southeast of Madagascar. These data have also highlighted the first evidence of an East Madagascar Undercurrent. However, the course of the EMC after it passes the southern most tip of Madagascar is still not immediately obvious.

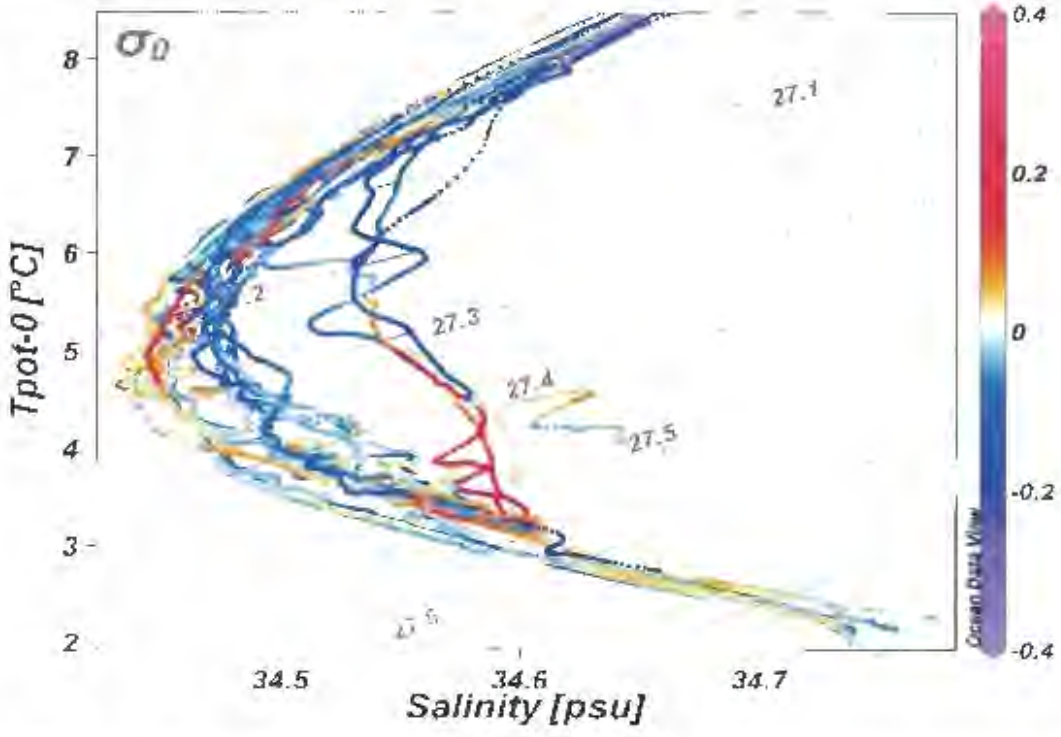

Figure 6.4. Potential temperature/Salinity plot of intermediate water in the ACSEX II sections B, C, D and E. Negative (blue colours) represents flow in the direction of the EMC and positive (red colours) represents flow in the direction of the EMC undercurrent.

There is a hint of the possible further course of the EMC in the LADCP data (Figure 6.1). These plots demonstrate that further offshore of the EMC there was a north (east) flow depicted in red. If there was a retroflection of the EMC, similar to the Agulhas Current, then it is expected that there would be an offshore flow like this. Compared to the EMC this offshore flow was relatively weak at only 0.2-0.6 m/s. The core position of this flow varied from 90 km off the coast to 335 km off the coast and the average depth of the flow was about 500 m. In order to display the absolute direction of this flow through the

sections the LADCP data were averaged over the first 500 m (Figure 6.5). In section B, D and E this flow was predominantly in a northeast direction, and in sections C this flow was strongest in an east southeast direction. This implies that this water was going against the general westerly background flow in the area (Figure 1.2). In the Swallow et al. study (1988) of the flow along 23°S, a counter flow to the EMC was also found at about 110-167 km from the coast. This flow was seen in their figure 7 to have a maximum velocity of only 0.08 m/s. Through a section along 23°S in 1975, Lutjeharms et al. (1981) found a flow with a northerly component of 0.50 m/s between about 250 and 300 km from the coast. Donahue and Toole (2003) have also shown northerly flow through a 1995 WOCE section along 25°S (left hand side panel of Figure 6.12). This flow counter to the EMC was positioned at 49°E (about 110 km from the coast). They interpreted this flow as being the western limb of a cyclonic eddy. This assessment was supported by the fact that the water properties of the northward flow did not completely match that of the EMC. The EMC was shown to have a low oxygen core at 150 m which was not present in the northward flow through the WOCE section. Furthermore the depth of the northward flow was only to 800 m while the EMC had a signal down to 1000 m. In the section of 1975 along 23°S (Lutjeharms et al., 1981) the northward flowing current was also seen to be shallower than the EMC (their figure 6). Whether the water that was flowing to the southeast and northeast in the ACSEX II data originated in the EMC or was the expression of an eddy still needs to be investigated.

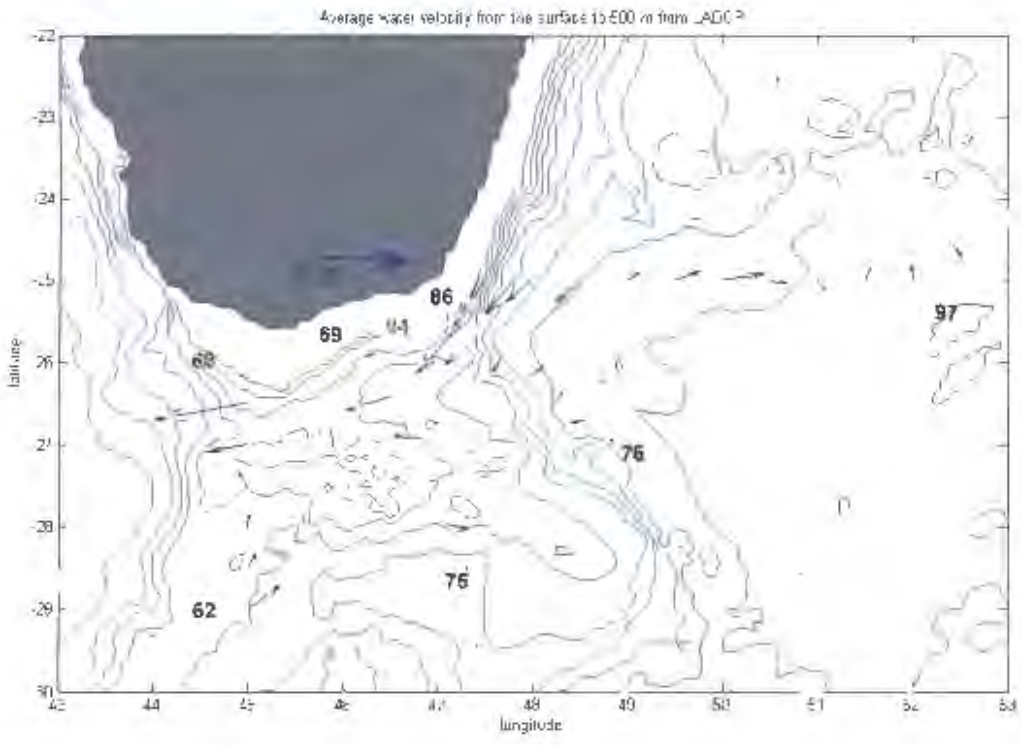

Figure 6.5. Average speed and direction of water in the upper 500 m for stations in sections B, C, D and E. South-eastward or north-eastward flow counter to the EMC is seen in all the sections.

Similar to the WOCE data of 1995, the core of the counter current seen in the ACSEX II sections was not as deep as the EMC (Figure 6.1). If the same rationale is applied as used by Donohue and Toole (2003) that a return current would have the same depth signal as its source current, then the counter current in the ACSEX II sections was most probably not a return current of the EMC. In order to further distinguish if the counter current was not an extension of the EMC the water characteristics were investigated.

The Θ/S diagrams of the water in the EMC (blue - green colours), and the counter current water (red - purple colours) are shown in Figure 6.6. The Θ/S plots of the EMC (stations 67, 71 and 82) showed interleaving in the upper 200 m, while the Θ/S plots of the counter current in sections B, C and D (stations 62, 74 and 79) were much smoother. In a density range between 23.5 and 25 kg.m^{-3} the Θ/S plots of the counter current in section B and D (stations 62 and 79) displayed saltier water than the EMC stations. The

oxygen profiles for the ACSEX II sections appear in Figure 6.7. The core of low dissolved oxygen concentration seen at 150 m within the EMC in the Donohue and Toole (2003) section was also present in the ACSEX II data. The low oxygen core was not as intense in section B though. As with the explanation of depth signal in the counter current flow compared to the EMC, a similarity in the oxygen concentration in the EMC and counter current flow could indicate a retroflection. However no low oxygen core as seen in the EMC was present in the counter current flow of station 62 (section B) and station 79 (section D). There were slightly lower oxygen concentrations in the counter flow at station 74 (section C) but this was around 210 $\mu mol.kg^{-1}$ and not as low as the 180 $\mu mol.kg^{-1}$ core seen in the EMC. Stations 92 and 93 also displayed lower oxygen concentrations in the counter current flow but this concentration was around 200 $\mu mol.kg^{-1}$ and also not as low as that seen in the EMC. The silicate concentrations for the sections are shown in Figure 6.8. The core of the EMC in all the sections had a silicate concentration from the surface to 100 m of around 2-3 $\mu mol.kg^{-1}$. In the counter current flow of section B (station 62) the silicate concentration was less than 1 $\mu mol.kg^{-1}$ from the surface to 100 m. The counter current flow of section C (station 74) was about 1.5 $\mu mol.kg^{-1}$ for the first 100 m. For section D (station 79) it was between 1-1.5 $\mu mol.kg^{-1}$ and for section E (stations 92 and 93) it was between about 1.5 and 2 $\mu mol.kg^{-1}$ in the first 100 m. It would seem that the counter current flow in all the ACSEX II sections had a lower silicate concentration than the EMC for the upper 100 m. This pattern of the EMC having a higher silicate concentration than the counter current flow was repeated on average for the deeper water down to 500 m. Thus, the EMC and the counter current flow appear to have had dissimilar water mass characteristics. This gives persuasive evidence that the north-eastward counter flow seen in sections B and D was not a direct extension of the EMC. Section C and E are perhaps not as clearly distinguished though. An additional means of detecting the existence of a retroflection is to study the pathway of drifters in the EMC.

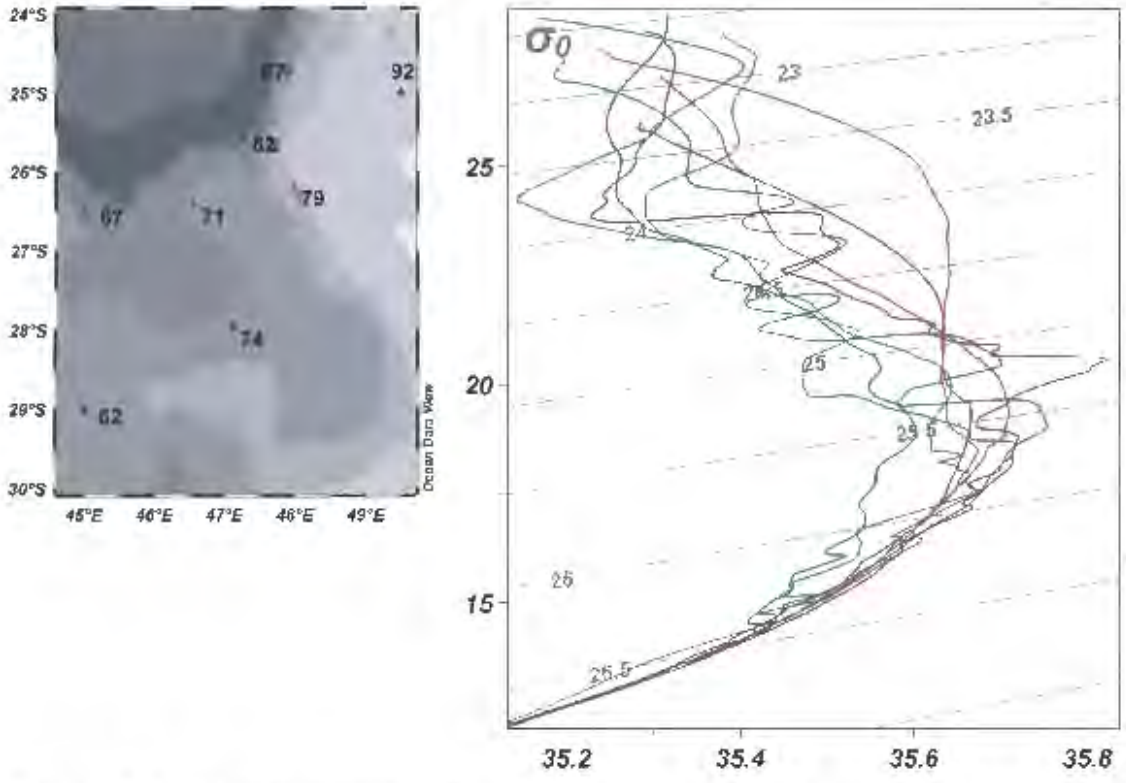

Figure 6.6. *Potential temperature/Salinity diagram comparing EMC surface water (green - blue colours) with the counter current water (red - purple colours). EMC water was generally seen to interleave more than counter current water. The counter current flow in station 62 and 79 was also seen to be slightly saltier than the EMC water at a density of between 23.5 and 25 kg.m^{-3}.*

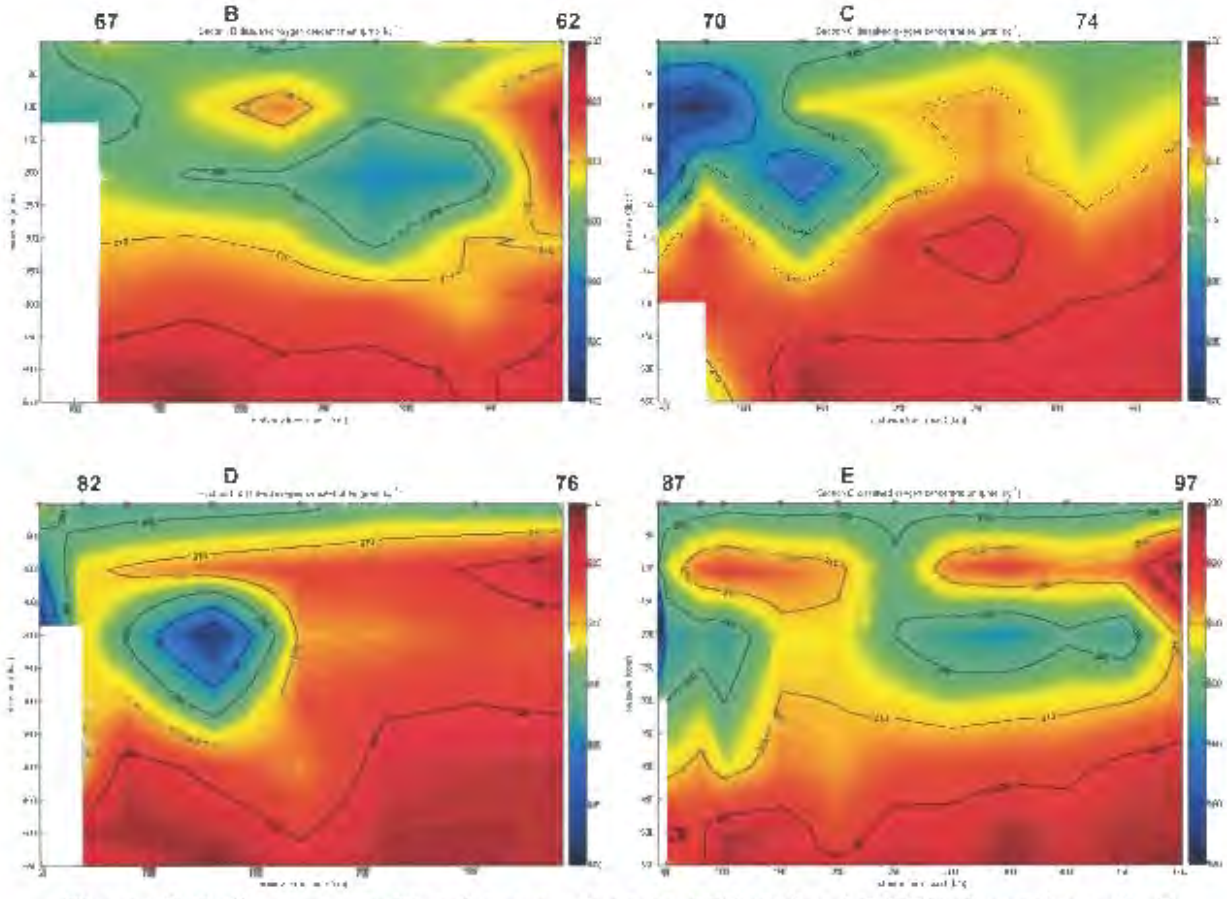

Figure 6.7. *Oxygen profiles from surface to 550 m for ACSEX II sections B, C, D and E. The EMC is seen to have a core of relatively low dissolved oxygen concentration at around 150 m (stations 67, 71, 82 and 87). The counter current flow at stations 62 and 79 do not display this low oxygen concentration. The counter current flow at stations 74 and 92 did have a slightly lower oxygen concentration but not as low as in the EMC core.*

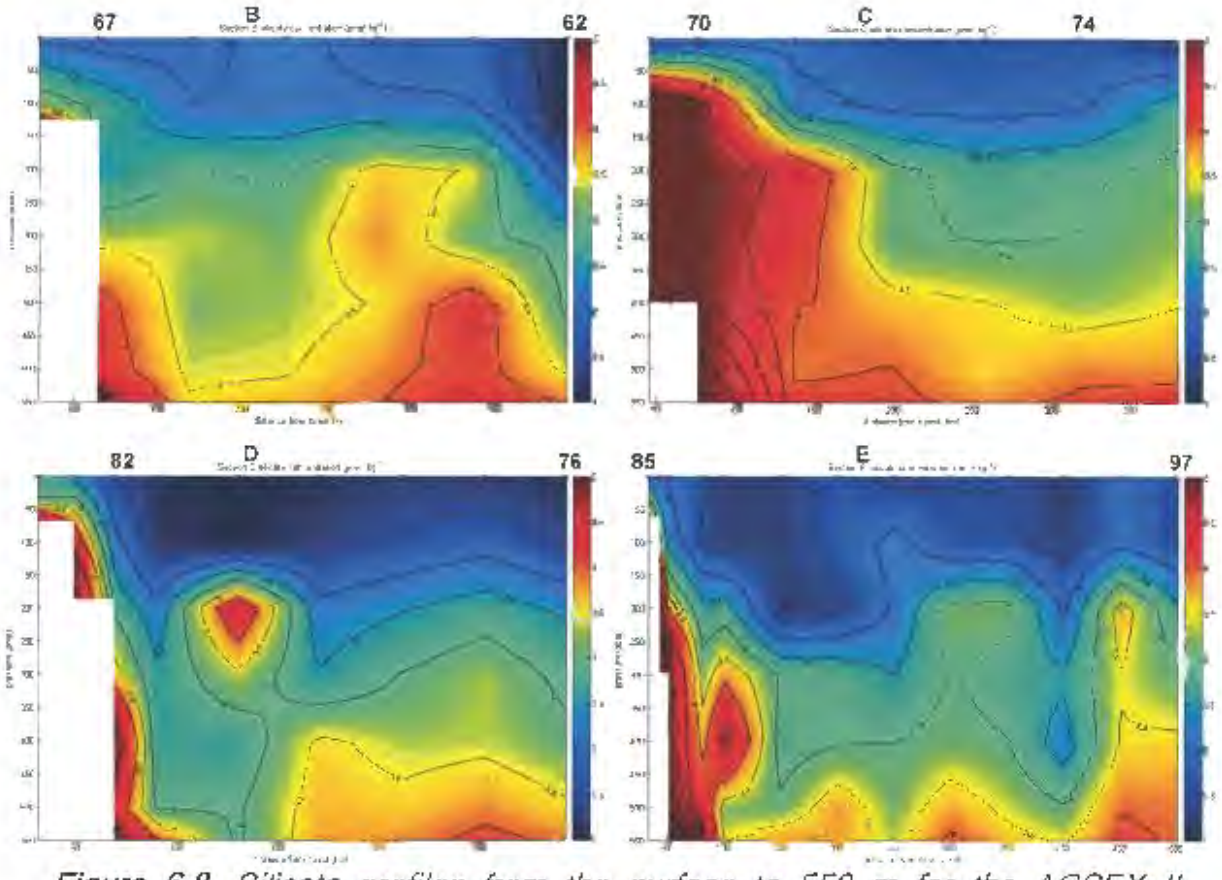

Figure 6.8. Silicate profiles from the surface to 550 m for the ACSEX II sections B, C, D and E. The silicate concentration in the EMC (stations 67, 71, 82 and 87) is generally higher than the counter current flow at stations 62, 74, 79 and 92 - 93.

Drifter analysis:

During the cruise two drifters were released into the core of the EMC. The tracks of these drifters superimposed on the Sea Level Anomaly (SLA), are shown in Figure 6.9. The SLA has been patched together so as to match the time the drifter was in the region of the patch as best as possible. As can be seen the drifters moved rapidly past the south-eastern tip of Madagascar. Drifter 28436 travelled from its deployment position to south of the southern tip of Madagascar at an average rate of 0.8 m/s. Drifter 28944 travelled from its deployment position until south of the southern tip of Madagascar at an average rate of 1.3 m/s. These speeds would suggest that the drifters were indeed caught in the flow of the EMC. The drifters did not follow a retroflecting path nor did they join the counter current flow seen to the east of the EMC. This evidence suggests that the counter current flow was not a continuation of

the EMC. However as the counter current water was moving against the background flow it has to have been forced by something.

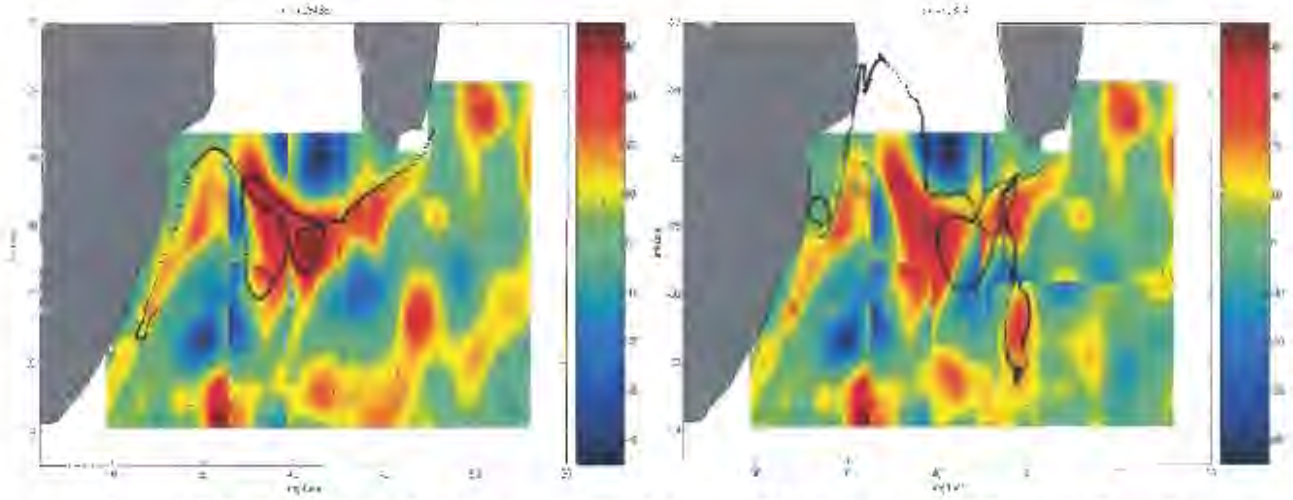

Figure 6.9. *Tracks of drifters released into the EMC during ACSEX II. The Sea Level Anomaly (SLA) pictures corresponding to the time a drifter was in a particular region have been patched together. The drifters did not retroflect southeast of Madagascar, but they did show interaction with eddies in the Natal Basin. Drifter 28436 stopped transmitting 92 days after deployment and drifter 28944 stopped transmitting after 173 days.*

During the drifters traverse across the Natal Basin (Figure 6.9) they appear to have been steered by eddies in this region as they were seen to complete a number of loops around eddies. Further drifters in the ARGOS data set have also been seen to undergo numerous loops to the southeast of Madagascar (Figure 6.10). From these observations the existence of eddies to the southeast of Madagascar are inferred. Therefore, it is possible that a cause for the counter current flow east of the EMC in the ACSEX II data could have been due to eddies in the region. Donohue and Toole (2003) have also explained the existence of the counter current flow seen in their WOCE section as being caused by a cyclonic eddy east of Madagascar.

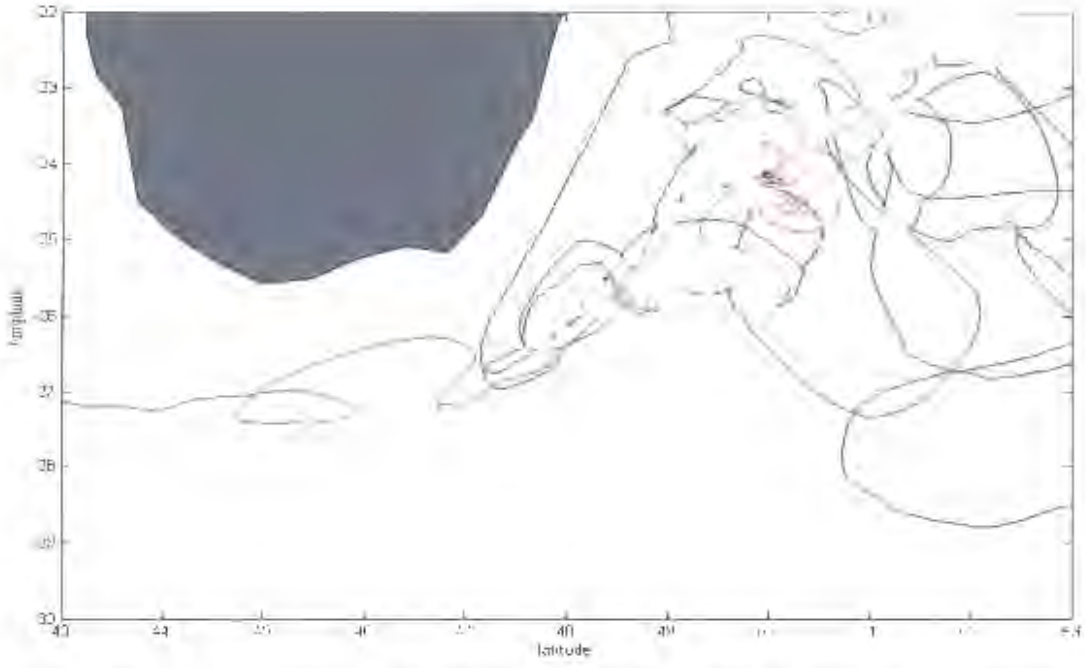

Figure 6.10. Examples of three separate drifter tracks southeast of Madagascar. Drifters have been seen to loop repeatedly as they are caught in eddies in this region.

In order to test this assumption the geostrophic currents from the SLA for the period of the ACSEX II cruise and for the WOCE cruise are shown next to the plot of surface currents as measured with the LADCP during ACSEX II (Figure 6.11) and the ship mounted ADCP (SADCP) from the WOCE cruise along 25°S (Figure 6.12). The origin of the arrows in the ADCP data are at the position where the measurements were taken and the length of the arrows represent the speed of the current. The key over the land shows the length of a 1 m/s arrow. The SLA is contoured in increments of 10 cm. Positive sea level anomalies (anticyclones) are depicted in the yellow to red colour range while negative (cyclones) are in the green to blue range. Looking at the SLA during the ACSEX II cruise (right hand side panel of Figure 6.11) there was an obvious large positive sea level anomaly centred at 27.7°S - 44.4°E with a maximum height of 25 cm above the mean. To the east of this feature there was a smaller positive anomaly centred at 27.7°S - 47.7°E. This smaller feature had a height of 15 cm above the mean. South of the large positive feature was a negative anomaly. The centre of this negative anomaly was at 30°S - 43.9°E and the height was 25 cm below the mean. Looking at the

LADCP arrows of surface water movement (left hand side panel of Figure 6.11) the first three stations from the coast of section B (stations 68, 67 and 66) showed a westerly flow. The second arrow of this representation of the EMC displays a flow speed of 1.1 m/s. This was the core of the EMC. Apart from the flow of the EMC, water movement through section B appears to have been mainly influenced by the large (anti-cyclonic) positive feature centred at 27.7°S - 44.4°E. The two arrows furthest offshore of section B which depict the counter current flow (station 62 and 63) matched the direction of flow indicated by the geostrophic flow arrows in the right hand side panel of Figure 6.11. This geostrophic flow was generated between the large positive feature at 27.7°S - 44.4°E and the negative feature at 30°S - 43.9°E.

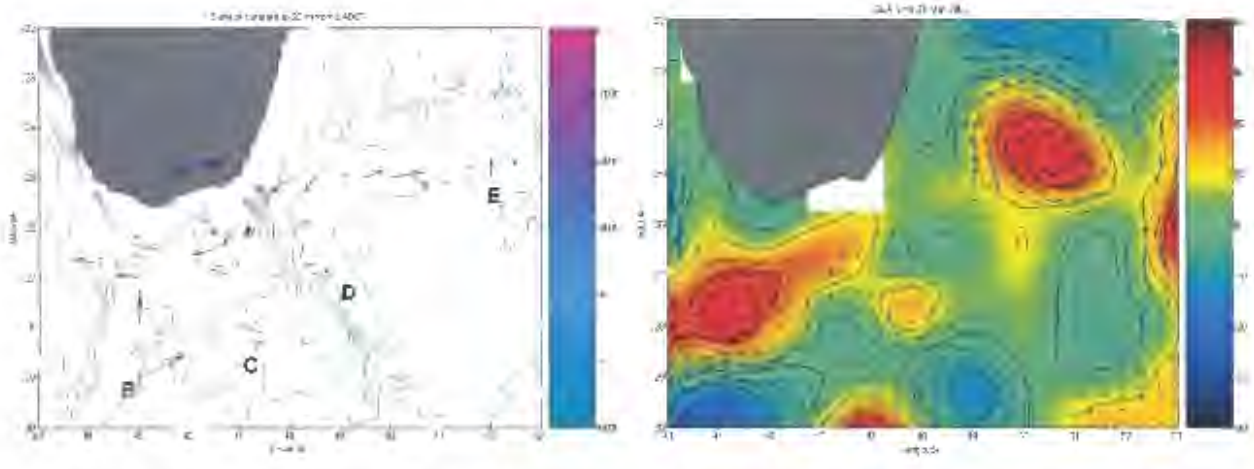

Figure 6.11. *Surface water movement as measured by LADCP during the ACSEX II cruise (left hand side panel) and. SLA and geostrophic flow for 21 March 2001 (right hand side panel). Comparing the two panels shows a strong parallel between the directly measured flow and the geostrophic currents calculated from the SLA.*

In section C the coastal most arrow showed south-eastward flow associated with the upwelling as discussed in chapter 7 'Upwelling in shore of the East Madagascar Current'. Only the third station from the coast (station 71) has an arrow depicting flow in the proposed direction of the EMC (this under representation of the EMC in section C has been discussed earlier). The eastward counter current flow seen in the LADCP data of section C seems to

have displayed an influence from the flow of water around the smaller positive feature centred at 27.7°S - 47.7°E.

There was another strongly positive feature seen in the right hand side panel of Figure 6.11 centred at 24.7°S - 50.5°E. Between the two strongly positive features in the figure was a weakly negative feature centred at 26.5°S - 48.2°E. Looking at the surface flows of section D (left hand side panel of Figure 6.11) the coastal most arrow showed offshore flow associated with the upwelling as with section C. The next two arrows from the coast (stations 82 and 81) represented the surface expression of the EMC. The remainder of the arrows on this section seem to have been influenced by the small slightly negative feature in the SLA centred at 26.25°S - 48.25°E. The four distal arrows on section D (stations 76-79) displayed a cyclonic flow around this smaller negative feature resulting in station 79 having a north-easterly counter current flow. The large positive feature centred at 24.75°S - 50.5°E appears to have had an influence on the flow at the distal end of section E. The last six arrows on this section (stations 92-97) are seen to indicate flow in an anticlockwise direction around the positive feature. From this analysis it would appear as though the SLA features influenced much of the water movement during the ACSEX II cruise. Similar affects have also been seen in a previous WOCE cruise (Donohue and Toole, 2003).

Looking at the sea surface velocity from the SADCP of the WOCE cruise (left hand side panel of Figure 6.12) and comparing it to the SLA geostrophic currents (right hand side panel of Figure 6.12) displays a very similar interaction to that seen in the ACSEX II data. Here, as was explained by Donohue and Toole (2003), the north-eastward flow of the counter current seen at around 48.5 to 50°E, seems to have been as a result of the flow around the large cyclonic feature that stretched from 25°S - 51°E to 28°S - 46°E. From studying the SLA, it now appears that the eddies around south-eastern Madagascar were largely responsible for the movement of water against the background flow in a northerly and easterly direction through the ACSEX II sections. However, the origin of these eddies is still to be determined.

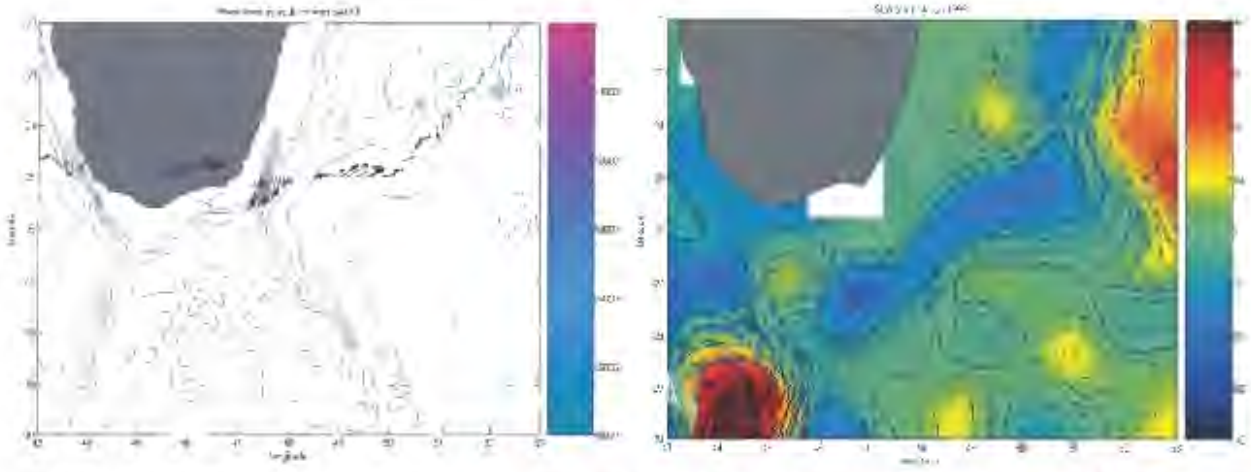

Figure 6.12. Surface water movement as measured by ship mounted ADCP during a WOCE cruise along 25°S and, SLA and geostrophic flow for the period of WOCE cruise. The eastward flow seen at 49°E in the SADCP seems to be caused by the cyclonic feature seen in the SLA.

In order to backtrack the eddies seen influencing the flow southeast of Madagascar an animation of the SLA figures was made. It was seen that anomalous features arrived at the southern tip of Madagascar from the east in the Indian Ocean. These features appeared to have originated at about 110°E. The eddies then travelled west towards Madagascar along a latitudinal range of 24 to 26°S. Quartly et al. (2006) and Schouten et al. (2002) have shown the same eddy route to the southern tip of Madagascar. The standard deviation of the SLA in the region of Madagascar for 1993 to 2005 is shown in Figure 6.13. In this figure the path taken by the SLA features from the east to southern Madagascar, where they have been shown to impact on the flow around southern Madagascar, is seen. An interesting feature of this path is that the SLA features seemed to intensify, as seen previously by Quartly et al. (2006), at 51°E (Figure 6.13 and Figure A.7). Looking at the bottom topography for the region (Figure 5.1) it is seen that the intensification of the features was probably associated with a change in bottom topography from abyssal plain to shelf edge. Furthermore the intensification that was seen south of Madagascar as the features pass en route to the Agulhas (De Ruijter

et al., 2004) also seems to be associated with topography. The Madagascar Ridge extends south from Madagascar with minimum depths of around 1000 m and features showed intensification as they travel over the ridge.

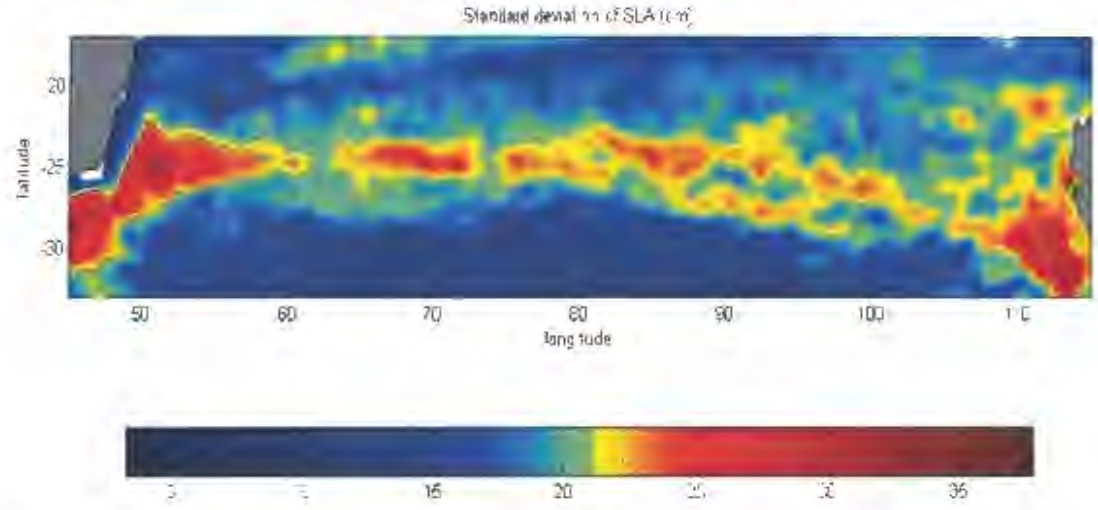

Figure 6.13. Standard deviation of SLA for 1993 to 2005. The general path taken by the anomalous features that arrive at south-eastern Madagascar from west of Australia can be seen between 23° to 27°S. The intensification of the features seen at about 53°E is probably due to the shallowing topography here.

A Hovmöller plot along 24°S to 26°S (Figure 6.14) shows that these SLA features travelled to the west at a speed of about 1.8 degrees per month (6 km per day). Results of Schouten et al. (2002) show these features arriving at south-eastern Madagascar at a rate of about six per year. After reaching the region south of Madagascar, where they have been shown to have an effect on the flow in this area, they carried on moving west to reach the east coast of southern Africa (De Ruijter et al., 2004). The origin of these SLA features is possibly in the Leeuwin Current (Morrow et al., 2004). Palastanga et al. (2007) report that it is also likely that the Rossby wave variability in the subtropical South Indian Ocean generated by baroclinic instability was the origin of these SLA features.

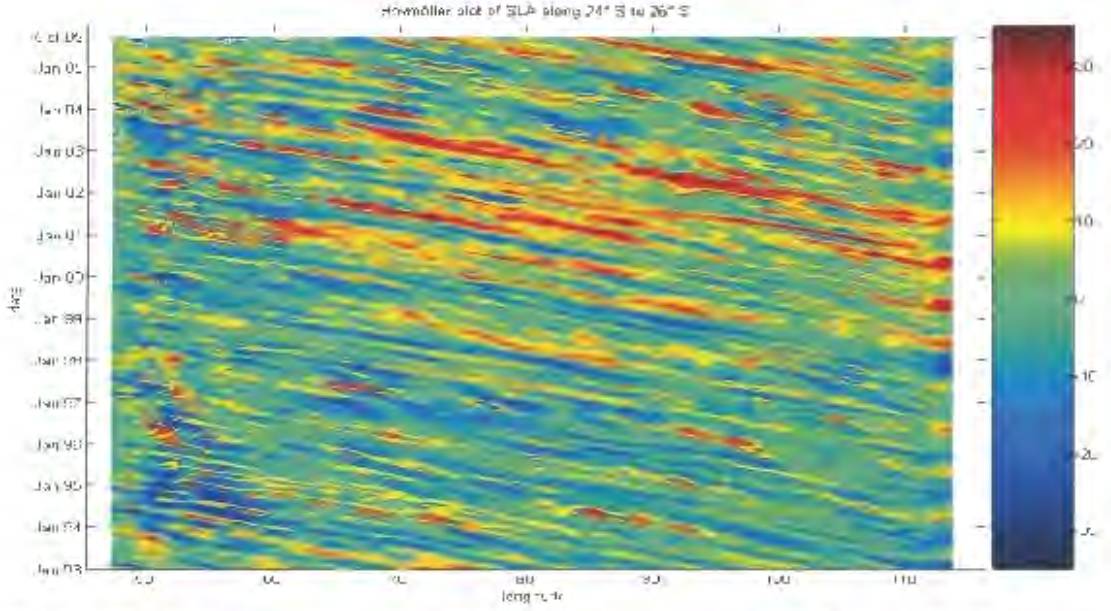

Figure 6.14. Hovmöller plot of SLA along a range of 24° to 26°S between Madagascar and west Australia. The period of the plot is from 1993 to October 2005. The positive and negative features seem to arrive at southeast Madagascar at a rate of about 6 a year. The translation speed of the features across the ocean is 1.8° per month.

The average flow direction of all drifters in the region for two thirds of a degree latitude by two thirds of a degree longitude for 1990 to 2005 is displayed in the left hand side panel of Figure 6.15. It is important to note that the drifter data are not evenly spread between 1990 and 2005 as the deployment of drifters has been irregular. The red arrows represent all flow in an easterly direction. Of interest is the easterly flow along 25°S. When comparing the drifter flow with the mean flow from SLA for 1993 to 2005 (right hand side panel of Figure 6.15) a match in this easterly flow was seen along 25°S. The geostrophic flow from SLA is a representation of the flow generated by transient eddies relative to the mean flow for 1993 to 1995 (SLA reference period). This geostrophic flow is not due to the mean flow as with Absolute Dynamic Topography (addendum Figure A.6). It would therefore appear that easterly flow seen in the average drifter plot along the 25°S could in part have been due to eddy – eddy interaction. Quartly et al. (2006) have suggested that previously reported signs of the EMC retroflection could possibly have been water from the current that was moved off to the east through the interaction of eddies. The

recently detected South Indian Counter Current (Palastanga et al., 2007; Siedler et al., 2006), are most probably also involved in the signs of retroflection of the EMC.

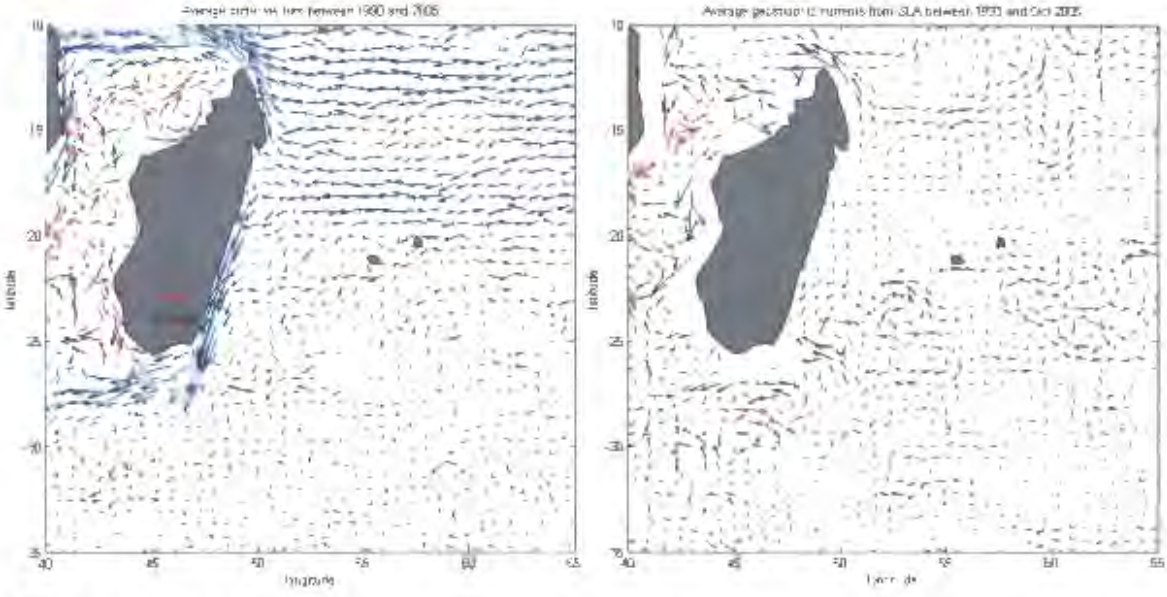

Figure 6.15. Average surface drifter movement between 1990 and 2005 (left panel) and mean flow relative to 1993 to 1995 as calculated from SLA between 1993 and October 2005 (right panel). The red arrows are used to highlight all flow that has an eastward component. When comparing the two panels a connection is seen between the drifter and geostrophic flows to the east of Madagascar in the region of 25°S.

This study has endeavoured to illuminate the flow patterns of the EMC. The EMC during the ACSEX II cruise was shown to flow at a maximum of 1.1 m/s and to have a width of about 100 m and depth of about 1000 m. However, no convincing proof of retroflection was seen in the ACSEX II data, although an eastward flow at the EMC termination was detected. SLA analysis and averaged drifter data suggest that eastward transport at the termination of the EMC could be related to eddy interaction. The clear signal of an EMC undercurrent was certainly an exciting find. This however, is not all that was possible from the ACSEX II data. The cruise track was planned so as to take the ship to the site of the proposed upwelling cell at the south-eastern tip of Madagascar. This hitherto under sampled region will be discussed in the next chapter.

7. Upwelling inshore of the East Madagascar Current

Does upwelling exist inshore of the EMC? This question was first tackled by Lutjeharms and Machu as well as by DiMarco et al. in 2000. These authors studied the remotely sensed sea surface temperature and colour data at the south-eastern tip of Madagascar. In these data they found evidence for an upwelling cell southeast of Madagascar, inshore of the EMC. Upwelling regions are typically cold, fresh, highly productive regimes with offshore volume transport in the upper layers. To verify and better understand the proposed upwelling component of this region of the EMC, it is essential that the associated physical, biological and chemical properties are studied and compared to the ambient water masses.

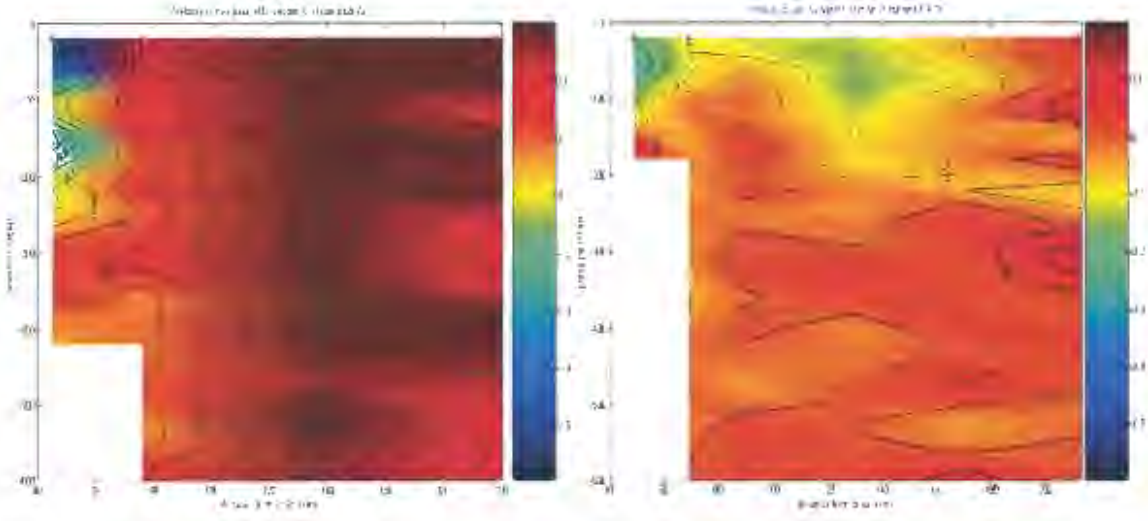

Figure 7.1. *Water flow parallel to section C (left side panel) and flow parallel to section D (right side panel). Measurements made with a Lowered Acoustic Doppler Current Profiler (LADCP). The offshore flow close to the coast is represented by blue to yellow.*

The *in situ* measurements taken during ACSEX II made it possible to investigate the properties of the suggested upwelling. The first of such data are those retrieved using the Lowered Acoustic Doppler Current Profiler (LADCP). The left panel of Figure 7.1 is a plot of the flow of water parallel to section C as was measured with the LADCP. In this representation the flow of

water either onshore or offshore along section C (map Figure 5.1) is depicted. An extensive region of flow towards the coast was apparent during the cruise and was depicted as the positive red areas on the plot. This onshore flow existed in the upper 100 m for 70 km from the coast to over 200 km from the coast. This flow extended over the full depth from about 85 km from the coast to over 200 km. However, at the station closest to the coast (45 km from the coast) there was a relatively strong flow offshore. This offshore flow went down to a depth of about 100 m and had a maximum speed of 0.5 m/s. Measurements made using radio tracked drifters in the surface waters off St Helena Bay, South Africa, have shown offshore flow rates of up to 0.15 m/s (Holden, 1985). A model run focusing on the Californian Current system has shown offshore flow rates of up to 0.4 m/s at the surface (Marchesiello et al. 2003).

The flow parallel to section D is represented on the right hand side panel of Figure 7.1. Unfortunately there were no LADCP measurements made at the north-westernmost station of section D (station 84). Although there were no current measurements made at station 84 this did not bias this section when comparing it to section C. This was because station 83 was 49 km from the shore which was similar to station 60 (north-westernmost station of section C) which was 45 km from the shore. Section D was also seen to have a predominant flow of water to the coast similar to the flow depicted in section C. There was also an offshore flow in section D. However although the offshore flow extended over a larger area in section D compared to section C the maximum speed of the offshore flow parallel to section D was only 0.2 m/s. The region of offshore flow extended from the surface to 150 m depth and extended from the coast to over 200 km from the coast.

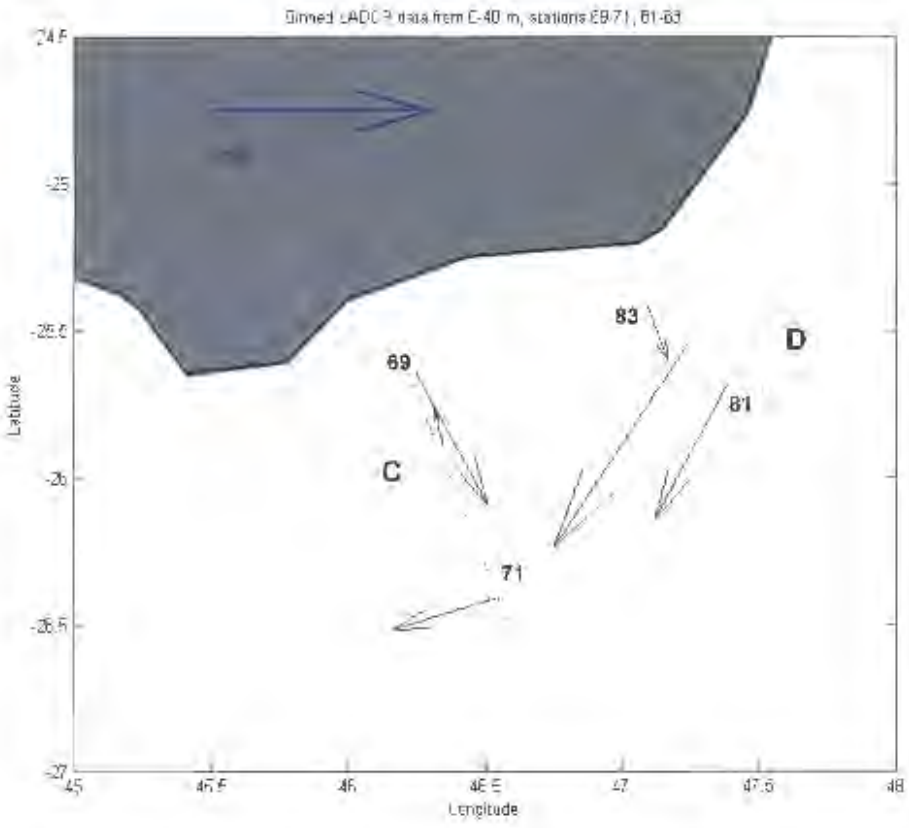

Figure 7.2. *Average speed and direction of water between the surface and 40 m for stations 69-71 and 81-83. The origin of each arrow is at the point where the measurement was taken. The offshore flow seen in Figure 7.1 is represented by the two arrows closest to the coast. The larger area of offshore flow depicted in the right side panel of Figure 7.1 is seen to be due to the section crossing the EMC at an angle.*

Arrows in Figure 7.2 show the average flow direction and speed in the region of interest. In this representation of the flow for the upper 40 m, true offshore flow was only present at the stations closest to the coast for which LADCP measurements were made in sections D and C. The larger area of offshore flow in section D (right hand side panel of Figure 7.1) was seen to be due to the relative flow direction of the EMC at an angle through the section. Whether the offshore flow seen in Figures 7.1 and 7.2 was in fact transporting water up from greater depths cannot be detected in the LADCP data. Remote sensing is however able to give a clearer picture of the origin of the water.

Upwelled water is colder than the surrounding surface water. This temperature difference has been used before in detecting upwelling regions in satellite remote sensing (Lutjeharms and Machu 2000; DiMarco et al., 2000). Figure 7.3 shows remotely sensed Sea Surface Temperature (SST) around the southern tip of Madagascar. These data were the average temperature for the three days up to and including 17 March 2001 on the left and 18 March on the right, as measured with the Tropical Rainfall Measuring Mission (TRMM) Microwave Imager (TMI) sensor. The large dilated land mask is an attempt to remove land contamination from which microwave sensors suffer. Unfortunately this masking covered part of the upwelling region of interest. However, a distinct patch of cooler water was detected in the south-eastern corner of Madagascar at 25,5°S - 46,3°E in the plot of 17 March. The temperature of this patch of cooler water was 26°C while the surrounding warmer water was up to 29°C. Also notable are two patches of cooler water seen at 24°S and 22.75°S - 48°E. These patches could possibly have been due to land contamination of the microwave data. Similar possible land contamination patches were seen at the same positions in the TMI data of 26 March (figure A.2), but were not seen in other remotely sensed SST data of 26 March (figure A.1). The cooler patch of water seen in the TMI data of 17 March at 25,5°S - 46.3°E was in the same general position as the offshore flow seen at station 69 in section C (Figure 7.2 and left side panel of Figure 7.1), as was measured on 18 March. The average remotely sensed SST for the three days up to and including 18 March is shown on the right side plot of Figure 7.3.

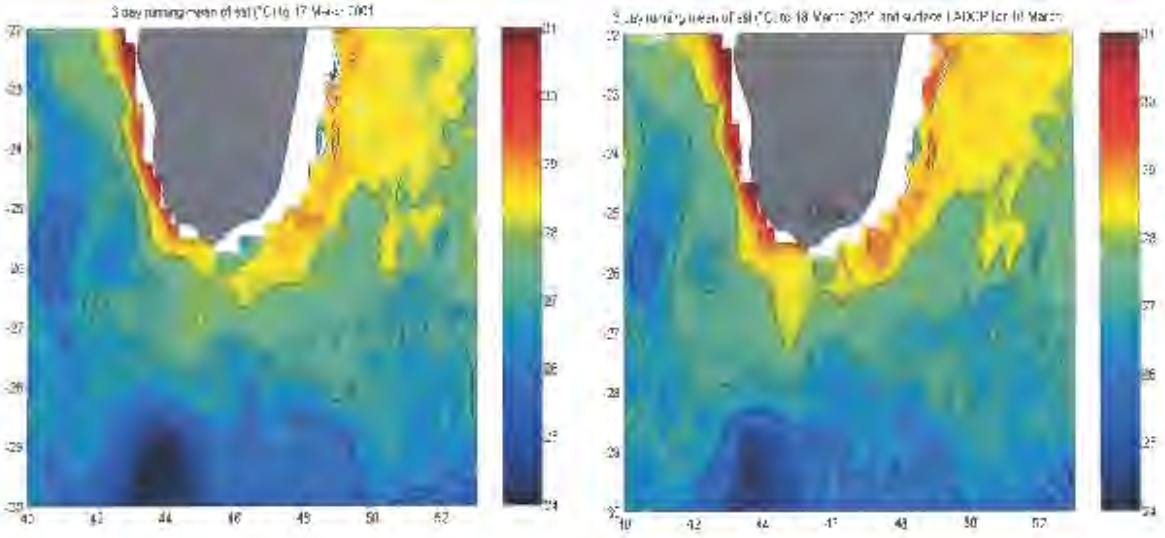

Figure 7.3. Mean sea surface temperature from the Tropical Rainfall Measuring Mission Microwave Imager. Data for the three days up to 17 March 2001 (left). A section of cooler water can be seen close to the coast at 25.5°S - 46.3°E. The plot on the right shows the surface current velocity arrows as measured with LADCP on 18 March 2001 superimposed on the mean sea surface temperature for the three days up to 18 March. A slightly cooler section of water is still seen next to the coast adjacent to the arrows. See also the fourth panel in Figure A.2. for the data up to 15 March to see quasi-permanence of feature.

The LADCP data for 18 March were superimposed on the temperature image. The lower temperatures of the cell that were seen so clearly in the left side plot of Figure 7.3 are not as distinct in the right side plot, but they are still noticeable. As this region receives high insolation, anomalously low sea surface temperatures are quickly raised to ambient temperatures (Quartly et al., 2006) and this could explain the sudden change in temperature. Although the remote microwave data does not give a very high resolution picture and has to have a large land mask, the data are not limited by cloud. The Advanced Very High Resolution Radiometer (AVHRR) is potentially better suited to accurately measure the upwelling cell, but it is unable to measure through cloud.

One of the few minimal cloud pictures of sea surface temperature for the duration of the cruise, as measured by AVHRR, is shown in Figure 7.4. In this

figure a patch of cooler water was seen adjacent to the coast at 25.3°S - 46.5°E. Additional filaments of cooler water were also seen further to the southwest and to the east. These filaments could have been upwelled water that had been entrained in the coastal edge of the current. From looking at the remotely sensed sea surface temperature it would appear that the offshore flow seen in the LADCP data (Figure 7.1) was most probably advecting cooler upwelled water offshore. One can be more certain of the origin of the cooler water seen in the satellite data by measuring the physical and chemical characteristics of the water *in situ*.

During the CTD deployments of the ACSEX II cruise, discrete water samples were taken at specified depths using the rosette sampler. The nutrient concentrations of these water samples were measured on-board during the cruise. The concentrations of nitrate, phosphate and silicate at around 100 m are shown in Figure 7.5, along with the water temperature measured at 100 m using the CTD. Contouring was not used in this representation because interpolation between the stations on different sections resulted in a misleading picture. The concentration of nitrate at the coastal station (69) of section C was 6.34 µmol/kg. At station 70, which was one station further offshore, the nitrate concentration was slightly less at 5.86 µmol/kg. The nitrate concentrations of the adjacent coastal stations of section B was 2.65 µmol/kg and the concentration of the adjacent station on section D (84) at 70 m was 2.3 µmol/kg. The nitrate concentration at 60 m for station 85 on section E was 2.45 µmol/kg. The concentrations of all the stations on all sections further offshore to the southeast were less than 1 µmol/kg. (The Potential temperature/Nitrate plot for all the stations can be seen in addendum Figure A.4.). This increase in nitrate concentration for the stations on the coastal shelf, and in particular at section C, is indicative of upwelling, and similar raised concentration levels should be seen in the other nutrients.

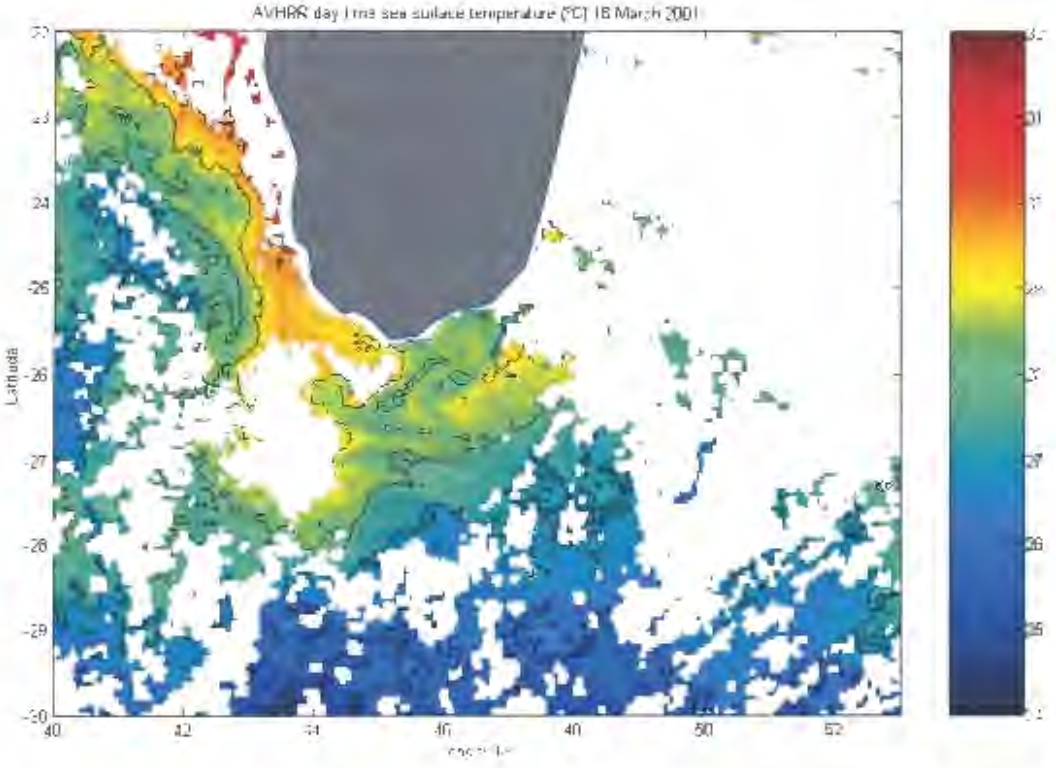

Figure 7.4. Sea surface temperature from the Advanced Very High Resolution Radiometer sensor carried on the NOAA-15 satellite. Data are for 18 March 2001. This higher resolution data shows the existence of a cooler patch of water at the south-eastern tip of Madagascar.

The concentration of phosphate at 100 m for the station on the coastal end of section C (69) was 0.53 µmol/kg while the coastal stations of the remaining sections at approximately this depth had a concentration of about 0.3 µmol/kg. The silicate concentration at 100 m for the coastal station on section C was 5.69 µmol/kg, and the next station on the section (70) had a concentration of 5.28 µmol/kg. Station 84 which was adjacent to 69 had a silicate concentration of 4.92 µmol/kg at 70 m depth, and station 68 had a concentration of 3.33 µmol/kg. The silicate concentration at 60 m for station 85 on section E was 3.76 µmol/kg. (The Potential temperature/Silicate plot for all the stations can be seen in addendum Figure A.5). The temperature of station 69 at 100 m was 18.43°C and station 70 was 19.27°C. The temperatures of the water at 100 m in the surrounding stations were in the region of 22°C.

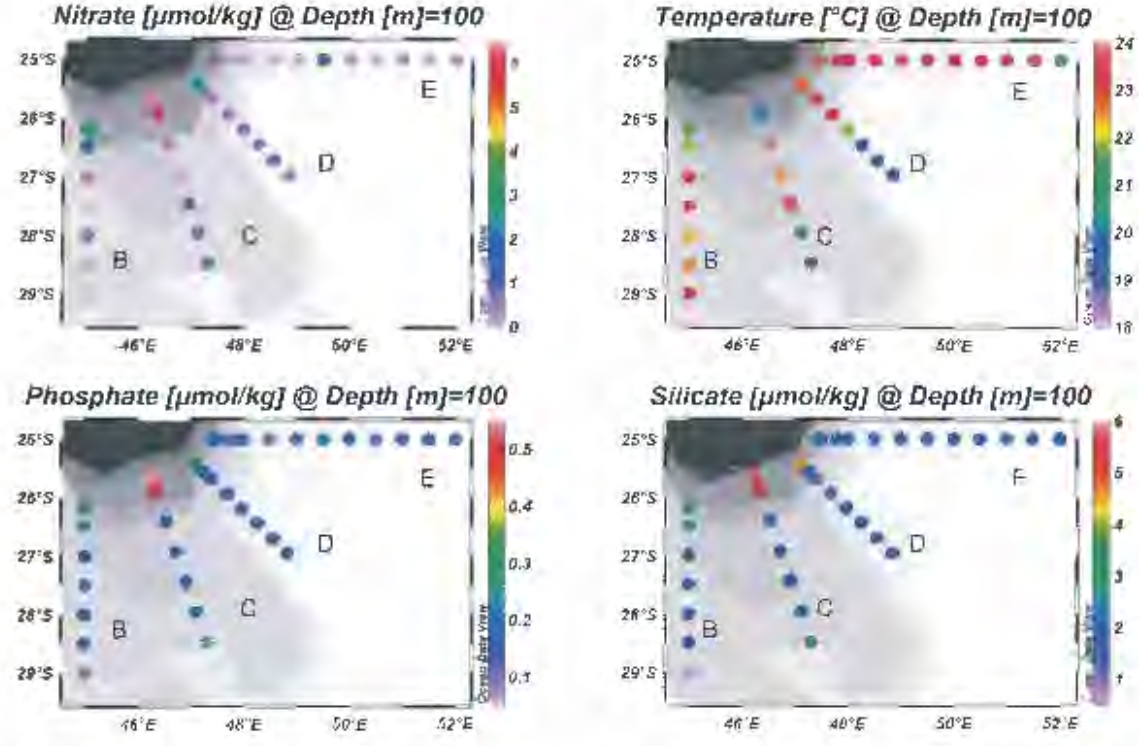

Figure 7.5. Nutrient and temperature distribution at 100 m for ACSEX II stations at the south-eastern tip of Madagascar. The two shelf stations of section C show a marked increase in nutrient concentration with an associated decrease in temperature. The shelf stations of the remaining sections exhibited the same trend but at a lesser intensity.

The nutrient and temperature data at 10 m are shown in Figure 7.6. The station closest to the coast on section D (station 84) had a surface temperature of 26.01°C which was the lowest surface temperature in the region of interest. This station also had the highest 10 m silicate concentration in the region at 2.69 µmol/kg. The second station from the coast on section C (70) was also shown to have had a relatively high nitrate concentration of 0.18 µmol/kg. The north-westernmost station of section C had a moderately low surface temperature of 27.58°C. The silicate concentration at 10 m for station 85 on section E was 2.21 µmol/kg. For clarity tables of the nutrient and temperature values for the stationed mentioned has been used (Table 7.1 and Table 7.2) These data are very instructive and give the definite impression that there was upwelled water in the region of the coastal stations of section C, D and E.

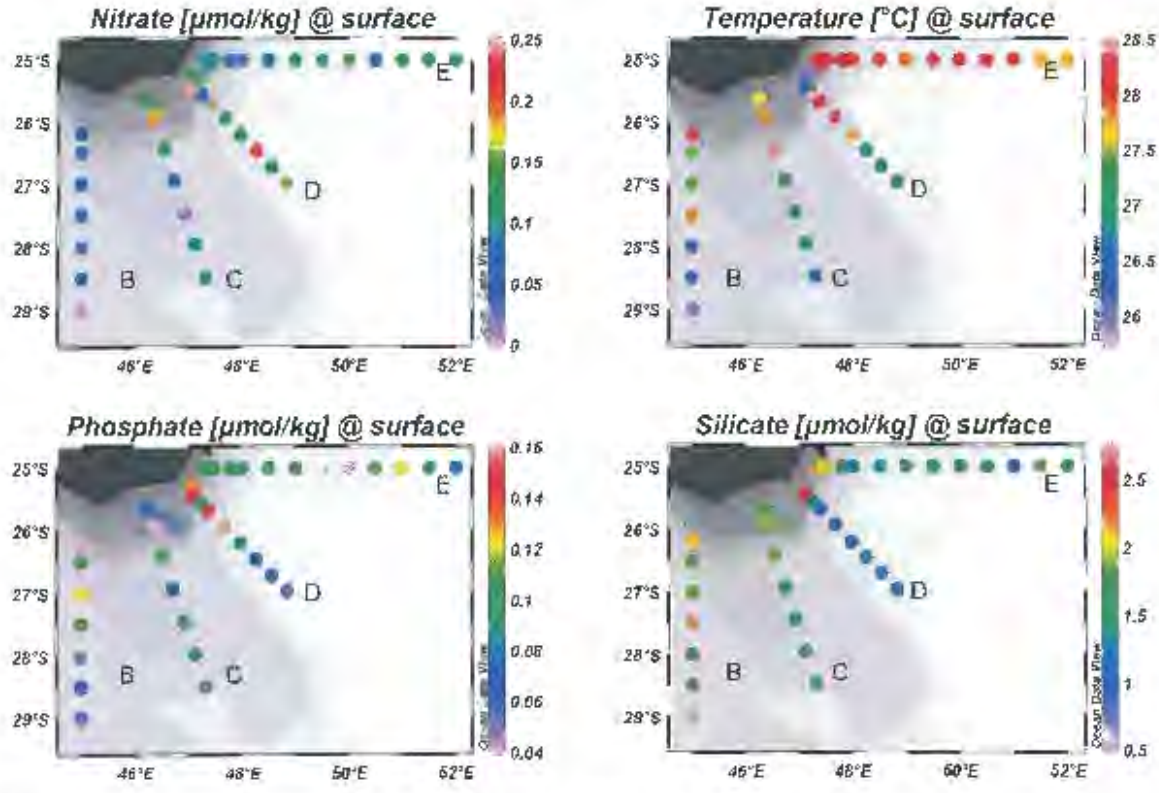

Figure 7.6. Nutrient and temperature distribution at the surface (10 m) for ACSEX II stations at the south-eastern tip of Madagascar. The two shelf stations of section D show a drop in temperature as well as an increase in silicate and phosphate concentration.

The temperature profile of the high resolution CTD data of section C, D and E (Figure 7.7) gives further evidence, and a clearer indication of the depth from which the upwelled water originated. In section C (left side panel of Figure 7.7) the dome shaped rise in isotherms at about 75 km from the coast shows the water to have been lifted by up to 150 m. This dome shape indicates the presence of a cyclonic eddy which will be discussed later. Section D (middle panel of Figure 7.7) displays a more gradual rise, with water having been lifted by about 30 m. The isotherms at the coast in section E appear to have been lifted by about 40 m. The presence of this colder nutrient rich water in the photic zone should result in an increased concentration of phytoplankton chlorophyll.

Table 7.1. Nutrient and temperature values at the surface for stations mentioned in the text.

Station position	Station	Depth	Temperature	Nitrate	Phosphate	Silicate
			°C	µmol/kg	µmol/kg	µmol/kg
B coastal	68	surface	27.58	0.07	0.04	2.1
C coastal	69	surface	27.59	0.13	0.06	1.89
C 2nd from coast	70	surface	27.76	0.18	0.04	1.97
D coastal	84	surface	26.01	0.13	0.13	2.69
E coastal	85	surface	28.19	0.09	0.1	2.21

Table 7.2. Nutrient and temperature values at around 100 m for stations mentioned in the text.

Station position	Station	Depth	Temperature	Nitrate	Phosphate	Silicate
			°C	µmol/kg	µmol/kg	µmol/kg
B coastal	68	100 m	21.52	2.65	0.3	3.33
C coastal	69	100 m	18.43	6.34	0.53	5.69
C 2nd from coast	70	100 m	19.27	5.86	0.48	5.28
D coastal	84	70 m	22.51	2.3	0.34	4.92
E coastal	85	60 m	21.69	2.45	0.31	3.76

The sea surface temperature and chlorophyll were continuously measured during the cruise by an AquaFlow system. Figure 7.8 shows the temperature and chlorophyll concentration measured along part of section D and E. At station 83 (map Figure 5.1) the AquaFlow system recorded a clear and sharp drop in the temperature from 28.5°C to 26.5°C. Associated with this marked temperature change was an increase in the chlorophyll concentration. The increase in surface chlorophyll concurrent with the drop in temperature suggests that this was a response to the upwelling and increased nutrient concentrations that were measured close to the coast. The chlorophyll concentration increased from 0.32 mg Chl-a/m^3 to around 0.63 mg Chl-a/m^3. This raised chlorophyll concentration was not particularly high, but the contrast was significant enough to demonstrate upwelling induced growth. The chlorophyll concentration was also seen to increase at 40 m depth by up to three times as much as the surface concentration in coastal stations 83-85 while stations further from the coast (stations 86 and 88) were seen to have a much lower fluorescence at this depth as can be seen in the Figure 7.9. The chlorophyll concentration may not have been representative of the typical intensity of the upwelling at this time of year. Ho et al. (2004) have shown that

the enhanced upwelling seen south of Madagascar each year in austral summer was not present in 2001.

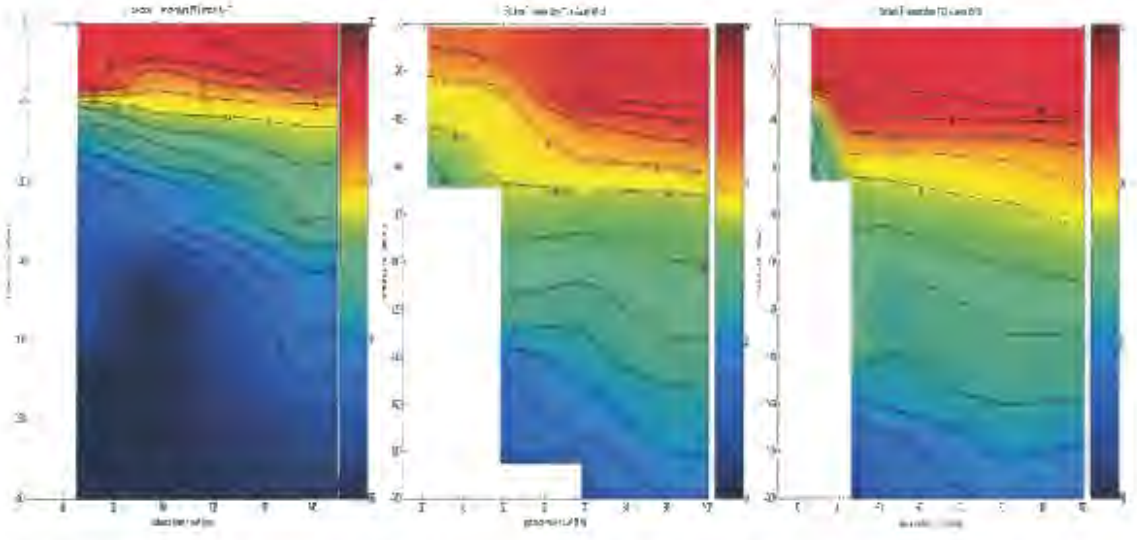

Figure 7.7. Temperature profile for section C (left panel), D (middle panel) and E (right panel). All the section show a rise in the isotherms close to the coast.

The dissolved oxygen concentrations as measured at 100 m are shown in Figure 7.10. The lowest relative concentrations (107.5 µmol/kg) were encountered at the coastal shelf stations of section C. Sections D and E also had relatively low dissolved oxygen concentrations at the upwelling stations on the coastal shelf. This possibly reflects the utilisation of oxygen in the bacterial remineralisation of dead organic matter (Machu et al., 2002). The dead organic matter having arrived at this depth from the upwelling induced chlorophyll rich region above. The complete spatial extent of the upwelling and associated chlorophyll bloom cannot be gleaned from the cruise track alone. A better method of getting an overall picture of the size of the chlorophyll bloom in the region is to use satellite remote sensing.

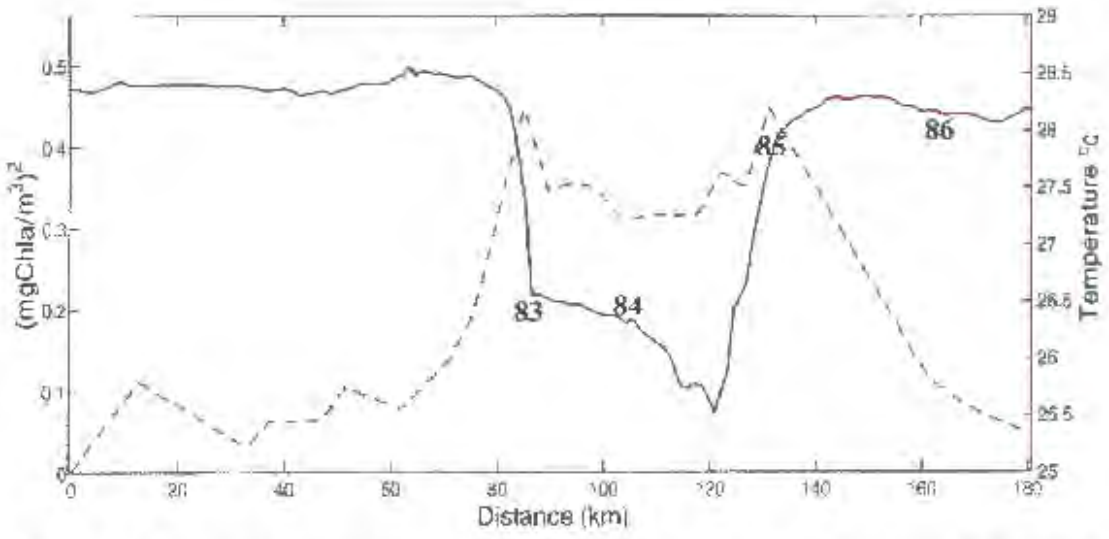

Figure 7.8. Surface temperature and chlorophyll plot as measured along the cruise track. The shelf stations of 83 and 84 on section D displayed sharply lower temperatures and higher chlorophyll concentrations when compared to the surrounding stations.

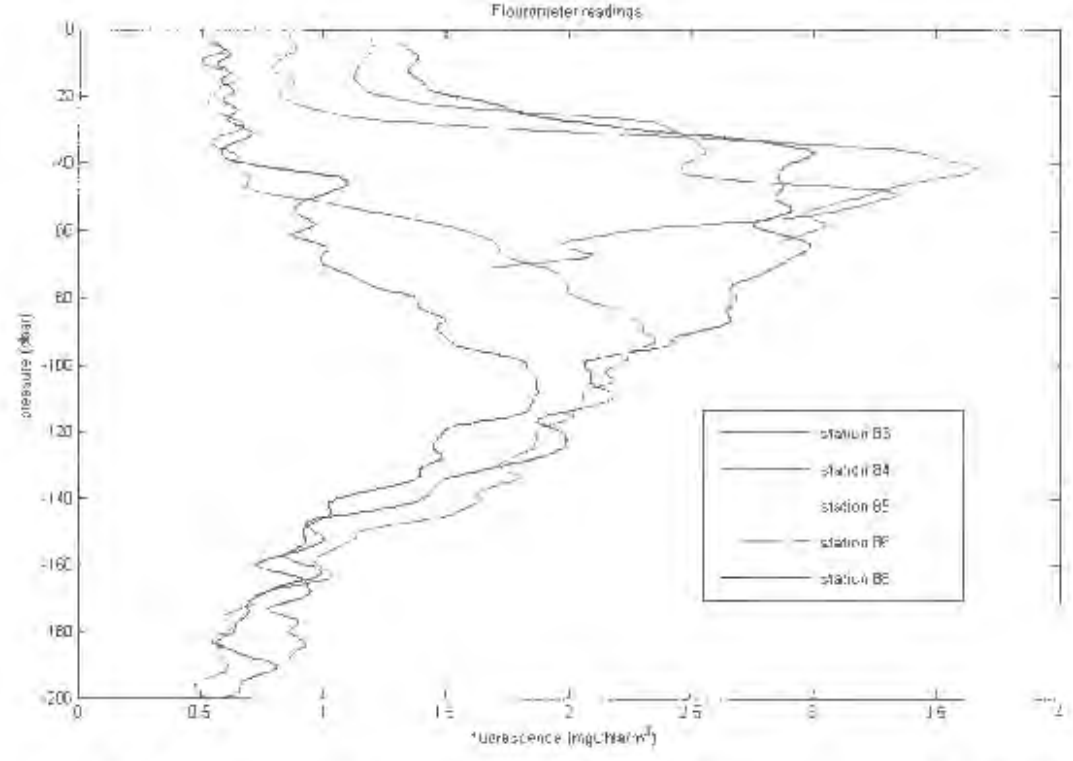

Figure 7.9. Fluorescence in mgChla/m^3 against depth in meters. Shelf stations 83, 84 and 85 show higher fluoresces at 50 m than the offshore stations.

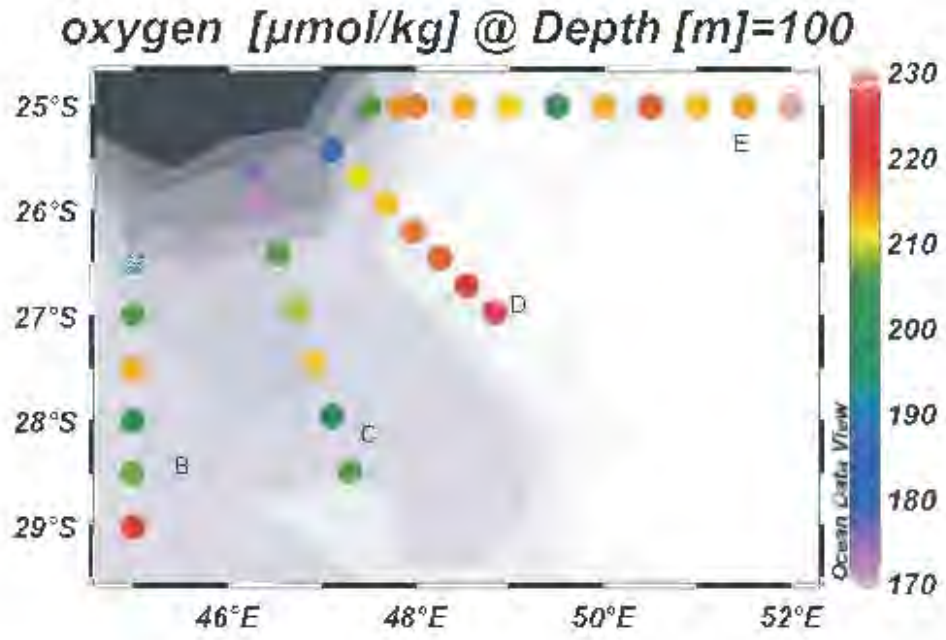

Figure 7.10. Dissolved oxygen concentrations at 100 m. The lowering of concentrations at the shelf stations could have been caused by bacterial remineralisation of dead chlorophyll.

Sea-viewing Wide Field-of-view Sensor (SeaWiFS) is a sensor that detects eight wavelength bands between 412-865 nm. Unfortunately cloud cover can prevent the measurement of these wavelengths from the sea surface. Figure 7.11 is a SeaWiFS chlorophyll false colour picture for 18 March 2001, a day on which there was minimal cloud cover over the region of interest. The plot shows a patch of heightened phytoplankton pigmentation at the south-eastern tip of Madagascar. This region of increased chlorophyll extends from 24.8°S - 47.3°E to 25.6°S - 45.7°E. The pigment concentration as measured by SeaWiFS in this productive region was about 0.5 mg Chl-a/m^3. This was a similar value to the concentration of chlorophyll in this vicinity as measured 2 days later by the ships underway-sampling system (Figure 7.8). The sharp front in chlorophyll concentration as indicated in the underway sampling was also seen in the SeaWiFS image between stations 82 and 83. The exact causes of the upwelling measured along the cruise track are still to be discovered.

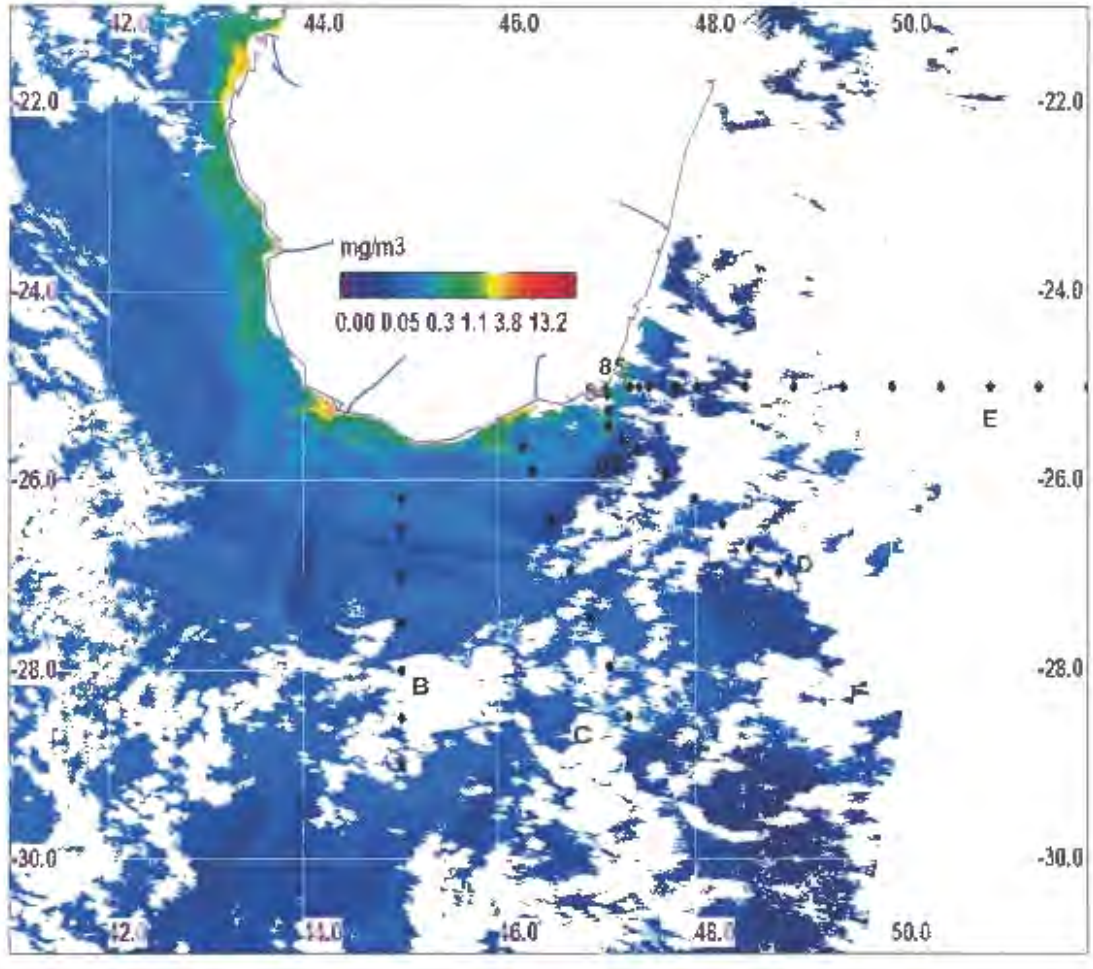

Figure 7.11. SeaWiFS false colour picture showing chlorophyll concentration on 18 March. The dots represent station positions occupied between 16 and 22 March. The sharp chlorophyll concentration front is seen between the second (83) and third (82) station from the coast on section D. The blue lines over the land represent rivers.

From the ACSEX data the presence of cooler, nutrient-rich, upwelled water and the linked increase in chlorophyll were certainly noticeable. The physical mechanisms forcing this upwelling are not as clear though. Wind is known as a common driving mechanism for coastal upwelling. The remotely measured wind stresses for the days leading up to the *in situ* measurement of the upwelling appear in Figure 7.12. The wind stresses over the region of interest were not particularly strong, but the direction was conducive to upwelling up to 19 March. However on 20 March (the date on which section D was measured) the stress dropped and the direction switched to onshore. DiMarco et al.

(2000) have said that the upwelling at the south-eastern tip of Madagascar is forced through a combination of favourable wind stress and frictional interaction between the EMC and the continental shelf slope. Gill and Schumann (1979) have explained the mechanics for current induced upwelling using the Agulhas Current close to Durban as an example.

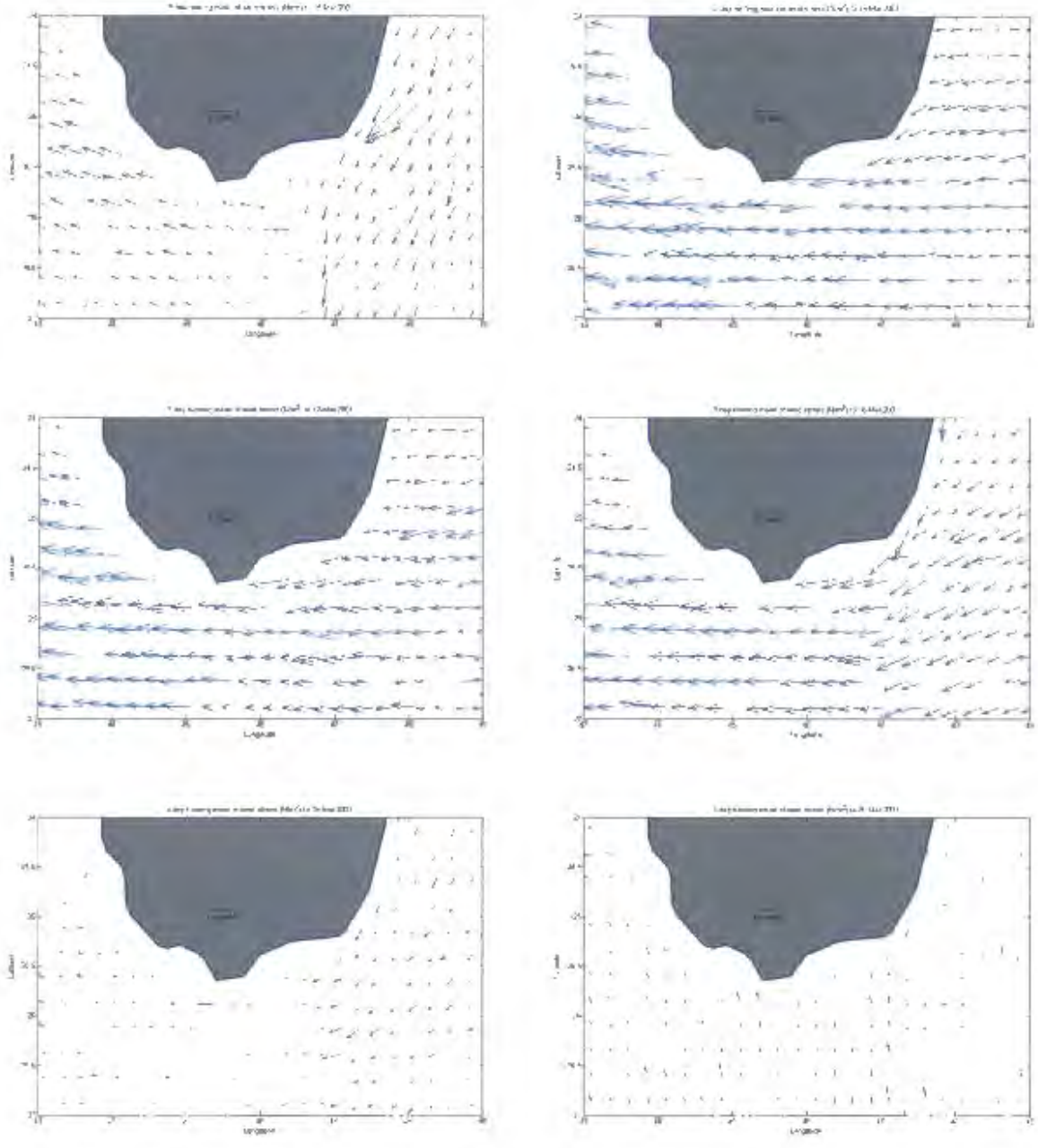

Figure 7.12. *Wind stress from 15 to 20 March 2001 as measured remotely by Quikscat. The days leading up to the cruise occupation of section C (18 March) had upwelling favourable wind stress. The days leading up to the occupation of section D (20 March) experienced a drop in the wind stress and a shift in the direction.*

A lee eddy trapped between the Madagascar coast and the current has been identified by Machu et al., 2002 as a possible driving mechanism for the upwelling. Figure 7.13 shows the same LADCP data as in Figure 7.2 but for the range 0-200 m. A rotational sense could be envisaged in the velocity arrows for these coastal shelf stations. In Figure 7.14, which represents the flow perpendicular to section C as measured with the LADCP, this cyclonic trapped lee eddy is also manifest. The positive values in this figure depict flow in a north-westerly direction. At the station closest to the coast there is a flow of about 0.2 m/s to the northwest, while the south-western arm of the eddy would be from 80 km from the coast to the EMC core at 140 km from the coast. The dome shape in the temperature profile at station 70 (Figure 7.7) could be caused by the presence of this cyclonic (divergent) eddy. Further evidence comes from the existence of higher nutrient concentrations at 100 m and the surface for station 70 than station 69 even though station 70 is further off the shelf than station 69 (Figure 7.6). The concave shape and widening of the shelf at the south-eastern tip of Madagascar could cause a trapped eddy as the current impinges on the shelf. A similar situation has also been reported on (Anderson et al., 1988; Meyer et al., 2002) where the concavity of the Natal Bight causes the existence of a permanent eddy inshore of the Agulhas Current. Lutjeharms and Jorge da Silva (1988) have also shown the existence of a Delagoa Bight eddy.

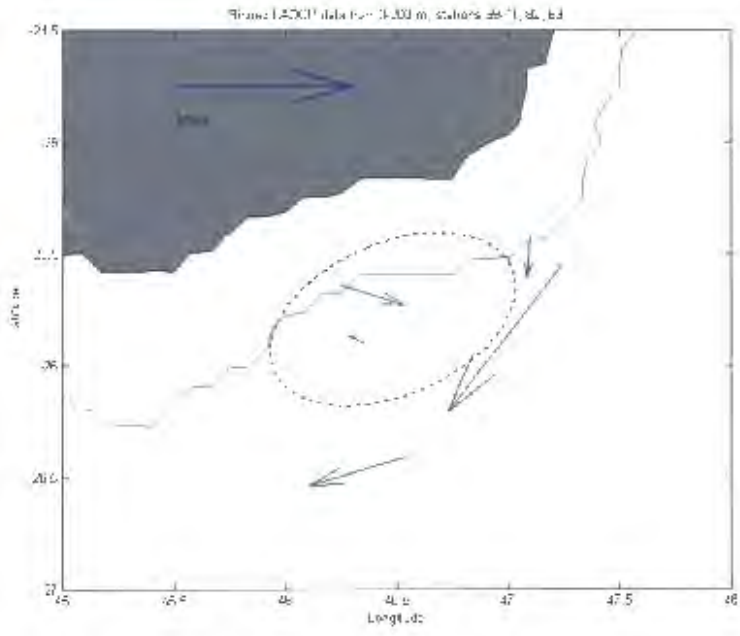

Figure 7.13. Average speed and direction of water between the surface and 200 m. Arrows origins depict flow at stations 69-71, 82 and 83. The dashed ellipse represents the position of the proposed lee eddy trapped between the EMC and the coast. The shelf edge at 300 m is shown in light blue.

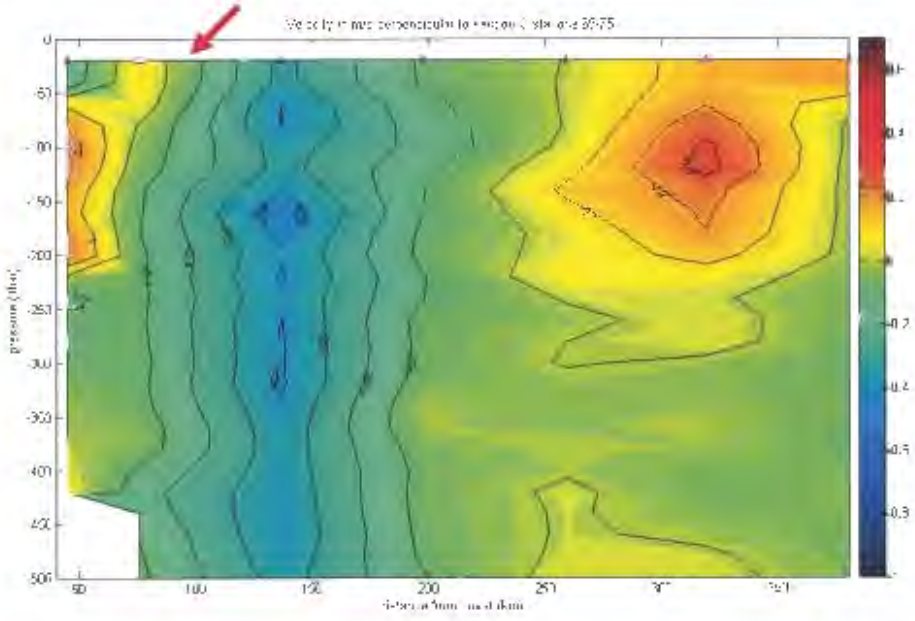

Figure 7.14. Water velocity in the upper 500 m through ACSEX II sections C. as measured by Lowered Acoustic Doppler Current Profiler. The core of a possible lee eddy is marked with an arrow in the current velocity perpendicular to section C as measured by LADCP.

An upwelling inshore of the EMC was certainly observed during ACSEX II. However the durability and full spatial extent of this upwelling cannot unfortunately be determined from one cruise. Remotely sensed data can aid in researching the upwelling over a larger region and longer time period, but cloud cover results in many uncertainties. The exact mechanism for the upwelling also remains unclear. Coastal upwelling cells are commonly wind driven. The wind stress before and during the cruise was shown to be in a direction which was upwelling favourable. A cyclonic eddy was also found to be centred at station 70 on section C and this could have accounted the upwelling seen here. The likelihood is strong that the total mechanism for upwelling at sections D and E was actually a combination of both wind forcing and current induced upwelling. The ACSEX data have certainly been instructive in highlighting this upwelling for the first time, but that was not the limit of the data. There was also the question of the proposed retroflection that has been looked at in the previous chapter as well as the discovery of the RSIW and the EMC undercurrent.

8. Conclusion

Many studies of the Agulhas Current have highlighted its nature and shown it to be an important link in the global thermohaline circulation (Lutjeharms, 1996). However the sources of this significant current remain understudied. One of the possible sources of the Agulhas Current is the East Madagascar Current (EMC). Past analysis of the EMC has studied the current at 23° and 25°S (Lutjeharms et al., 1981, Swallow et al., 1988, Donohue and Toole, 2003), but no dedicated cruise has previously focused on the termination of the EMC. The ACSEX II (Agulhas Current Sources EXperiment) set out to investigate the termination of the EMC with a series of hydrographic stations (Lutjeharms et al., 2001).

The data from the cruise and complementary data have been used in answering the key questions as laid out in chapter 3 'What is unknown about the East Madagascar Current termination?'.

8.1 What are the main water masses at the southern termination of the EMC?

Analysis of the ACSEX II data in this study has verified the previously suggested water masses in the surface, central and intermediate depths of the EMC (Swallow et al., 1988). Previous studies indicated the presence of Tropical Surface Water; Subtropical Surface Water; South Indian Central Water and Antarctic Intermediate Water. Due to the limitation on the maximum cast depth of the hydrographic stations in the ACSEX II cruise only the upper layers of the deep water masses could be studied. Closer investigation revealed a differentiation between fresher North Indian Deep Water (NIDW) with its higher silicate/lower oxygen concentration and more saline North Atlantic Deep Water (NADW) and Circumpolar Deep Water (CDW). Unfortunately, further limitations on cable depth to 800 m meant it was impossible to make deep hydrographic casts in the Mascarene basin to verify the deep water masses here.

Although Red Sea Intermediate Water has been noted in sections off the north of Madagascar (Swallow et al., 1988), it has never been conclusively reported at the southern end of the EMC. The relatively high density of the ACSEX II shelf stations have made it possible to highlight Red Sea Intermediate Water for the first time. The Red Sea Intermediate Water with its characteristic high salinity (34.5 psu) low oxygen signal (140 $\mu mol.kg^{-1}$) was found adjacent to the shelf at a depth of between 800 and 1250 m and at temperatures of between 4 and 6.5° C. The discovery of RSIW in the southern EMC is important as it verifies that RSIW can also enter the Southwest Indian Ocean east of Madagascar and not only through the Mozambique Channel.

8.2 What is the probable trajectory of the termination of EMC?

Numerous methods have been employed to analyse the general trajectory of the EMC. A comprehensive review of these studies has been given in chapter 2 'What is known about the East Madagascar Current?'. Notwithstanding all the previous work done on the trajectory of the EMC there is no certainty in the description of the path of the termination of the EMC. The ACSEX II cruise was planned as a means to clarify this picture.

The salient points of the study are that the EMC had a maximum speed of 1.1 m/s, the maximum width of the current was about 100 km and the depth was 1000 m. This resulted in a maximum calculated volume flux through the ACSEX II sections of 39.3 Sv. This value compares well with previous results. Furthermore conclusive evidence was found of an EMC undercurrent that flowed in a north-easterly direction. The depth range of the EMC undercurrent was from 1000 to 2000 m and the maximum speed was 0.3 m/s. This resulted in a maximum calculated volume flux by the EMC undercurrent of 0.8 Sv. The Red Sea Intermediate Water was shown to be partially entrained in the EMC undercurrent flow, but the majority of the Red Sea Intermediate Water was seen to be flowing south, away from its source.

Although there were signs of surface water flowing counter to the EMC, closer inspection of the Θ/S, oxygen and silicate data did not provide substantial evidence that the water was directly fed by an EMC retroflection loop. After

studying the sea level anomaly in the area it was decided that the counter current flow was due to eddy features in the region. These sea level anomalies were shown to originate at about 110° E and were seen to arrive at the south-eastern tip of Madagascar along a path positioned between 24-26°S. The propagation speed of the features along the path was about 1.8° per month, and they arrived east of Madagascar at a rate of about 6 per year. The average direction of the surface drifters in the region matched the mean flow relative to 1993 – 1995 which was derived from the SLA. This further supports the idea that eddies in the region caused eastward flow at the termination of the EMC and could have resulted in a temporary retroflection of the EMC on other occasions. The new results for ACSEX II therefore have not been able to provide a definitive answer to the question of retroflection.

8.3 Does upwelling exist inshore of the EMC termination?

Upwelling at the south-eastern tip of Madagascar has been reported on previously (Lutjeharms and Machu, 2000; Di Marco et al., 2000; Ho et al., 2004). These studies have, however, relied exclusively on remotely sensed data to outline the upwelling inshore of the EMC.

The ACSEX II cruise made it possible to survey the site of the proposed upwelling and take *in situ* measurements. The data showed that there was indeed upwelling, indicated by a drop in sea surface temperature of up to 3° C. Closely associated with this sharp drop in temperature was a more than doubling in chlorophyll concentration. An increase in nutrient concentrations at the sea surface also pointed to upwelling. Examination of the temperature and nutrient profiles showed that the source of the cooler nutrient rich surface water was from water around 40 m deeper. Lower dissolved oxygen concentrations were also found under the upwelling cell at 100 m. It was theorised (Machu et al., 2002) that this decrease in oxygen was due to bacterial consumption of the decaying organic matter from the upwelling cell above.

The LADCP data showed that there was a surface offshore flow of up to 0.5 m/s perpendicular to the coast during the cruise. The causes of the offshore

flow and associated upwelling have been difficult to detect. The shelf configuration in the region of the upwelling makes current-induced upwelling, as explained by Gill and Schumann (1979), a very likely mechanism. The wind stress before and during the cruise was also shown to be in a direction which was upwelling favourable. Furthermore the data from the cruise revealed the possibility of a trapped lee eddy causing dynamic upwelling at section C. It is most likely that the total mechanism is actually a combination of all these forces.

At present mesoscale features such as the trapped lee eddy inshore of the EMC and the possible retroflection of the EMC are not adequately resolved in Absolute Dynamic Topography (ADT) (http://www.jason.oceanobs.com/html/-donnees/produits/hauteurs/global/madt_uk.html) but hopefully new and exciting satellite developments (http://www.csr.utexas.edu/grace/-overview.html) will make it possible to calculate ADT and geostrophic flow with much more certainty in the future. For now regular placement of drifters directly into the EMC could make possible a statistical inference on the permanence of a retroflection. Furthermore, in order to study an EMC retroflection directly will require a longer term analysis such as judiciously placed moorings as have been initiated in 2005 (Quartly et al., 2006). Although it is impossible to plan a cruise to coincide with a retroflection, more regular cruises to the termination of the EMC might result in the retroflection being sampled fortuitously. Although further work is required on the interesting topic of the EMC retroflection, a study of the forcing of the upwelling inshore of the EMC could also benefit from regular cruises to the EMC termination.